Hydrogeology of the Karst of Puerto Rico

GEOLOGICAL SURVEY PROFESSIONAL PAPER 1012

JMR

HYDROGEOLOGY OF THE KARST OF PUERTO RICO

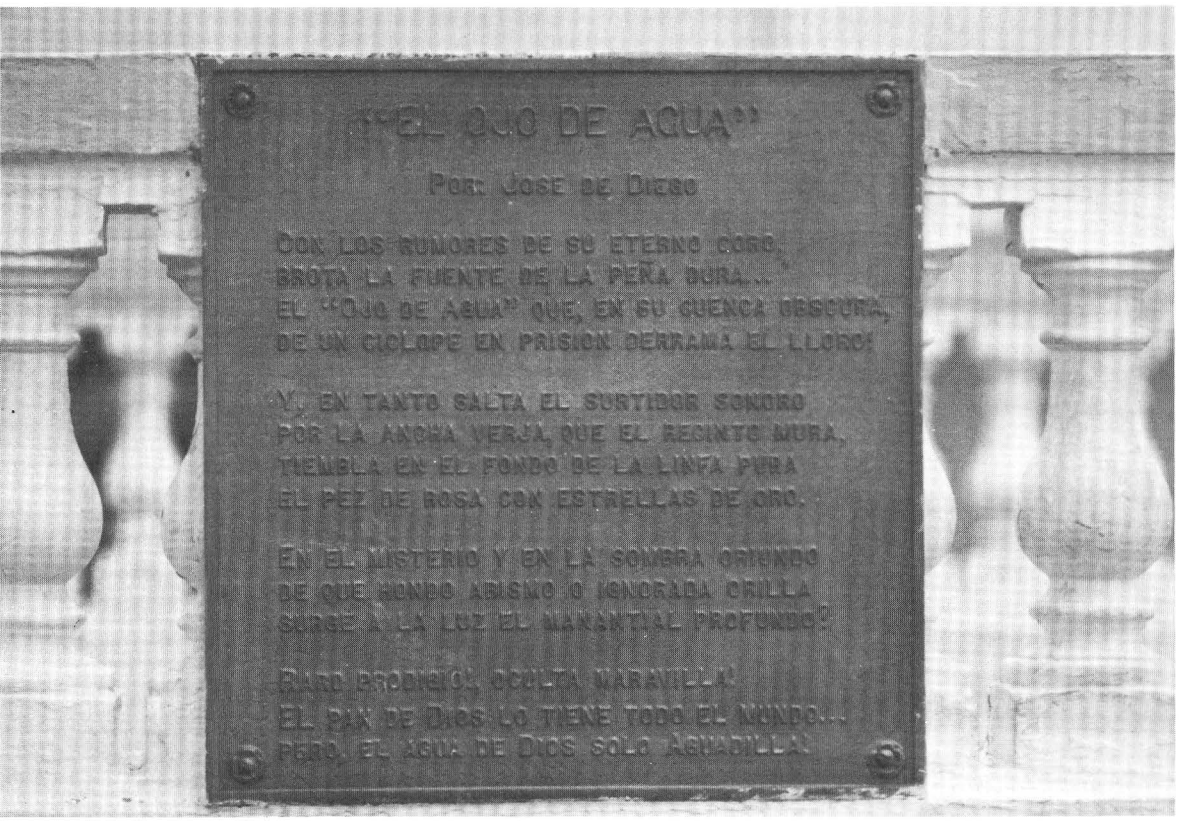

Poem by a foremost Puerto Rican concerning the "Karstic Spring" at Aguadilla, Puerto Rico.

Hydrogeology of the Karst of Puerto Rico

By ENNIO V. GIUSTI

GEOLOGICAL SURVEY PROFESSIONAL PAPER 1012

UNITED STATES GOVERNMENT PRINTING OFFICE, WASHINGTON : 1978

UNITED STATES DEPARTMENT OF THE INTERIOR

CECIL D. ANDRUS, *Secretary*

GEOLOGICAL SURVEY

V. E. McKelvey, ***Director***

Library of Congress Cataloging in Publication Data

Giusti, Ennio V
Hydrogeology of the karst of Puerto Rico.
(Geological Survey professional paper ; 1012)
Bibliography: p.
Supt. of Docs. no.: I 19.16:1012
1. Water, Underground—Puerto Rico. 2. Karst—Puerto Rico. 3. Geology—Puerto Rico. I. Title. II Series: United States. Geological Survey. Professional paper ; 1012.
GB1055.G58 551.4'9'097295 76-26183

For sale by the Superintendent of Documents, U.S. Government Printing Office
Washington, D.C. 20402
Stock Number 024-001-03031-4

CONTENTS

ILLUSTRATIONS

TABLES

CONVERSION FACTORS

Metric units	*Conversion factor*	*Foot-pound-second units*	*Remarks*
meter (m)	3.28	foot (ft)	
millimeter (mm)	.039	inch (in.)	
kilometer (km)	.62	mile (mi)	
square kilometer (km^2)	.386	square mile (mi^2)	
degree Celsius (° C)	1.8	degree Farenheit (° F)	add 17.8 to ° C
liter per second (L/s)	15.9	gallon per minute (gal/min)	
kilogram per square centimeter (kg/cm^2)	14.22	pound per square inch (lb/in^2)	
centimeter per second (cm/s)	2,850	foot per day (ft/d)	
cubic meter per second (m^3/s)	35.4	cubic foot per second (ft^3/s)	
milligram per liter (mg/L)	~1	parts per million (ppm)	for dilute solutions
gram per cubic centimeter (g/cm^3)	62.5	pound per cubic foot (lb/ft^3)	
gram (g)	.0022	pound (lb)	
tonne per year (t/yr)	1.1	short ton per year (ton /yr)	

NOTE:—Multiply units in first column by the conversion factor to obtain units of third column. The order of the units shown follows that used in the report.

HYDROGEOLOGY OF THE KARST OF PUERTO RICO

By ENNIO V. GIUSTI

ABSTRACT

About one-fifth of Puerto Rico is covered by a tropical karst formed on a series of six limestone formations ranging in age from middle-Oligocene to middle Miocene. These formations strike east to west and crop out over the north coast of the island. Structurally, the rocks form a simple wedge abutting southward against a mountain chain of volcanic origin and thickening northward to about 1,400 meters by the seashore. All stages of karstification are present: from the incipient, found at the western end of the belt to the residual, found at the eastern end. Maximum development of sinkholes occurs on the Aguada Limestone and upper part of the Aymamón Limestone. These formations have a $CaCO_3$ content range from about 85 to 95 percent. The semi-impermeable Cibao Formation has developed a fluvial drainage. An analysis of stream channel orientations indicates that the present topographic drainage oriented toward the northeast is superimposed on a former drainage system oriented toward the northwest. Transition from the northwestern to the northeastern drainage orientation is ascribed to Pleistocene eastward tilting of the Puerto Rican platform. This tilt is thought to have affected the subterranean drainage pattern as well, so that springs are found mainly on the western wall of northward-oriented valleys. Estimates of the water budget indicate that the karstic stream basins behave on an annual basis much as other stream basins that are not on limestone terrane. Average incoming solar radiation (expressed as evaporated water) and rainfall (2,900 mm and 1,750 mm, respectively) result in an evapotranspiration of about 1,100 mm (millimeters) annually and a discharge of 650 mm. This discharge is accommodated fluvially in areas underlain by the Cibao Formation and by the lower part of the Lares Limestone and subterraneally through the karst elsewhere.

Base flow of streams in limestone in Puerto Rico is less than in streams in volcanic terrane, owing to fast disposal of rainfall through networks of subterranean solution channels. Ground water is found under water-table conditions in the Aymamón and Aguada and under artesian conditions in parts of the Cibao and the Lares. The unconfined groundwater discharges along a strip near the shoreline into swamps and lagoons; the artesian water discharges through a submarine face an unknown distance from the coast and possibly, in part, along a presumed fault near the coast. In the western part of the belt, ground water discharges through the sea bottom, possibly as springs. Permeability is found to decrease exponentially with stratigraphic depth.

Except for lake waters resting on terra rossa, most waters of the limestone belt are saturated or supersaturated with respect to calcite, and as much as 86 percent of the solution is computed to arise mainly from enrichment of rainwater with CO_2 in the soil from the decomposition of organic acids. The denudation rate of the limestone belt through solution is computed as 0.070 mm per year with some evidence that abrasion may increase the denudation rate locally by as much as 40 percent. Calculations based on a projected initial limestone surface and the computed solution rate reveal that the limestone belt emerged from the sea about 4 million years ago and that the eastward tilt of the Puerto Rican platform, reported in the literature, occurred about 1 million years ago. Of the factors pertinent to karst development, aquifer permeability, both vertical and lateral, and primary rock porosity are thought to be the basic control for the existence and morphology of the karst. Assuming sufficiently pure limestone, climate is considered of secondary importance.

INTRODUCTION

Most men of science of ancient times thought that all the water about them originated from large underground caverns, perennially replenished by the sea or by condensation of moist air. This view, along with most scientific theories prevailing at that time, was the legacy of Aristotelian thinking; and it is interesting, within the context of this report, to speculate that only a karst land—the Grecian one, in this instance—could have been responsible for fostering such a theory. Only the karst develops underground rivers, and only carbonate and other soluble rock terranes develop karst. However, not all limestone terranes become karst, and not all karsts contain underground rivers. A great range of conditions occur in many limestone regions; some areas show little effects of solutional erosion, whereas other areas show advanced stages of karst development. A limestone area can occupy any intermediate position within these two limiting conditions; one of the objectives of this report is to place the north coast limestone area of Puerto Rico within such a perspective. The main purpose is to describe the hydrologic and geologic conditions of the karst terrane of the north coast of Puerto Rico.

The writer appreciates the cooperation of the Puerto Rico Aqueduct and Sewer Authority for providing data on well logs and pumpage and for providing a crew to drill holes in well casings to measure water levels.

DATA AVAILABLE AND PREVIOUS INVESTIGATIONS

Areal photographs are available for the area, and topographic quadrangle maps may be obtained at the scale of 1:20,000 with contour intervals of 5–10 m in regions of high relief, and of 1 m in regions of low relief. Geologic maps, also at a scale of 1:20,000, have been published for each quadrangle in the region. Meteorological data include records from about 25 daily rainfall stations scattered throughout the north coast limestone belt and the nearby mountain slopes, and records from 5 evaporation sites at different altitudes in the area. Hydrologic data available prior to this study were limited to monthly water levels from a skeleton network of 5 wells, and miscellaneous low-flow discharge measurements from 20 sites. In addition to these hydrologic data from the limestone area proper, data were available from three long-term (more than 10 year of record), and two short-term (2 years of record) streamflow stations located in the volcanic area near the contact of the limestone belt. Chemical analyses of ground and surface water have been published in basic-data reports.

Reports on the limestone belt include geologic mapping, principally by Monroe (1962, 1968a, 1969a), Briggs (1961, 1966), and Briggs and Akers (1965) and the excellent studies of the karst morphology by Monroe (1964, 1966, 1968b, 1969b). Detailed work on a portion of the area but with conclusions significantly applicable to the limestone belt in general can be found in Williams (1965). Older and more general works, such as those of Lobeck (1922), Meyeroff (1933), and Zapp and others (1948), yield much useful information on the geology and geomorphology of the limestones. The coastal features and shoreline investigation of Kaye (1959), and various geophysical investigations such as the gravity work of Myers (1955) and Shurbet and Ewing (1956), provide information for a better understanding of the three-dimensional boundaries of the limestone belt.

An investigation of the hydrogeology of Puerto Rico, which includes a comprehensive study of the ground-water conditions of the north coast limestone area, was made by McGuinness (1948). Birot and others (1967) present a quantitative evaluation of the water budget of a karst stream basin, and field-analyzed chemical data of karstic water. Bennett and Giusti (1972) evaluated the hydrology of the Laguna Tortuguero area; Diaz (1973 mapped the chemical quality at the Caño Tiburones; and Jordan (1970) reported on ground-water movement in the upper Río Tanamá basin.

THE LIMESTONE AREAS OF PUERTO RICO

The limestones of Puerto Rico are found scattered throughout the island as caps of mountains or as belts draped over the north and south coasts. These limestones (see fig. 1) range in age from early Cretaceous (Briggs and Akers, 1965), the oldest of the patches being found in the interior, to middle Miocene and perhaps as young as middle Pliocene (G. Seiglie, oral commun., 1969), the youngest proposed age for the youngest formation found in the north coast belt. The limestones of the interior represent the remnants of reefs that fringed the Cretaceous volcanoes of Puerto Rico (Meyerhoff, 1933), whereas the north and south belts, were deposited later over the eroded volcanic core, in shallow clear-water environments with open circulation, on a generally stable shelf.

The limestones of the north coast cover an area about 125 km (kilometers) in length from Aguada to Loiza and as much as 22 km in width near Arecibo, encompassing about 1,600 km^2, or one-fifth of the land area of Puerto Rico. The altitude of the north coast belt is about 400 m (meters) at the contact with the volcanic core and decreases northward to sea level.

The discussion in this report is confined to the north coast belt west of the Río de la Plata because it contains important aquifers; moreover, it is the only area that has developed prominent karst topography.

GEOLOGY

VOLCANIC BASEMENT

The limestones of the north coast belt rest unconformably on a faulted and folded volcanic base that is no younger than Eocene in age (Briggs, 1961). The surface of the volcanic rocks beneath the limestone is highly irregular as evidenced by the variability of the angles of the dips and their azimuths reported from seismic reflection work carried out in the search for oil structures (Myers, 1955).

LIMESTONES

The limestones on the north coast were deposited in shallow clear water with open circulation, on a

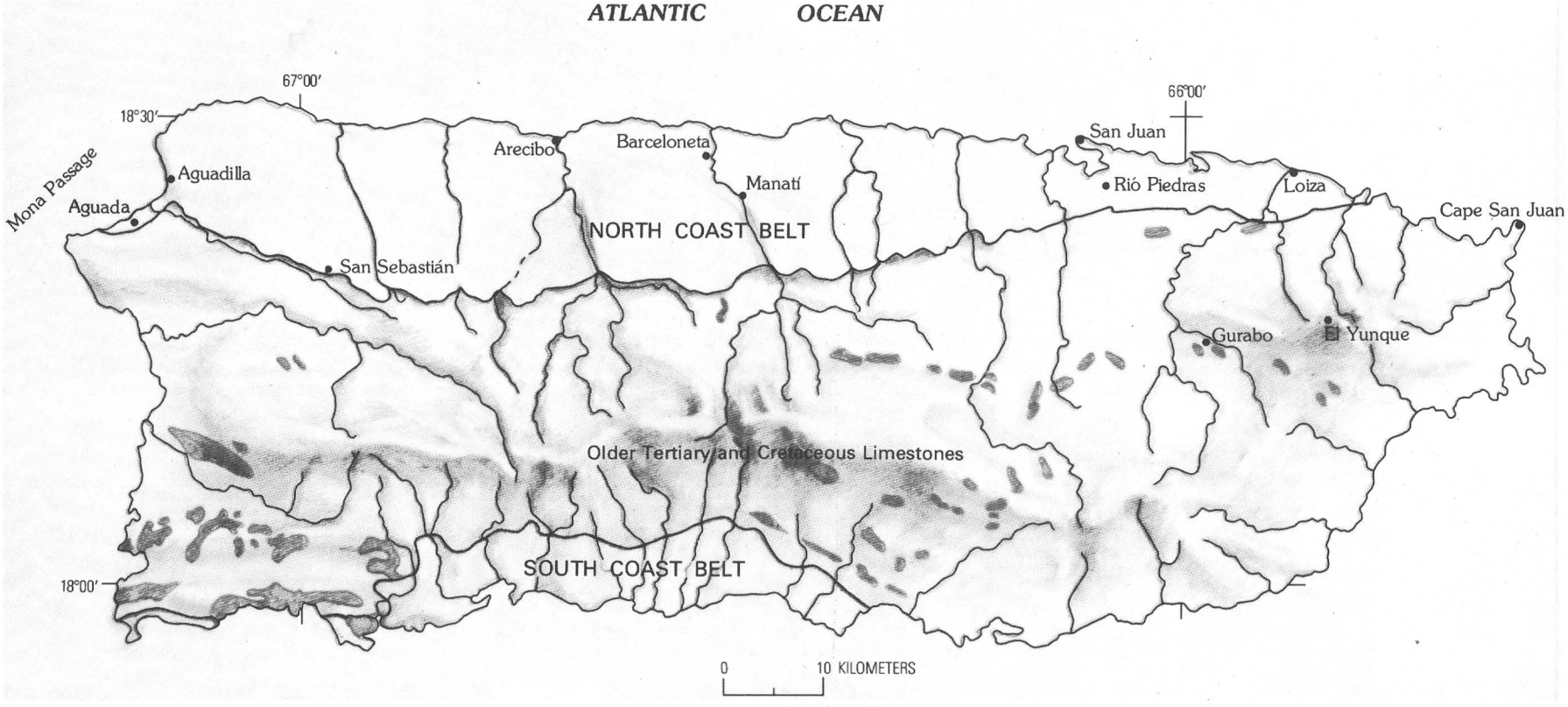

FIGURE 1.—Location of the limestone areas (slightly modified from Briggs and Akers, 1965).

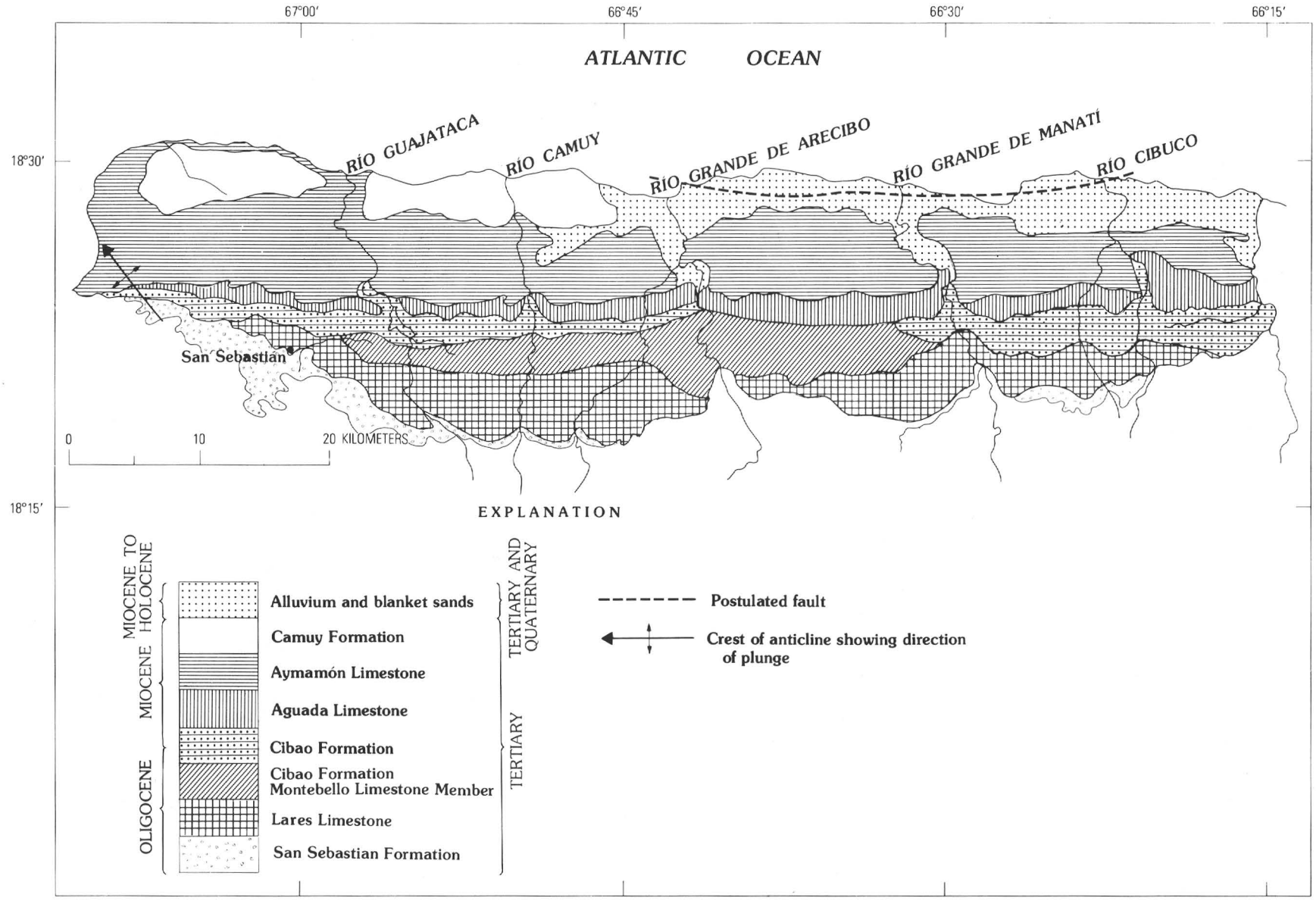

FIGURE 2.—Geologic formations of the north coast limestone area (adapted from Briggs and Akers, 1965).

generally stable shelf, and have undergone little postdepositional structure changes. Most investigators consider the age of the limestones to range from middle Oligocene to middle Miocene.

Above the volcanic base, six formations are recogized (fig. 2); these are described herewith from oldest to youngest (lithology of the rocks units are adapted from the several reports of Briggs and Monroe.).

SAN SEBASTIÁN FORMATION

Essentially the Formation is a poorly cemented shaly bedded claystone, but contains layers of siltstone, sandstone, conglomerate, and locally has lenses of limestone and lignite. The thickness ranges from zero in the middle part of the belt to about 300 m near the town of San Sebastián. The age is controversial. Most investigators consider it to be of middle Oligocene age; Gordon (1959), however, believes that no rock of the north coast Tertiary sequence is older than Miocene. Generally the San Sebastián is too impermeable to serve as a source of ground water and acts as a confining bed in most of the area. In the vicinity of San Juan, however, conglomerate and sandstone zones form part of an important aquifer.

LARES LIMESTONE

The Lares gradationally overlies the San Sebastián. It is a thin-bedded limestone at the base, changing upward to a thick-bedded and massive dense limestone. In the center of the belt it is a very pure limestone about 300 m thick; but it thins both eastward and westward and eventually pinches out at the margins of the belt. The age controversy of the San Sebastián applies to the Lares, but most investigators consider it to be of middle and late Oligocene age. The Lares is a poor aquifer where it crops out because of low permeability; however, in the center of the belt where it is overlain by younger rocks it becomes an important aquifer because of high potentiometric head.

CIBAO FORMATION

The Cibao is the most variable formation of the north coast, to the extent that at least two members are recognized: The Montebello Limestone Member and the Quebrada Arenas Member.

Generally the Cibao is an interbedded sequence of marl, chalk, limestone, sand, and clay as much as 230 m thick. In the eastern and western parts of the belt, clastics are predominant. In the middle part, limestones are predominant.

The Cibao Formation acts either as a confining bed or as an aquifer, depending upon the lithology. In the San Juan area, an artesian aquifer capped by clays that are in turn overlain by water-bearing limestones are all part of the Cibao Formation.

The Quebrada Arenas and the Montebello Members are present in the middle of the belt. These members are thick-bedded to massive finely crystalline to granular limestones. The Montebello Member, which is chalky in some places, is among the purest limestones of the north coast. The Montebello Member at depth is an important artesian aquifer in the middle part of the limestone belt.

The Cibao Formation ranges from Oligocene to Miocene in age, or, according to Gordon (1959), is entirely Miocene.

AGUADA LIMESTONE

The Aguada consists of hard thick-bedded to massive calcarenite, locally rubbly to finely crystalline, alternating with beds of clayey limestone. Maximum thickness is about 90 m. The age is early Miocene. Water-bearing properties of the Aguada are considered to range from poor to fair, reflecting differences in lithology.

AYMAMÓN LIMESTONE

The basal part of the Aymamón is a massive to thick-bedded limestone, finely crystalline, about 70 m in thickness. The middle and upper parts are very pure chalky limestone, riddled with solution channels. Total thickness is about 300 m; the age is early Miocene. The basal part of the Aymamón is similar to the Aguada in its water-bearing properties. The middle and upper parts of the limestone are highly permeable.

CAMUY FORMATION

The youngest limestone formation of the north coast belt is areally extensive only west of Arecibo. The lithology of the rock unit varies from a calcarenite to a limestone conglomerate in a clayey matrix. Some parts of the Camuy are quartz sandstone. Maximum thickness is about 200 m. The age is middle Miocene according to most investigators but may be as young as Pliocene according to micropaleontological work by G. A. Seiglie of the University of Puerto Rico, (oral commun., 1969). In general, the Camuy is not an aquifer because it is above the water table.

UNCONSOLIDATED DEPOSITS

BLANKET SANDS

Overlying the limestone formations are the so-called blanket sands. A sandy-silty-clayey mixture, they fill most depressions of the north coast belt surface to an average depth of about 10 m, though an infill of 30 m is not uncommon nearer the coast. There are some debatable points concerning their formation—some workers attribute them to a reworking of marine sediments (Monroe, 1969b); others (Briggs, 1966) favor a fluvial origin. The latter view appears to be more plausible (Williams, 1965) in view of the fact that no fossils have been found in the blanket sands. Briggs believes the blanket sands to be contemporary with arching of the Puerto Rican platform, being therefore the deposits of the first rivers flowing from the newly risen island. These deposits were later augmented by the insoluble residues of solution of the limestone formations (especially the clastic Camuy). The age of the blanket sands would range, therefore, from late Miocene (or Pliocene) to the present. The blanket sands are important as recharge media, but insignificant as aquifers.

QUATERNARY DEPOSITS

The Quaternary deposits of the north coast belt include the alluvium of the river flood plains, a mixture of unconsolidated sand, gravel, and clay ranging in thickness from 0 to about 100 m. Locally the alluvium is a good aquifer. Other Quaternary deposits include the carbonaceous muck in lagoons and swampy areas, some landslide material at the foot of limestone escarpments, cemented sand dunes along the coast, and recent beach deposits. Some of them, especially the cemented sand dunes, provide important clues to the geologic past of the island (Kaye, 1959). Except for the swamps, which mark areas of ground-water discharge, none of these deposits are involved materially in the hydrogeology of the north coast limestone belt. The geologic map of figure 2 shows the most important unconsolidated deposits.

STRUCTURE

The general attitude of the limestone sequence is that of a homocline gently inclined to the north. Figure 3 shows histograms of the angle and azimuths of the dips. In terms of average values the limestone formations dip 5° in a direction N. 0° 47′ E.

A plot of dip angles with latitude is shown in figure 4. Although there is extensive scatter, a relation line can be drawn through the field of points to show a decrease in dip toward the coast. The decrease of dip angles with latitude (northward) reflects the steeper inclination that the limestone belt must have had near the center of the island, at the contact with the volcanic core, when it arched up in Miocene and Pliocene time. This steeper dip of the Tertiary belt in the interior of the island was noted by Briggs (1961), who stated that the dips ranged from about 3° at the Aymamón-Aguada contact to as much as 6° in the older formations. In the same paper, Briggs discusses the thickening of the formations in a seaward direction as shown in an analysis of the rock material drilled by a deep oil test that penetrated the entire Tertiary sequence.

Shurbet and Ewing (1956), on the strength of gravity data and assumed rock densities, inferred a structure for the north coast limestone belt that showed a thickening of rock seaward. Figure 5, a generalized geologic section through longitude 66° 43′, is derived from the relation line of figure 4 and the structural interpretation made by Shurbet and Ewing.

This sample wedge structure contains a few gentle folds such as the one described by Monroe (1962) in the Manatí area. Most of the folds probably reflect structural features of the basement complex and do not inherently affect the overall struc-

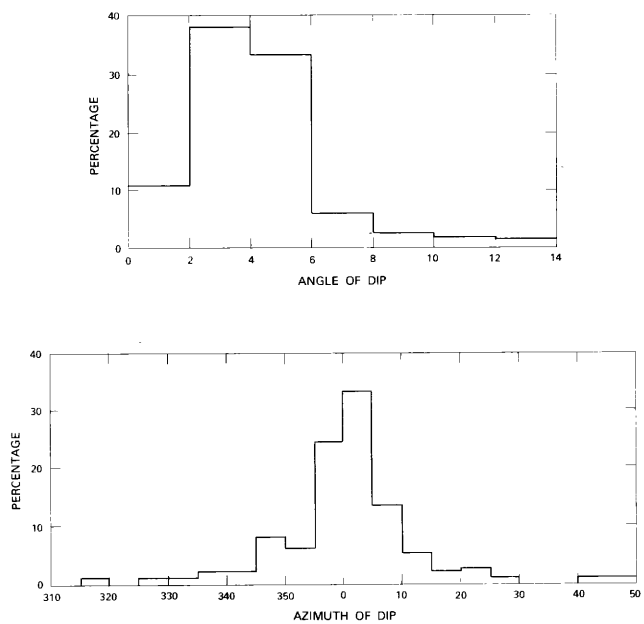

FIGURE 3.—Histograms of north coast limestone dips and orientations.

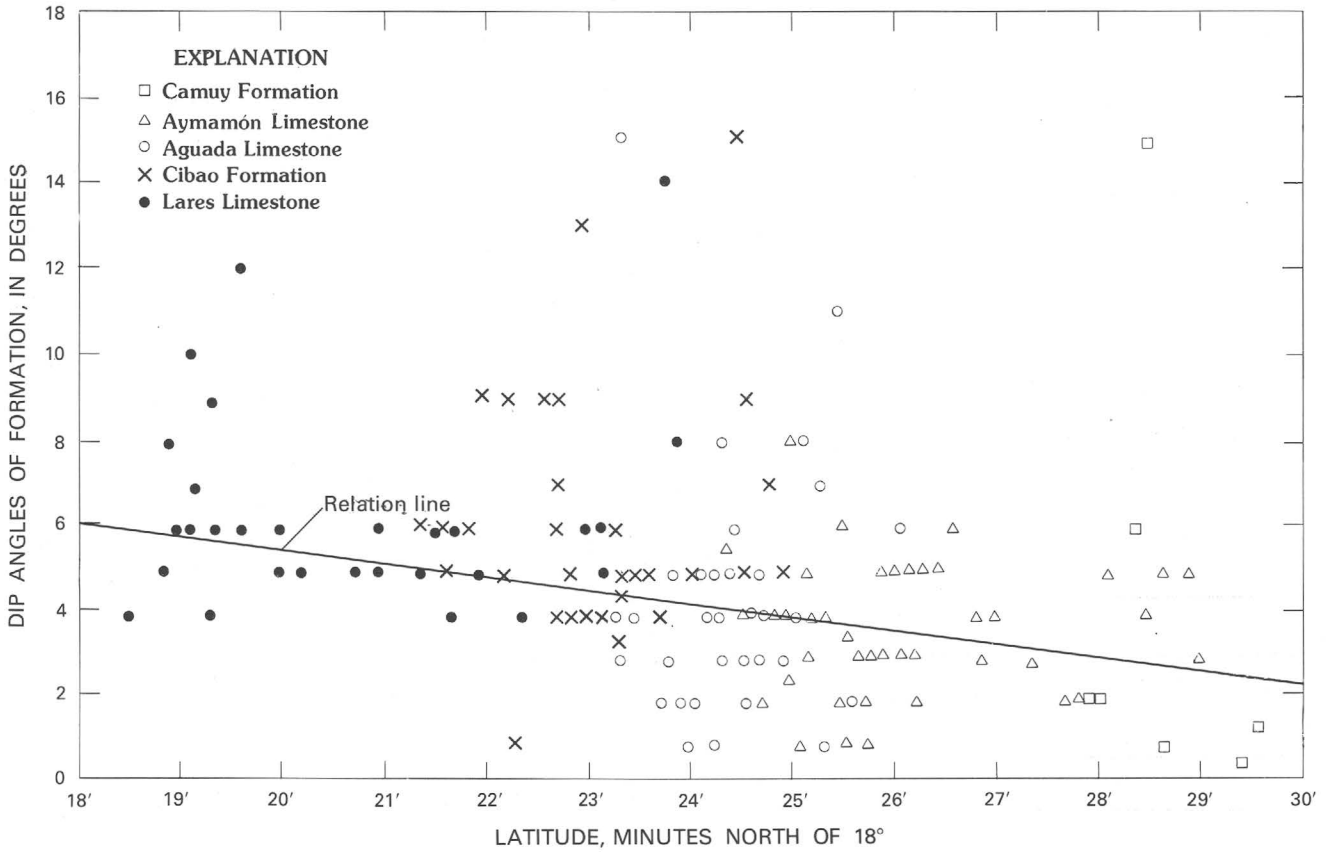

FIGURE 4.—The dip of the limestone decreases in a seaward direction.

tural aspect of the north coast belt. One exception toward the western margin of the belt, southeast of Aguadilla, is a northwest plunging anticline (see fig. 2) accompanied by a few normal faults also alined in a northwest-southeast direction (Monroe, 1969a); possibly there is ongoing tectonic activity related to the Puerto Rican trench and Mona Passage, both known to be seismically active. This anticline and associated faults are probably related to the raised shoreline of the western part of the limestone belt.

Briggs (1961) postulated a major strike fault along the north coast extending from Arecibo east to the Río Cibuco (see fig. 2)—a distance of nearly 40 km.

LANDFORMS—THE KARST

An aerial view of the north coast belt shows the karst as a flat, highly pitted surface lapping against the mountains of the central core (fig. 6). This surface is crossed by two large valleys in the eastern part; westward one can barely discern the sinuous trace of three or four river valleys, not wide enough to provide a clear gap in the flat surface. The terrain, on closer inspection, appears as clusters of hills separated from each other by rounded depressions (fig. 7)—the "lunar landscape" of Monroe (1968b).

A common feature of limestone surfaces is depressions (sinkholes) that drain internally. The areal distribution of sinkholes may be used to draw inferences on the physical-chemical properties of the rocks and on the hydrology of the area. The quantitative map of karst development in figure 8 was prepared from topographic maps by dividing the

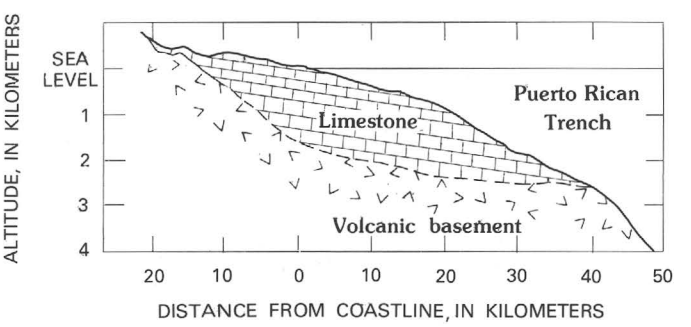

FIGURE 5.—Section of the north coast limestone belt through longitude 66°43′ (adapted from Shurbet and Ewing, 1956).

FIGURE 6.—The karst is a highly pitted surface lapping against the central volcanic core of the island.

FIGURE 7.—Rounded depressions mark the bottom of the karst. Here the depressions have coalesced to form a narrow valley.

region into rectangles of 1-minute longitude by 1-minute latitude, and measuring the percentage of the area of each rectangle falling within closed topographic contours. The topographic maps used were at the scale of 1:20,000 with contour intervals of 5 and 10 m. The maximum karst development (100 percent) as defined by this topograhic method occurs where half of the chosen sample area is covered by closed contoured depressions and half by hills separating them. A close correlation between geologic properties of the formations and degree of karst development is indicated. (Compare figs. 2 and 8.)

Some degree of karstification has taken place on all the limestones with the exception of the predominantly clastic San Sebastián Formation. In the far western part of the area the Lares Limestone has a normal fluvial development of streams that drain southward to the Río Culebrinas. Eastward, however, the Lares Limestone has developed slight to moderate karstification. The Cibao Formation shows but slight karst development in the eastern and western parts of the area, where it is predominantly clastic (figs. 9 and 10). In the center of the north coast belt, however, where the Cibao Formation is a pure limestone (Montebello Limestone Member), an extensive karst has developed. Karstification increases northward in the overlying Aguada Limestone and reaches its maximum development in the southern outcrop area of the Aymamón Limestone;

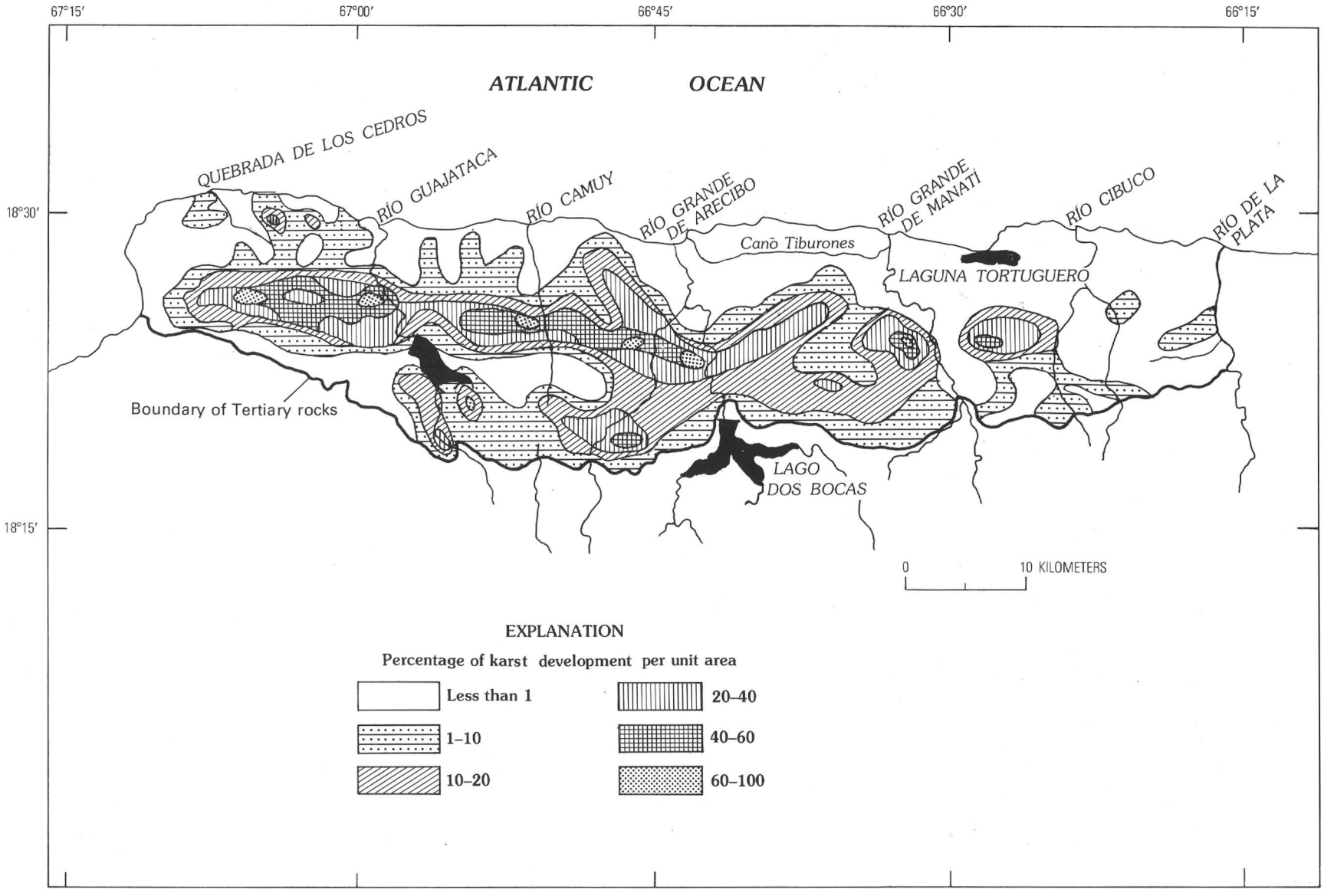

FIGURE 8.—Karst development of the north coast limestone belt.

FIGURE 9.—The Cibao topography is one of rolling hills—no karst. Aguada karst in background.

it then decreases seaward. The small degree of karstification in the northwestern part of the belt reflects a youthful stage of incipient karst development. The equal lack of karstification in the northeastern part of the belt reflects the opposite—a mature to old stage which marks the final dissolution phase.

Monroe (1966, 1968b) believes that the formation of the Puerto Rican karst is the result of limestone solution and reprecipitation, with the karst morphology depending on the lithology and structure of the limestones. He describes the surface of the limestone hills as a pitted hardened shell, a few meters thick at most, covering a soft interior. This feature can be seen in most roadcuts. The hard shell, as well as the asymmetry of the hills (mogotes), which show a flatter gradient on the eastern side, is explained in terms of the preferential soaking of the eastern side by rain, wind, driven from the east, and in terms of reprecipitation of calcium carbonate supersaturated overland flow near the foot of the hills. The flat areas of land between mogotes are, in Monroe's view, where the limestone is actively being dissolved at the contact beneath the cover of the blanket sands. Organic acids, which are associated with the dense vegetation growing on the limestones and washed down into the blanket sand-covered depressions, greatly increase the solubility of the limestones. The influence of the lithology and structure on the different landforms of the karst is related to the purity of the limestones and to their bedding thickness. Thus, areas in warm and humid climates underlain by massive pure limestone can develop into cockpit karst (Kegelkarst) marked by subconical hills separated by steep-walled valleys. Mogotes, typified by subconical hills rising out of a blanket-sand covered plain are found on the pure somewhat chalky Aymamón Limestone. Zanjones, or trenchlike elongated depressions somewhat parallel to each other, have developed where limestone is thin bedded and brittle. Caves and natural bridges have formed in areas of alternating beds of hard and soft limestone.

FIGURE 10.—Rolling topography of the Quebrada Arenas Limestone Member of the Cibao Formation.

In this report, the mogote karst is regarded as a phase of the karst development, being somewhat the equivalent of the monadnocks of the Piedmont region of the eastern continental United States, representing the last geomorphic expression prior to complete obliteration of land relief. From the classical geomorphic approach of stage development, the northwestern area of the north coast limestone represents the youthful stage: it is marked by a plateaulike surface slightly pitted with shallow closed depressions. The next or mature stage is represented by the rugged cockpit karst found throughout the Aguada Limestone and lower part of the Aymamón Limestone in the middle of the belt, and in patches on the Lares Limestone. The next phase, or old stage, would be the mogote karst. It, in turn, would further degrade to a fluvial drainage developed on blanket sands, evidence of which appears in the eastern part of the north coast belt. These stages, of course, allow for local features caused by lithologic and structural differences; however, in general, attributing morphology to the purity and thickness of limestone is not sufficient to explain the landform development other than in a restricted area.

The mogote karst may once have been a cockpit karst; the cockpit may develop into mogote karst in due time—just as the plateaulike northwestern part of the belt will mature into a cockpit area eventually. Figure 11 illustrates the relation between karst development and topographic altitude; this figure was constructed from the results of the analysis of percent karst development that were utilized in constructing figure 8. The horizontal axes in figure 11 represent karst development in percent, as previously defined, and topographic relief in meters. Frequency of occurrence, shown on the vertical axis, represents the number of 1-minute map rectangles at a given average altitude which exhibit a given percent of karst development. The maximum development of the karst—the cockpit karst—is in areas where the relief ranges from about 80 to 120 m. Beyond this range of relief the author interprets figure 11 to imply that the karst

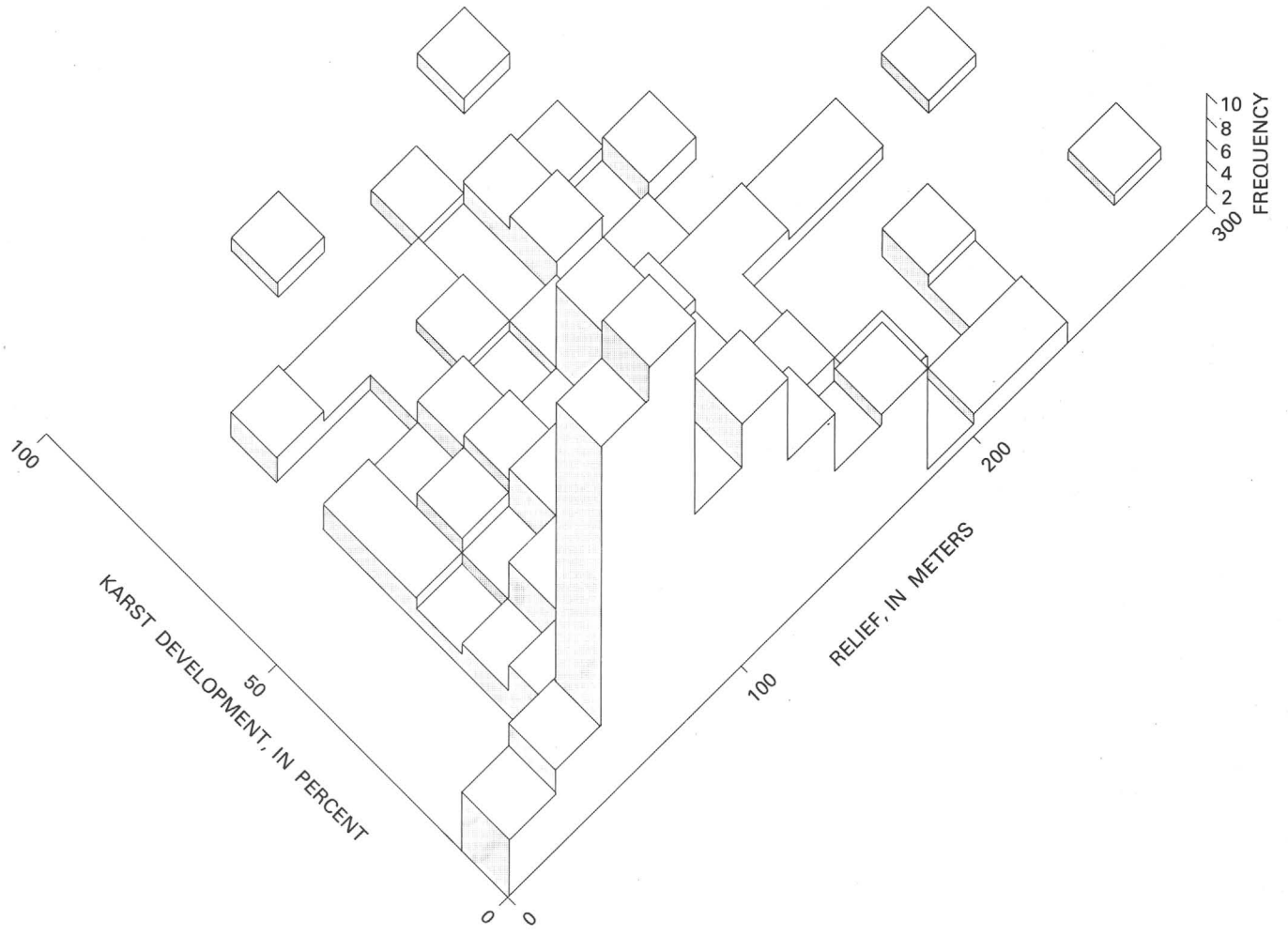

FIGURE 11.—Distribution surface of karst areas.

decreases by collapse of underground caves or surfaces erosion and that the stream courses begin to develop.

STREAM NETWORK

The limestone belt is traversed by six rivers whose headwaters are found in the volcanic terrane to the south. Figure 12 shows the stream network developed on the north coast limestone, the major springs, and the altitude contours of land surface. (The stream network is shown in more detail in pl. 1.) The contours represent the mean altitude above sea level of each 1-minute square of the limestone belt. The mean altitudes were computed by dividing each 1-minute square into 25 grid points, and averaging the altitude of these points as taken from a topographic map. The average direction (azimuth) of the topographic slope is about N. 5° E. compared with a geologic dip direction essentially due north. The major rivers generally cross the belt in a direction west of north (Williams, 1965, p. 160–182).

In the general area southeast of Lago de Guajataca (fig. 13) the alinement of the sinkholes area is peculiarly in a northwesterly direction. The portion of Río Guajataca shown in the southwestern corner of the map of figure 13 was probably formed by the collapse of a series of these northwesterly oriented sinkholes. There is an indication that this preferential alinement is related to the drainage patterns of the original fluvial system that formed at the time of emergence of the Puerto Rican platform from the sea.

Whatever major tributaries there are enter the rivers from the west within the limestone belt. The short segments of streams shown about the middle of figure 12 reflect the fluvial development formed on top of the Cibao Formation; and it should be noted that even these short segments tend to orient themselves so that they would, if

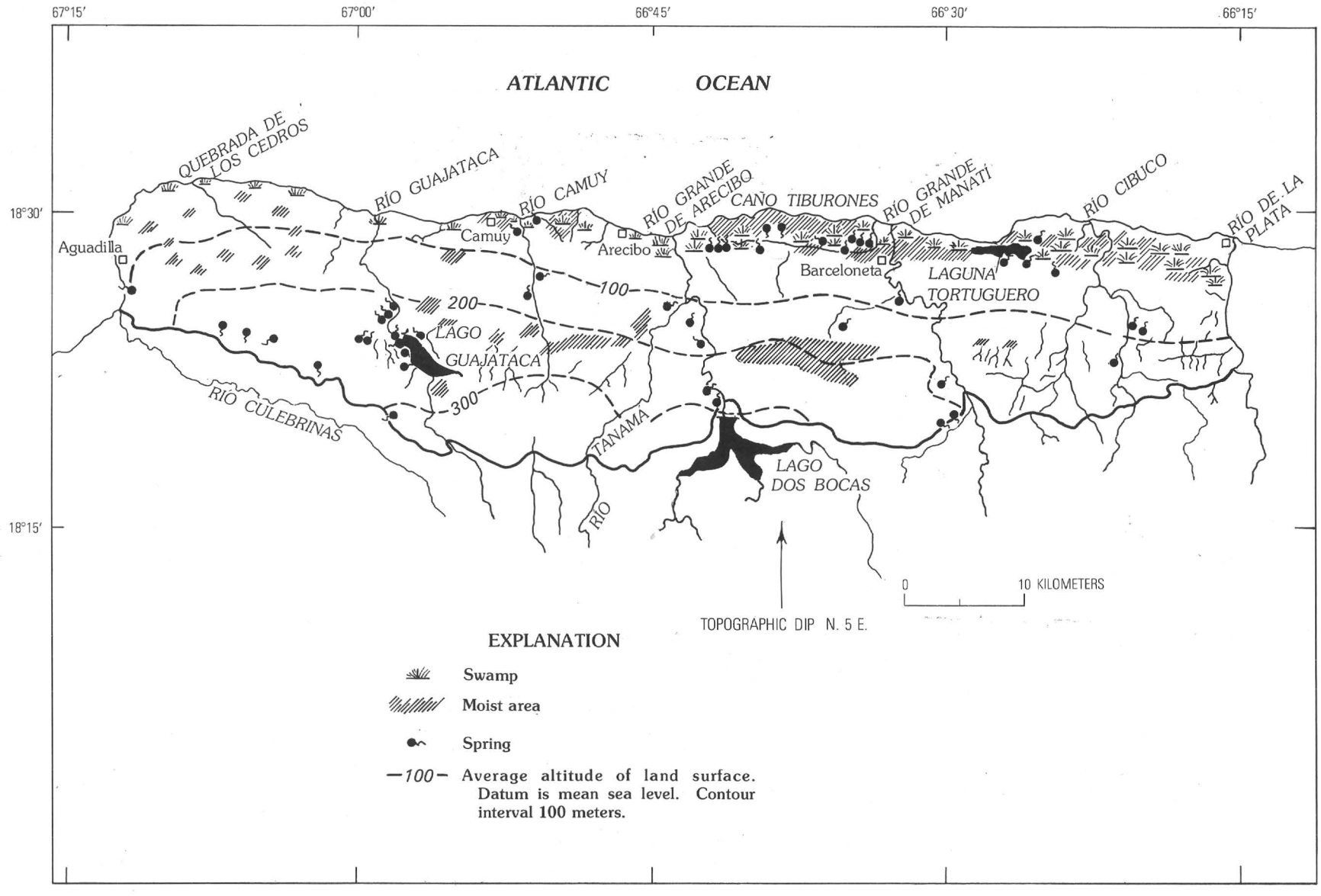

FIGURE 12.—Average altitude of land surface, stream network, and major springs of the limestone belt.

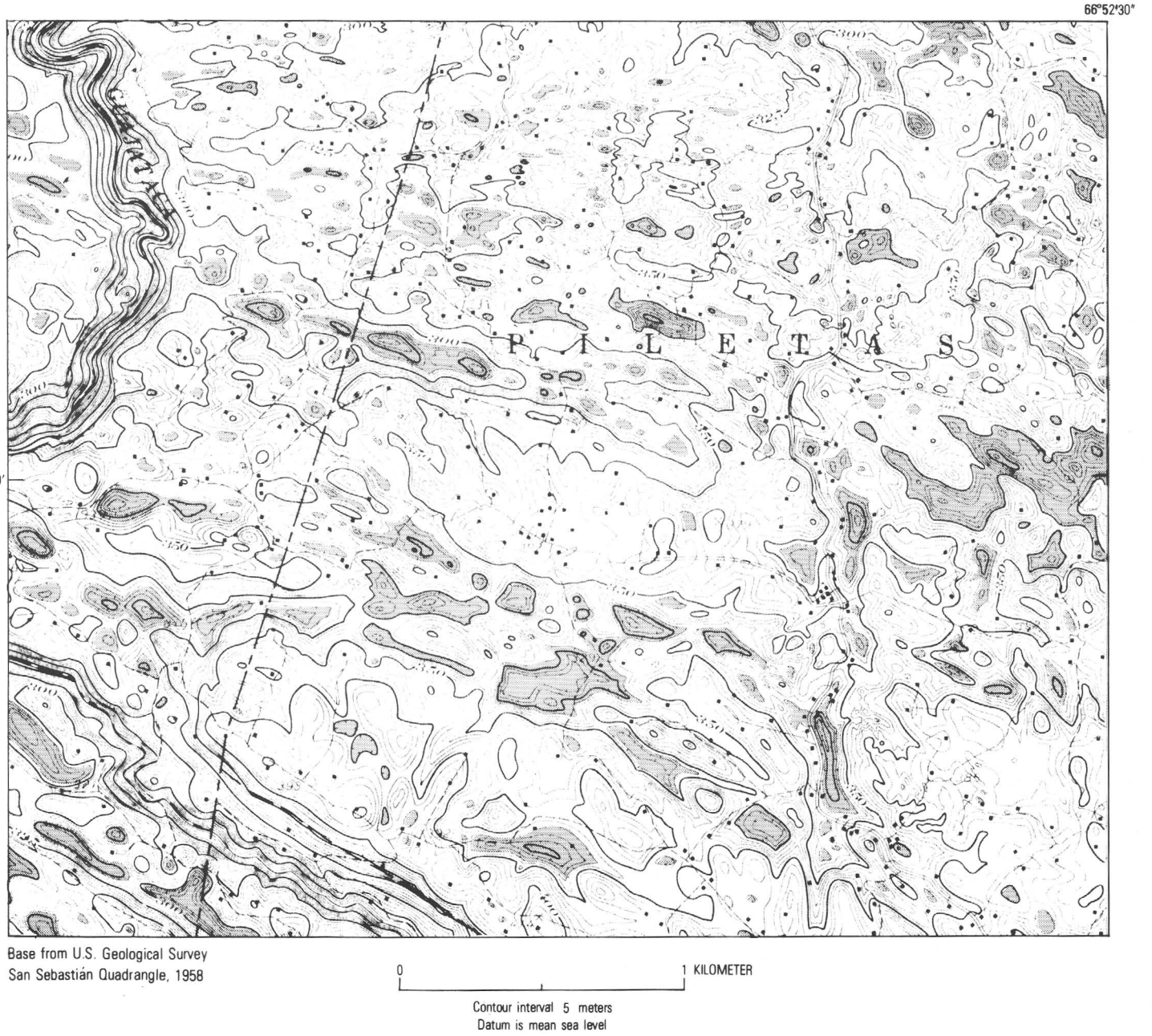

FIGURE 13.—Northwest-southeast alinement of the sinkholes in the Lares Limestone southeast of Lago de Guajataca.

linearly extended, enter the main rivers from the west. This preferential alinement could not develop on a lithologically uniform surface dipping gently northward. The main reason for the anomaly is to be found in the eastward tilt of the entire Puerto Rican platform. This tilt, which was argued for by Lobeck (1933) and Meyerhoff (1933) on the basis of the raised coastline found along the western margin of the north coast, is thought to have occurred sometime during the Pleistocene. Monroe

(1968a) found terraces at altitudes of 40 to 70 m on top of the raised limestone platform in the west, which he dates from the Pleistocene, though he favors eustatic rather than tectonic movements to explain the existence of the raised beach deposits.

Most of the rivers flow in normal valleys open to the sky, but both the Río Camuy and the Río Tanamá flow underground for some stretches. The Río Camuy disappears underground soon after entering the limestone and emerges at a straight-line distance of about 6 km downstream. The surface where the Río Camuy flows underground is marked by "lines of steep-walled collapsed sinks" (Monroe, 1968b). The Río Camuy flows through the lower part of a series of caves lying at different levels; they have been only partly explored (Gurnee, R. H., and others, 1966). The Río Tanamá flows underground at different points, for distances of less than a kilometer. Its course can readily be interpolated between its points of disappearances and reappearances. Clearly, at least parts of these river courses have formed through the collapse of caves or sinkholes.

Another river, the Río Guajataca, shows evidence of collapsed caves, the floor of its canyon being strewn in places with a chaotic rubble of collapsed blocks of limestone. In fact, at places the arch of former caves can be easily reconstructed (fig. 14). The Río Guajataca is probably an example of the next stage of development that follows that of the Río Tanamá; a canyon has been opened to the sky, but except for some isolated inland reaches and a short interval near the coast, there has been no development of a proper channel with river banks and a flood plain. The development of a proper channel, which is usually concurrent with the development of meandering, marks the approach to the equilibrium stage described by Mackin (1948). In the north coast belt, the equilibrium stage is achieved by the Río Grande de Manatí (fig. 15), Río Grande de Arecibo (fig. 16), and the Río Cibuco.

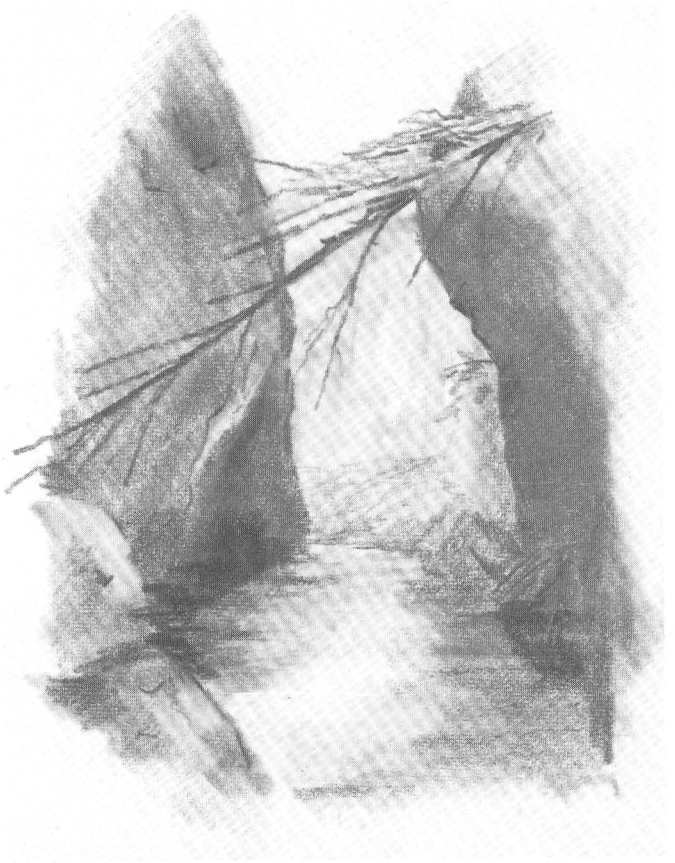

FIGURE 14.—Former cave of the Río Guajataca.

DRAINAGE AREAS

The computation of water balances of river basins required the quantitative assessment of rainfall, evaporation, and streamflow as well as the determination of storage changes; thus the area of the drainage basins were needed.

It became apparent early in the study that drainage divides in the karst areas could not be unequivocally determined from the available maps. Because the divides about many sinkholes occurred at the same altitude, it was not known whether a given sinkhole area was to be assigned to one river basin or to another. Two criteria were used to obtain at least a first estimate of interbasin boundaries and thus of drainage areas:

1. Any sinkhole was assumed to drain to the neighboring sinkhole of lowest altitude.
2. Where neighboring sinkholes lay at the same altitude the preferential path was chosen according to the general orientation of stream courses. An example of the application of these criteria is shown on a portion of a topographic map in figure 17.

A number of indeterminate drainage areas that did not seem to belong to any stream basin were found; their probable drainage pattern is discussed later with the streamflow data. The results of the water-balance computation were themselves used to evaluate the reliability of the computed drainage areas. An error made in the drainage area evaluation, therefore, would have affected the results of the water-balance computations.

FIGURE 15.—The Río Grande de Manatí exhibits a well developed flood plain.

OTHER LANDFORMS

The limestone terminates abruptly near the coast west of Arecibo (figs. 18 and 19) in sea cliffs, or is separated from the sea by a narrow strip of beach (Kaye, 1959). East of Arecibo large swampy areas have formed, the Caño Tiburones between the Río Grande de Manatí and the Río Grande de Arecibo, and Laguna Tortuguero between the Río Grande de Manatí and the Río Cibuco are prominent features of this swampy terrain, and are notable for the large amounts of nearly freshwater they discharge. The alinement of these areas of freshwater outflow was taken by Briggs (1961) as suggesting, though he qualified the evidence as circumstantial, the presence of a large strike fault (discussed in the chapter on structure). Stringfield (written commun., 1971) interpreted these swamps as drowned karst features that formed during a low stand of the Pleistocene sea. Other landforms found in a narrow belt north of the swampy areas, along the coast, and even drowned offshore, are sea cliffs and cemented sand dunes; these are described by Kaye (1959).

CLIMATE

The climate of northern Puerto Rico is humid tropical (Picó, 1950). As an aid to numerical comparison, climate can be conveniently represented as a function of rainfall and evaporation only; the latter integrating the effects of solar radiation, wind, and temperature. In terms of the climatic index of Thornthwaite (1931), northern Puerto Rico has an index of about 90 (Giusti and Lopez, 1967), which correlates with the meteorologically based description of humid, or, on the basis of vegetation pattern, with the forest province. Thus, the north coast belt is climatically consonant with the popular image of Puerto Rico.

RAINFALL, TEMPERATURE, AND WIND

The average annual rainfall on the north coast limestones is 1,800 mm (millimeters), and rainfall

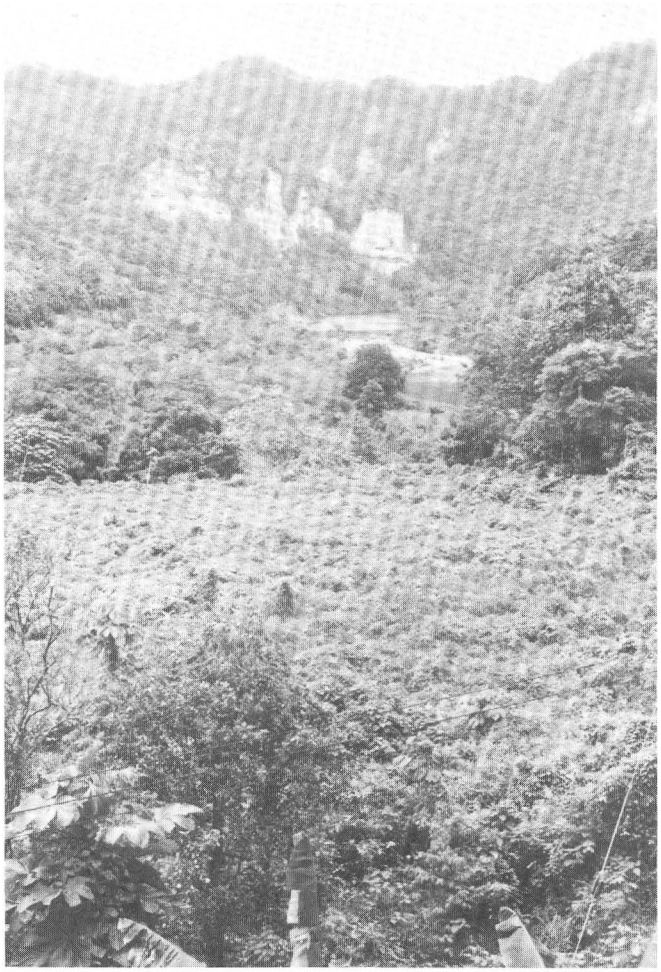

FIGURE 16.—The flood plain (foreground) of the Río Grande de Arecibo begins where the river emerges from the canyon.

ranges from 1,550 mm on the coast to 2,300 mm inland in the areas where the limestones are in contact with the mountains of the central core. To the extent that rainfall in Puerto Rico increases rapidly with altitude, the small range of rainfall found on the north coast belt reflects the slight differences of relief. The variability within the year follows an islandwide trend: a generally dry period that begins in December and usually ends in March or April, a spring rainfall period in April and May, an erratic, semidry period in June-July, and a wet season from August through November. Greatest monthly rainfall is in September. The hurricane season is from June through October and in any 1 year can produce a very wet June or July.

The average annual air temperature is 24° C on the north coast belt and varies but a few degrees from winter to summer.

Puerto Rico lies in the path of the easterly trade winds which are almost constantly blowing across the island. Data published by Briscoe (1966) indicate that the winds vary from month to month and that there is a yearly average ranging from 16 km/h (kilometers per hour) at Cabezas de San Juan on the east coast to 5 km/h at Gurabo in the interior. In general, there are more constant and stronger winds in the coastal areas than in the interior areas. Differential heating between the sea and land also produces an onshore breeze during the day and an offshore breeze at night.

EVAPOTRANSPIRATION

Evapotranspiration is a major factor in the water balance of the north coast limestone region. Unfortunately, field data on evapotranspiration are sparse; for this reason it is desirable to establish a relation between evapotranspiration and a more readily available hydrologic parameter. Because reasonably good rainfall records are available for the karst region, an analysis was made to relate evapotranspiration to precipitation. Before presenting the results of this analysis, certain theoretical concepts will be reviewed, with the aim of showing that a relationship between evapotranspiration and precipitation can be accepted with reasonable confidence.

Potential evapotranspiration represents the maximum possible rate of evapotranspiration from an area—that is, the rate which is observed under a full plant cover, when an unlimited supply of water is available for evapotranspiration. Actual evapotranspiration depends upon the available water supply, and is generally much less than potential evapotranspiration. Potential evapotranspiration is a function of such factors as solar radiation and the moisture content of the atmosphere. Actual evapotranspiration also depends upon these factors, but depends as well upon the available water and the plant cover. In the limiting case of a desert area, potential evapotranspiration is very high, whereas actual evapotranspiration is low because of the lack of available water. In more humid areas potential evapotranspiration is lower because of reduced solar radiation and increased humidity, while actual evapotranspiration is higher. In permanently wet areas, such as a rain forest, the theory of Bouchet (1963), verified by the work of Morton (1965) and Solomon (1967), predicts that potential evapotranspiration and actual evapotranspiration should approach the same value, equal to one-half the absorbed solar radiation as expressed in millimeters

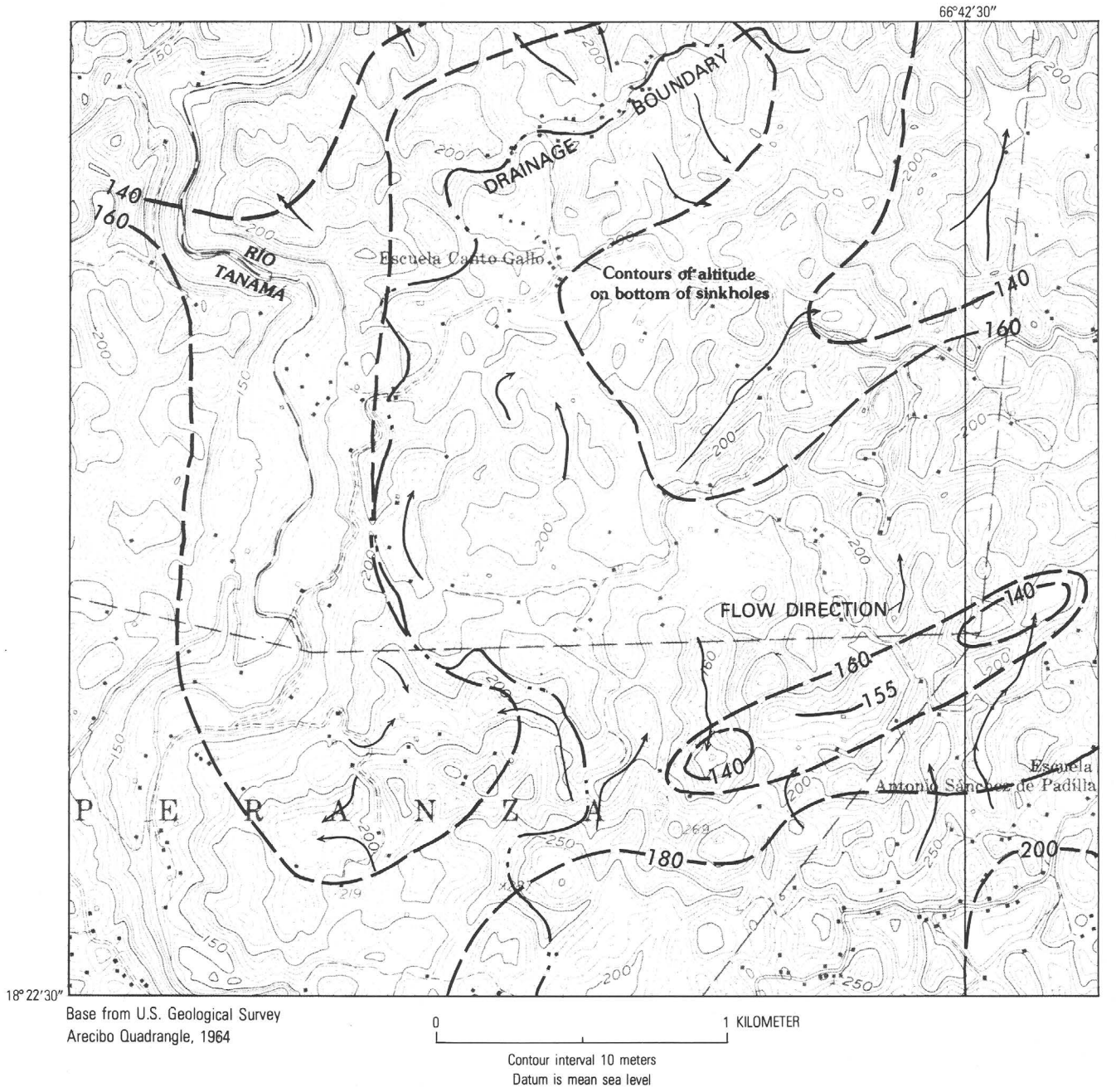

FIGURE 17.—Example of criteria used to delineate drainage boundaries in karst terrane. The dashed lines are contours of the altitude on the bottom of the sinkholes.

of evaporated water. Thus potential values should decrease with increasing precipitation, while actual values should increase with increasing precipitation, until the two become approximately equal for the limiting case of a very humid region.

As a first step in developing a relation between evapotranspiration and precipitation, an analysis was made of the relation between solar radiation and precipitation in the north coast area. The basic assumption was that a relation between evapotranspiration and precipitation would follow from an underlying relation between solar radiation and precipitation. This approach also provided a means of estimating solar radiation in areas (or over periods) for which direct data were lacking.

The theoretical annual extraterrestrial solar

FIGURE 18.—Coastline west of Arecibo. Raised shoreline in the distance.

radiation—that is the radiation at the upper limit of the atmosphere—is equivalent to 5,000 mm of evaporated water per year, at the latitude of Puerto Rico (Smithsonian Meteorological Tables, 1966). This very high total is distributed monthly as shown in figure 20. Figure 21 shows a plot of the ratio Rg/Ra versus precipitation, where Rg is the observed annual incoming radiation, and Ra is the theoretical annual extraterrestrial radiation, 5,000 mm of water per year. The observed radiation values are based upon a few years of record (M. Capiel, oral commun., 1970) and averages (Briscoe, 1966) of total incoming solar radiation. For values of rainfall between 500 and 2,500 mm, the line whose equation is

$$\frac{Rg}{Ra} = (0.73 - 0.00009P) \qquad (1)$$

where

P = rainfall, in millimeters

provides a fair fit to the data. For an average Ra of 5,000 mm for the island

$$Rg = 3{,}650 - 0.45P. \qquad (2)$$

FIGURE 19.—Sea caves on Aymamón Limestone cliffs, west of Arecibo.

The equation of Glover and MacCullock, as given by Roche (1963), may be used to show the relation indicated in figure 21, and equation 2 gives results which fall within reasonable limits. Their equation is

$$\frac{Rg}{Ra} = 0.29\cos\lambda + 0.52\frac{n}{N} \qquad (3)$$

where

Rg and Ra are as previously defined, and
λ = latitude in degrees,
n = number of observed hours of insolation, and
N = number of maximum possible hour of insolation.

To obtain an upper limit for Rg/Ra, the fraction n/N may be set equal to 1.0, approximating a condition of zero rainfall—that is, maximum insolation; to obtain a lower limit, n/N may be set equal to zero, corresponding to a condition of no days of sunshine. For the latitude of Puerto Rico, taking n/N as 1.0 gives a maximum value for Rg/Ra of

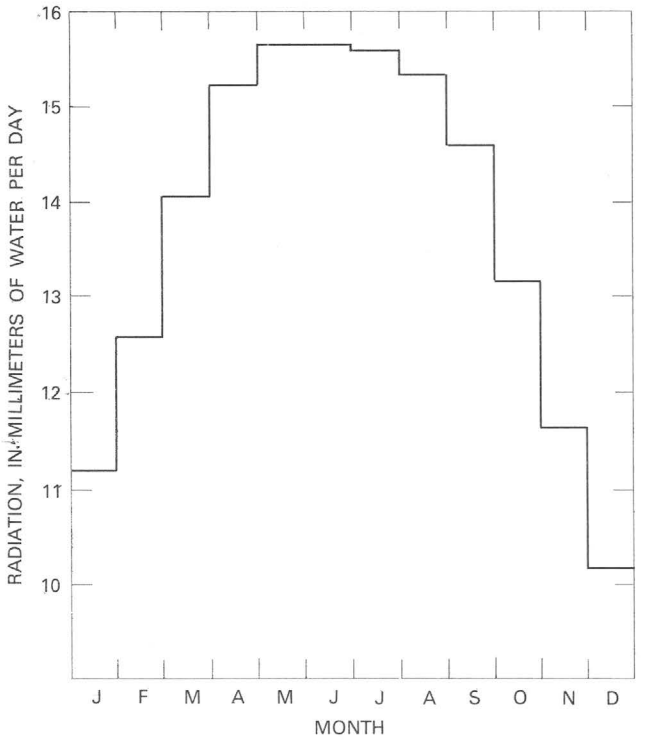

FIGURE 20.—Mid-monthly theoretical solar radiation in equivalent evaporated water for Puerto Rico.

about 0.8. This would presumably correspond to a condition of zero rainfall. The equation of Glover and MacCullock gives 0.28 as a minimum value of Rg/Ra; however, because of the very low probability of occurrence of a year with no days of sunshine, a value of 0.35 is probably a more realistic lower limit for Rg/Ra, corresponding to a year of very high precipitation. Examination of figure 21 shows that these limiting values bracket the field data very reasonably.

Bouchet (1963) gives the equation

$$Ep+ET=(1-a)Rg \qquad (4)$$

Where Ep represents potential evapotranspiration; ET is actual evapotranspiration; Rg, as before, is solar radiation (expressed as equivalent evaporated water); and a is the albedo of the region. The term $(1-a)Rg$ represents the absorbed solar radiation. Equation 4 is applicable provided the underlying assumption of the theory, that there is no net exchange of energy between the region and its surrounding areas, is satisfied. Where such border exchanges (termed "oasis effects" in the theory) do occur, deviations can be expected.

In terms of equation 4, the limiting conditions referred to previously may be expressed as follows:

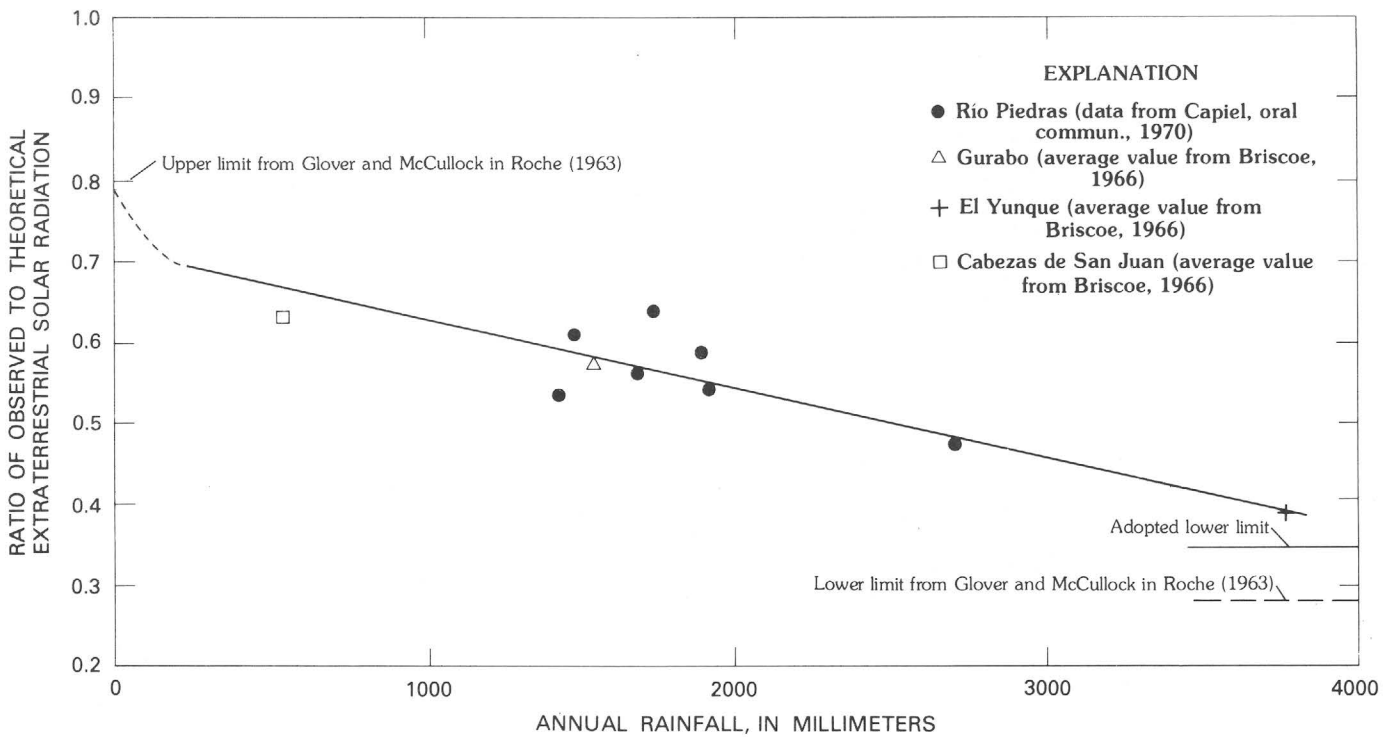

FIGURE 21.—Variation of fractional radiation (ratio of observed to theoretical solar radiation) with rainfall, annual values.

for rainless regions,

$$ET = 0 \text{ and } Ep = (1-a)\ Rg \quad (5)$$

for permanently wet regions,

$$ET = Ep = 0.5(1-a)Rg \quad (6)$$

Thus the ratio $Ep/((1-a)Rg)$ decreases from a maximum of 1.0 at no precipitation to a minimum of 0.5 at very high values of precipitation; while the ratio $ET/((1-a)Rg)$ increases from a minimum of zero at no precipitation to a maximum of 0.5 at very high values of precipitation.

Figure 22 shows a plot of the ratios $E/((1-a)Rg)$ and $ET/((1-a)Rg)$ versus precipitation, where E represents pan evaporation and ET represents regional evapotranspiration as determined by local water budget calculations. The values of Rg used in forming these ratios were taken from figure 21. Pan evaporation, E, may be taken here as an approximate measure of potential evapotranspiration, Ep. The estimates of actual evapotranspiration were made by considering closed basins in various parts of Puerto Rico for which net inflow and outflow of ground water could reasonably be considered zero, over periods for which the storage change was zero, and computing the difference between precipitation and stream discharge.

The relations shown in figure 22 conform closely to the behavior predicted by Bouchet's theory. Although there is scatter due to data errors and due to border ("oasis") effects near the coast, the limiting conditions established by the theory are clearly satisfied.

In figure 23, values of annual pan evaporation

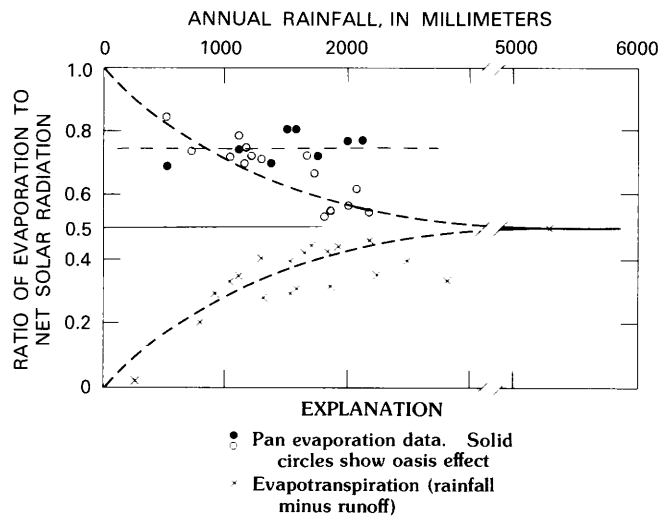

FIGURE 22.—Evaporation to net solar radiation ratio as a function of rainfall in Puerto Rico.

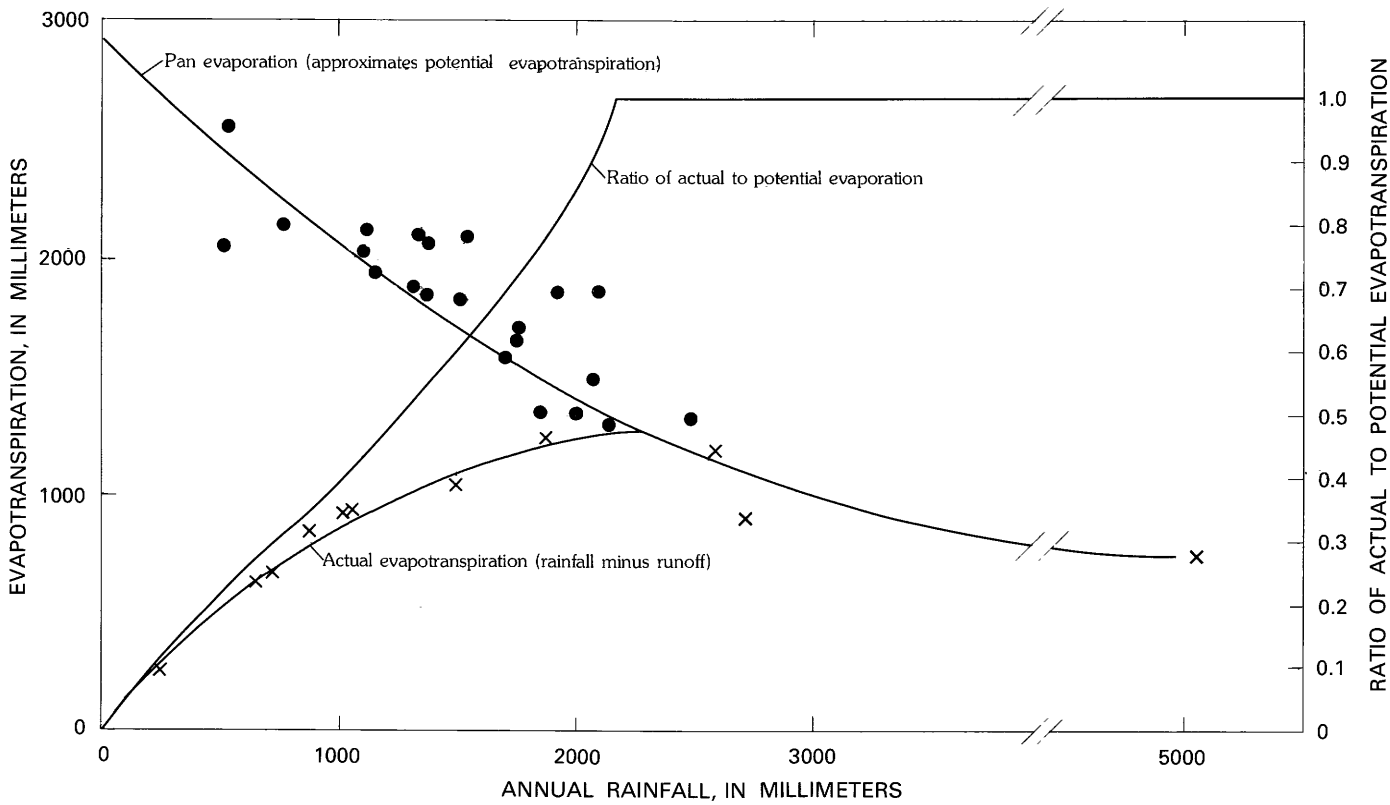

FIGURE 23.—Potential and actual evaporation and their ratio as a function of rainfall.

and evapotranspiration, and values of the ratio of evapotranspiration to pan evaporation, are plotted as functions of annual precipitation. From this graph, the average evapotranspiration from the north coast limestone area, corresponding to the average annual rainfall of 1,800 mm, appears to be about 1,150 mm. Taking pan evaporation as roughly equivalent to potential evapotranspiration, the corresponding average value of ET/Ep is about 0.76. However, it should be noted that this is an average value; the actual value of the ratio depends upon precipitation. The relationship shown in figure 23 was utilized in a water-budget analysis for the limestone area to compute actual evapotranspiration from pan evaporation and precipitation data; this is described in a later section of the report.

HYDROLOGY

The decision at the beginning of this investigation was that the most practical approach to the study of the area would be to obtain a water balance of the entire limestone belt. This goal required assessment of all inflows and outflows; therefore, 10 stream inflows from the volcanic terrane were gaged continuously where they entered the limestone belt, and 12 stream outflow points from the limestone were gaged as far downstream as possible. The difference between the discharge of the upstream and downstream sites constitutes the contribution to streamflow from the limestone area. Rainfall and pan evaporation (potential evaporation) were obtained from the available data published by the National Weather Service, supplemented by data from a few temporary sites to fill some gaps in the areal distribution of the existing meteorological network. Rainfall and pan evaporation data were collected at 25 and 5 sites respectively. About 40 wells were used to gather information on the water-table configuration.

GROUND WATER

WATER-TABLE LEVELS

A contour map of the water-table surface is shown on plate 1. River-bed altitudes were used as control points in constructing this map. In the pattern of ground-water flow suggested by these contours, recharge in the topographically high areas moves radially outward toward the streams and the coast. The streams, the swampy features along the coast, and to some extent the sea floor itself thus all function as drains for the ground-water system. Within the most seaward part of the Aymamón Limestone, the altitude of the water table is just above mean sea level, with an average slope of about 0.0007, reflecting the high permeability of the Aymamón in this area. Southward the gradient steepens to about 0.045 within a transition zone which varies locally, but that in general includes the less permeable lower part of the Aymamón and Aguada Limestone. The gradient flattens again to about 0.003 within the Cibao Formation and the Lares Limestone, possibly indicating higher permeability or a smaller component of lateral ground-water movement.

ARTESIAN ZONES

Until July 1968, the known aquifers in the area were under water-table conditions, although conditions of local confinement had apparently been encountered occasionally by well drillers. No large-yield flowing well had ever been drilled in the north coast limestone belt; however, no well deeper than about 250 m had ever been drilled in the area. In July 1968, a disposal well was drilled in the Cruce Dávila area of Barceloneta. To obtain permission to use the well for disposal of certain industrial effluents, the law required that the well reach salty water. Therefore, the well was drilled deeper than any other water well in Puerto Rico. At a depth of about 350 m below the surface the well penetrated a "crumbly limestone layer" from which water flowed at a rate of 160 L/s (liters per second) with about 7 kg/cm^2 (kilograms per square centimeter)/ of shut in pressure at the land surface. The water was fresh.

The artesian zone occurs within the Montebello Limestone Member of the Cibao Formation which, in the outcrop area, is a very pure chalky limestone. The driller's report indicates that a massive limestone layer was penetrated above the crumbly limestone of the artesian aquifer, while W. H. Monroe (written commun., 1970) reports several meters of clay above the artesian zone. Both types of material undoubtedly contribute to the confinement of the Montebello artesian zone.

A second artesian zone was found at a depth of about 500 m, in the Lares Limestone. Since 1968 several more deep wells have been drilled in the same vicinity; all have penetrated the upper artesian zone and some the lower zone. A first approximation to an average potentiometric surface for the artesian zones is shown in cross section $C-C'$ of plate 2. This surface was constructed by linear interpolation between an average water-table altitude in the

Cibao-Lares outcrop area, and an average static head in the artesian wells at Cruce Dávila.

Drilling in the Tortuguero area in 1972 confirmed the existence of a very limited artesian zone in the Cibao in that area, together with a thick and well-defined artesian zone in the Lares. However, only in the east-central part of the limestone belt, between Río Grande de Arecibo and Río Cibuco, has it been proved that ground water flows under water-table conditions within the Aymamón and possibly the Aguada Limestones, and under artesian head within the Montebello Member of the Cibao Formation and the Lares Limestone. Elsewhere there is only indirect evidence to indicate probable paths of flow.

PERMEABILITY DISTRIBUTION AND GROUND-WATER FLOW

To compute the ground-water flow requires a knowledge of the permeability of the aquifer, as well as information on the head gradient and the cross-sectional area of the flow. These factors are utilized in Darcy's Law to compute the rate of ground-water flow, under the assumption that the flow approximates uniform movement through a porous medium when considered on a regional scale. Because of the possibility that in limestone the flow may be concentrated locally in "pipes" or along bedding planes or through fractures, Darcy's Law may not be applicable in a local sense. However, at the scale of regional flow it is assumed that the networks of solution pipes, fractures, and bedding planes are interconnected and spaced so as to approximate flow through a porous medium. The degree to which results from the application of Darcy's Law agree with the water-budget evaluation will give an indication of the reasonableness of these assumptions.

Estimates of permeability for the water-producing intervals of the rocks were obtained using specific capacity data from all wells in the north-coast limestone area for which information on lithology and well construction was available. The method of estimation was based on Thiem's equation for steady-state radial flow to a pumping well, and thus again involved the assumption that Darcy's Law was applicable in a general sense over the area of influence of the well. The equation used was

$$K = 37\frac{Q}{SM}\log\frac{re}{rw} \qquad (7)$$

where

K = permeability, in centimeters per second;
Q = well discharge, in cubic meters per second;
S = drawdown, in meters;
M = screened or open intervals of the well, in meters;
re = the radius of a plan view of the cone of depression, in meters, taken arbitrarily as 150 meters in all cases; and
rw = radius of casing, in meters.

The error involved in using an assumed radius of influence is probably small. Because the term re/rw appears in the logarithm, an error in K of only 100 percent is introduced when re is in error by 1,000 percent.

The permeability values computed in this way ranged from less than 10^{-4} cm/s (centimeter per second) to about 1 cm/s. The estimated average permeability south of Caño Tiburones is shown in figure 24. An estimate of the ground-water flow through the area south of Caño Tiburones can be made substituting the values for permeabilities from figure 24 and the gradients from plate 2 in the equation for Darcy's Law. For 1-kilometer width of aquifer:

$$Q = 10\,K\,I\,t \qquad (8)$$

where

Q = discharge, in cubic meters per second;
K = permeability, in centimeters per second;
I = head gradient, dimensionless; and
t = thickness of aquifer, in meters.

For the Aymamón and Aguada Limestones, the head gradient was taken as the water-table gradient; for the Cibao and Lares formations, the gradient was taken as the difference between the average water-table altitude in the Cibao-Lares outcrop area and the average artesian level in the wells at Cruce Dávila, divided by the distance of flow. The discharges for the various aquifers are as follows:

Aymamón
$Q = 10 \times 0.2 \times 0.00095 \times 60 = 0.11$ m³/s

Aguada
$Q = 10 \times 0.02 \times 0.00095 \times 100 = 0.02$ m³/s

Cibao (Montebello Limestone Member)
$Q = 10 \times 0.005 \times 0.0021 \times 180 = 0.02$ m³/s

Lares
$Q = 10 \times 0.0002 \times 0.0021 \times 75 = 0.0003$ m³/s

The flow through the entire limestone section south of Caño Tiburones, calculated using a width of 15 km (derived from the flow pattern shown on plate 1), amounts to about 2.3 m³/s or 0.15 m³/s per kilometer width.

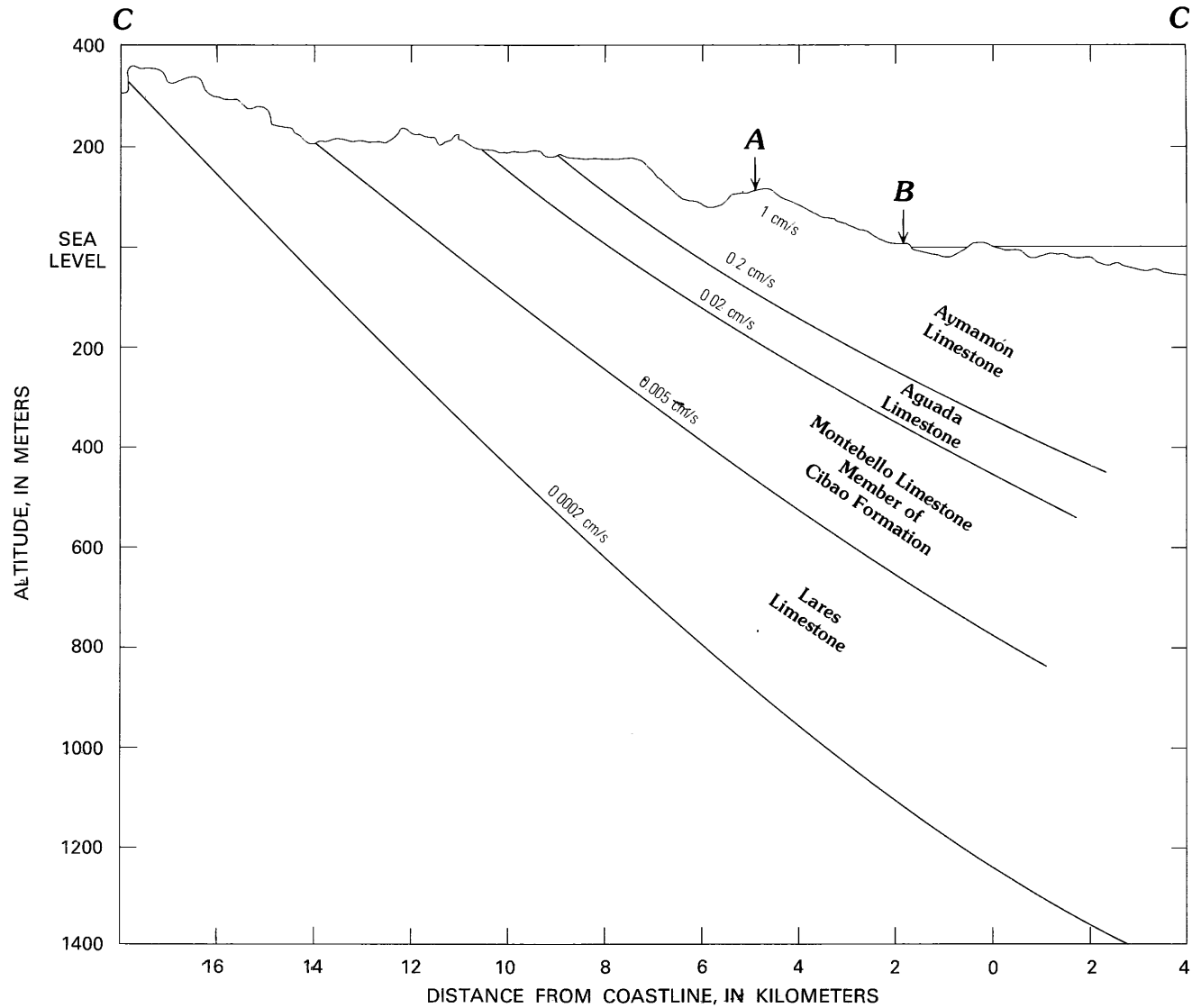

FIGURE 24.—Average permeability distribution within cross section *C–C'* through the Caño Tiburones area between points A and B. See plate 1 for location of cross section.

Similar calculations carried out for various sections shown on plate 2 are summarized in table 1. The results for the sections through the Río Cibuco basin, Laguna Tortuguero, Caño Tiburones, and the Río Camuy basin are more reliable than the results for the sections through the Río Guajataca basin and through the westernmost part of the belt, which were based on data projected from sections to the east. These results will be compared later in this report with the budget results computed from streamflow and meteorological data.

The data in figure 24 clearly show a permeability decrease from a high in the Aymamón to a low in the Lares. A plot showing all the computed permeabilities as a function of stratigraphic depth, measured from the projected top of the Aymamón Limestone, is shown in figure 25. The plot is semilogarithmic, and the average straight line indicates an exponential decrease in permeability with stratigraphic depth. However, this relationship refers only to the permeability of the aquifer intervals and should not be inferred to mean a continuous change of permeability with depth. Low permeability layers —that is, aquitards (for which no permeability calculations were made)—are found intermixed with the more permeable zones. The permeability of the massive limestone found on top of the artesian aquifers south of Caño Tiburones is orders of magnitude lower than that of either the overlying or the underlying layers.

TABLE 1.—*Ground-water flow of the north coast limestones*
[Sections are shown on plate 2]

Formation	Thickness (meters)	Slope	Permeability (cm./s)	Discharge (m^3/s per km width)
Vega Alta-La Plata				
Aymamón Limestone	60	0.00076	0.1	0.046
Aguada Limestone	75	.00076 ?	.02	.011
Cibao Limestone	150	.0028 ?	.002	.008
Lares Limestone	130	.0028 ?	.0005	.002
Total	---	------	-----	.067 = .80 for 12 km
Manatí-Tortuguero				
Aymamón Limestone	90	0.00057	0.1	0.0510
Aguada Limestone	60	.00057 ?	.005	.0020
Cibao Limestone	170	.0028	.0005	.0024
Lares Limestone	110	.0028 ?	.0002	.0006
Total	---	------	-----	.0560= .67 per 12 km
Arecibo-Barceloneta				
Aymamón Limestone	60	0.00095	0.2	0.1140
Aguada Limestone	100	.00095 ?	.02	.0190
Cibao Formation	180	.0021	.005	.0190
Lares Limestone	75	.0021	.0002	.0003
Total	---	------	-----	.1523=2.28 for 15 km
Camuy-Arecibo				
Aymamón Limestone	60	0.001	0.05	0.0300
Aguada Limestone	90	.001	.002	.0018
Cibao Limestone	170	.003 ?	.001	.0051
Lares Limestone	300	.003 ?	.0002	.0018
Total	---	------	-----	.0387= .43 for 11 km
Guajataca-Camuy				
Aymamón Limestone	60	0.001 ?	0.02	0.0120
Aguada Limestone	90	.001 ?	.002	.0018
Cibao Limestone	200	.003 ?	.0005 ?	.0030
Lares Limestone	300	.003 ?	.0002 ?	.0018
Total	---	------	-----	.0186= .20 for 11 km
Aguadilla-Guajataca				
Aymamón Limestone	60	0.001 ?	.02 ?	.0120
Aguada Limestone	90	.001 ?	.002 ?	.0018
Cibao Limestone	200	.001 ?	.0005 ?	.0010
Total	---	------	-----	.0148= .25 for 17 km

NOTE: Total for entire belt = 4.6 m^3/s.

GROUND-WATER FLOW PATTERNS

The caves found in the karst of the north coast belt are almost invariably tunnellike and develop from limestone solution along bedding planes. As a result, the regional ground-water flow lines tend to follow the bedding of the limestone layers down dip, presumably along preferential paths of higher permeability.

ARTESIAN FLOW PATTERNS

In the section through the Caño Tiburones area in figure 26, three possible patterns of ground-water outflow from the artesian zones are illustrated. The simplest pattern is direct discharge to sea in a submarine outflow area; it is illustrated by the arrows in the lower right corner of figure 26. In such submarine outflow, the ground water must discharge against the static head exerted by the column of seawater above the outflow area. This head can be measured in terms of an equivalent freshwater potentiometric head, defined as the height above sea level to which freshwater would rise in a piezometer inserted to the seabed. This equivalent freshwater head increases seaward as the depth of saltwater increases. The solid line above the sea surface in figure 26 shows the trend of the equivalent freshwater head.

The potentiometric head of the artesian zones beneath the sea can presumably be found by extending the artesian-head gradients measured on land. Extensions of the potentiometric head of the artesian aquifers seaward in this manner involves the assumptions that there are no changes in permeability within the artesian zones and that there is no gradual loss of flow from these zones by upward leakage. If these assumptions are satisfied, the

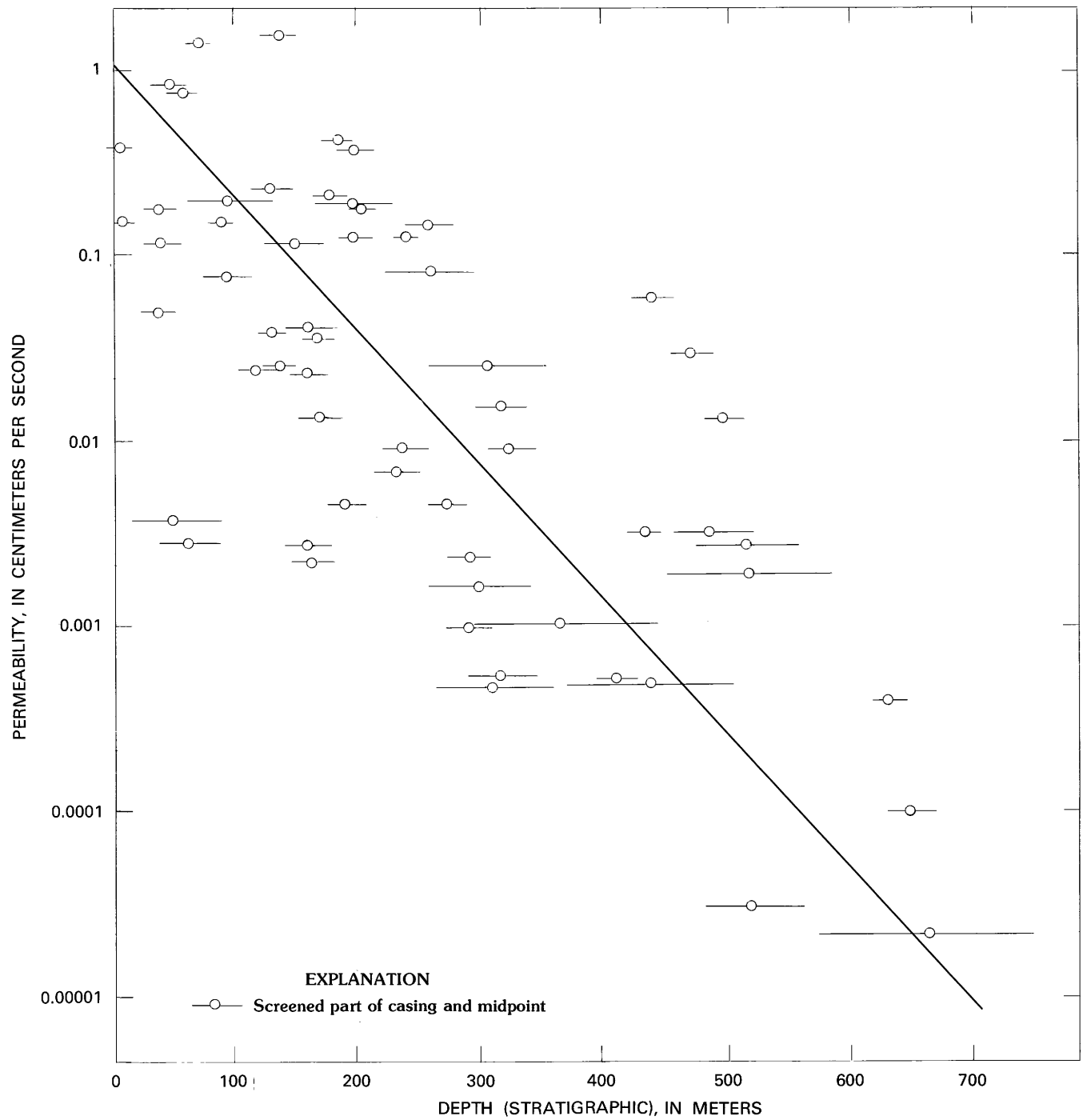

FIGURE 25.—Variability of permeability with stratigraphic depth from projected top of Aymamón Limestone.

upper dashed line in figure 26 is obtained as an average potentiometric surface for the Cibao and Lares systems. Discharge at a submarine area requires that the artesian head in the aquifer balance the equivalent freshwater head of the column of sea water above the discharge area. In figure 26, this condition is indicated by the intersection of the dashed line representing artesian head with the solid line representing equivalent freshwater head at the sea floor. This intersection occurs approximately 30 kilometers offshore; this is in reasonable agreement with locations of the submarine outcrops of the artesian zones, as obtained by extrapolation of the dip seaward. However, the extrap-

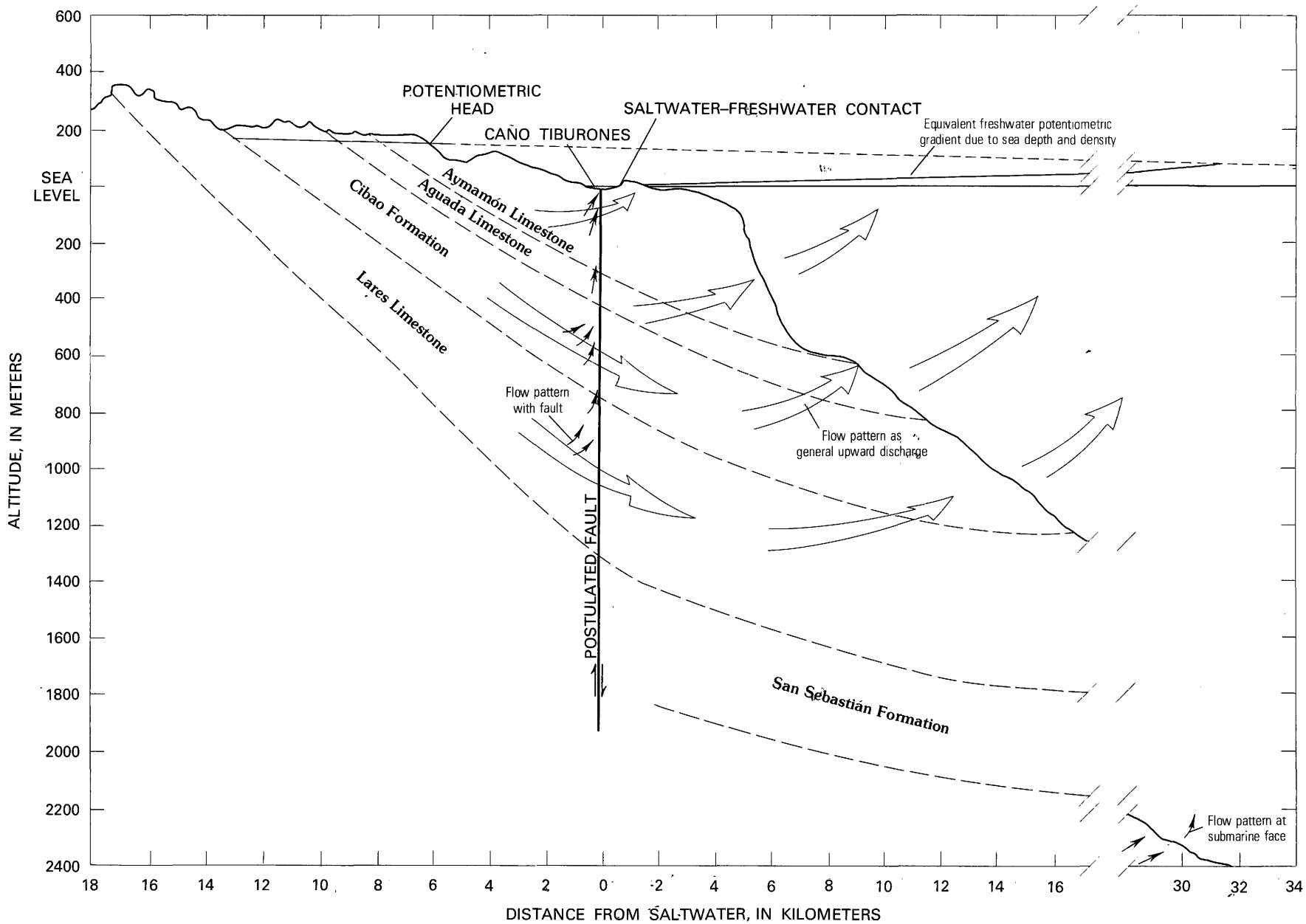

FIGURE 26.—Possible patterns of ground-water flow in Caño Tiburones area.

olation of head gradients and geologic dips for tens of kilometers is questionable, and this agreement may be no more than fortuitous.

A second possible pattern of ground-water discharge is shown by the large arrows in figure 26. If the permeability of the artesian zones decreases seaward, the head gradient in the aquifer cannot be linear, and the above extrapolation of heads would not be valid. Rather, the loss in head per kilometer would increase seaward, and the artesian head would be dissipated much closer to shore than 30 km. If a permeability decrease were gradual with distance and with the stratigraphic depth, the result would probably be a widespread upward discharge of ground water through the confining beds (large arrows of figure 26). Some of this upward seepage would probably escape through the sea floor and some through discharge areas on land.

A third possible pattern of discharge is related to the faulting postulated by Briggs (1961) in the Caño Tiburones area. Such faulting would presumably have thrown rock of low permeability against the artesian zones, and the barrier so created would block or impede flow seaward and force discharge upward. It is possible that fracturing associated with the postulated faulting could have produced a zone of high vertical permeability along the fault trace, creating conditions favorable to vertical outflow. The pattern of ground-water flow that might result from these conditions is shown by the small solid arrows in figure 26.

WATER-TABLE FLOW PATTERNS

Throughout the limestone area, but particularly east of Arecibo, ground water under water-table conditions discharges through springs and by areal seepage, either directly to sea or to the swampy areas along the coast. These swampy areas discharge, in turn, by evapotranspiration or by surface drainage to the sea.

A two-dimensional steady-state electric analog analysis of conditions south of Laguna Tortuguero was made by G. D. Bennett (Bennett and Giusti, 1972). The results of this analysis are shown in figure 27. The model, made of conducting paper of fixed resistance, was designed to simulate the water-table aquifer with a vertical to horizontal ratio of permeability of 1 to 10. The results of measuring the electric current at the boundaries, equivalent to measuring the ground-water flow, indicated that 75 percent of the outflow takes place inland from the coast and is disposed of through Laguna Tortuguero's direct outflow to sea, and by evapotranspiration from swampy areas, while 25 percent of the outflow takes place along the sea bottom in a zone a few hundred meters wide. Conditions in the Río Cibuco basin can be expected to be very similar to those in the Tortuguero area. Original conditions in the Caño Tiburones area were probably also similar. At the present time, however, agricultural drainage within the Caño Tiburones has lowered the water table several feet, so that all ground-water flow toward the coast enters the Caño Tiburones itself and discharges either by evapotranspiration or into drains, from which it is pumped to the sea. The water table in the northern part of the Caño Tiburones has in fact been lowered below sea level, inducing a substantial inflow of sea water, which makes up roughly one-third of the total pumpage from the drain system of the Caño.

West of Arecibo the conditions of ground-water outflow in the water-table zone are more speculative. From water-budget data to be presented later, it appears that the Río Tanamá, Camuy, and Guajataca act as highly efficient ground-water drains, and therefore only a small part of the regional flow from the areas between these rivers can be expected to discharge to coastal swampy areas or through the sea bottom.

The coastline west of Arecibo is formed by cliffs that rise several meters above the sea. No springs were noticed issuing from these cliffs. A few ponds and swampy areas occur at the foot of the sea cliffs, but these are the only evidence of ground-water outflow inland from the coast. No large freshwater springs are known to occur at sea with the exception of one unverified report about such an offshore spring near the town of Camuy. The evidence points to ground-water outflow mainly as the base flow of streams.

The pattern of ground-water outflow in the westernmost part of the limestone belt, between Río Guajataca and the west coast, remains unknown. In the southernmost part of this region, the outcrop area of the Lares is drained southward by streams tributary to Río Culebrinas (fig. 12). The Cibao Formation in this area is a nearly impermeable clayey marl.

In the northern part of this area west of the Guajataca, the karst is well developed in the Augada and lower part of the Aymamón. The younger Camuy Formation crops out on a flat surface of youthful stage karst. The estimate of ground-water outflow to the north, given in table 1, is much larger than the estimated maximum evapotranspiration outflow from swampy areas at the foot of the sea

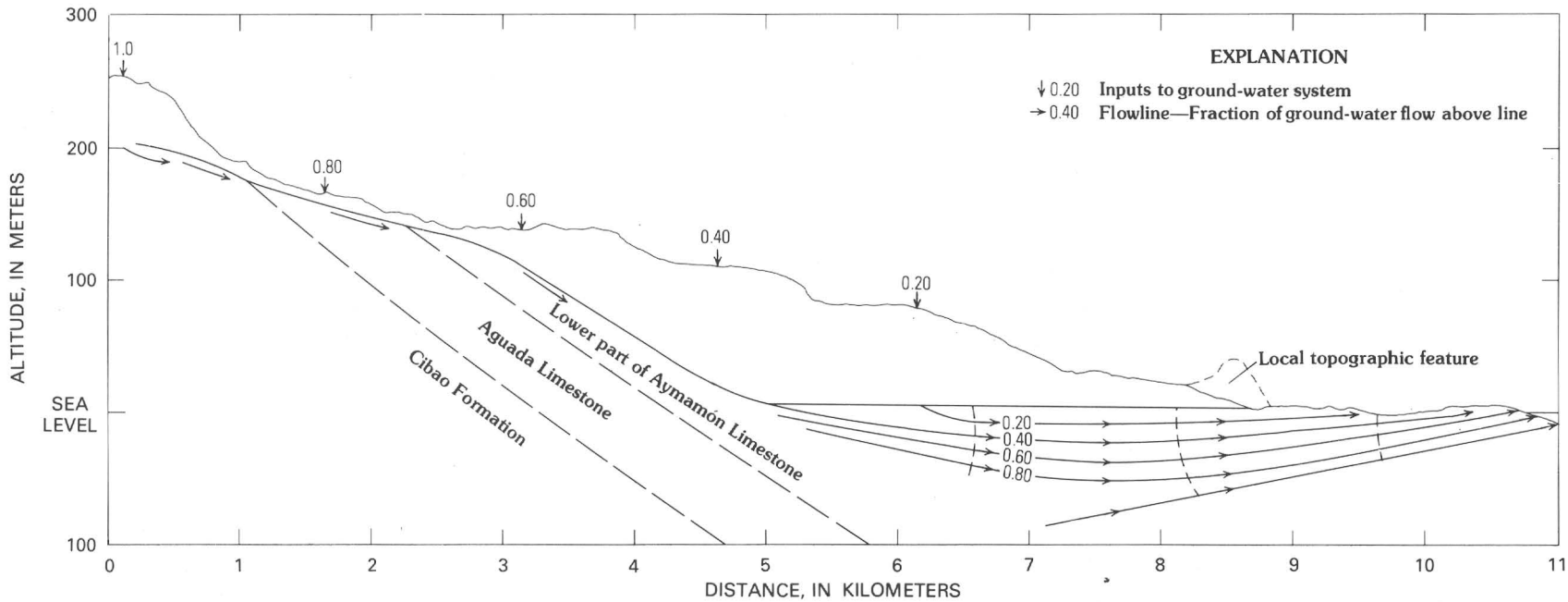

FIGURE 27.—Ground-water flow pattern in the Tortuguero area (Bennett and Giusti, 1972).

cliffs. Quebrada de los Cedros, the only stream in the area, is normally dry. Thus the most reasonable explanation at this time is that the ground-water outflow from the northwestern corner of the limestone belt is mainly through the sea bottom.

SPRINGS

There are thousands of springs within the limestone area. Those springs of large yield which were found in the field are located on the map of figure 12. The springs discharging near the coast rise through the blanket sands or swamp deposits, and give rise to Caño Tiburones (figs. 28 and 29) and to Laguna Tortuguero. Springs contributing water to rivers issue from cliffs (figs. 30 and 31) or emerge through the alluvium. A few springs (fig. 32) flow only after heavy rains; during droughts they stand as nearly circular pools of water marking the surface of the water table.

In regions where horizontal strata are cut by a river, one would normally expect to find an equal

FIGURE 29.—Large spring at the south end of Caño Tiburones.

FIGURE 28.—Small spring (cancora) in the Caño Tiburones area. Hundreds of such springs flow upward through the muck of this former lagoon.

FIGURE 30.—Salto Collazo Spring, from the Lares Limestone, discharges southward to the Río Culebrinas drainage system.

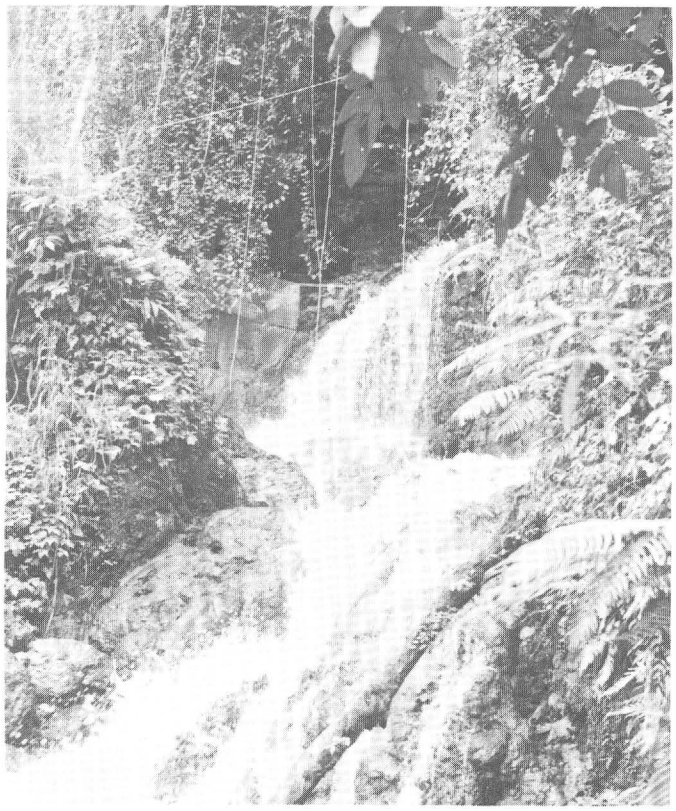

FIGURE 31.—Spring El Chorro to Río Grande de Arecibo—note travertine deposits in lower right.

FIGURE 32.—Spring in flood plain of Río Grande de Arecibo. This spring flows only after heavy rains.

number of springs on both sides of the river valley. Instead, springs along the rivers in the north coast limestone occur mainly on the west sides of the river valleys. Their position suggests that the eastward tilt of the Puerto Rican platform has affected the pattern of drainage of ground water.

STREAMFLOW AND WATER BUDGET

To test whether the results of water-budget calculations would yield important clues to the groundwater movement in the north coast limestones, data were collected for a period of approximately a year and a half on streamflow, rainfall, and pan evaporation in the limestone drainage basins. For those streams draining both volcanic and limestone terranes, the streamflow was recorded both where the streams entered the limestone belt and at their mouths; by difference, therefore, the contribution from the limestone part of the basin could be assessed. The data shown in table 2 cover selected drainage basins for 1 year of record—the period between November 1969 and October 1970. This choice of period reflects the most reliable data; the streamflow at the beginning and at the end of this period was nearly equal.

In table 2, the drainage basins are grouped geologically into those draining volcanic terrane and those draining limestone terrane. Measurement sites are indicated by number and by the name of the gaged stream, and are located on the map of plate 1. The numbers in column 1 are the rainfall in millimeters over the basin, as obtained from Thiessen averaging. Column 2 lists the evapotranspiration, computed by multiplying a Thiessen averaged pan evaporation (shown in column 6) by the ratio of evapotranspiration to pan evaporation; this ratio was taken from figure 23, as a function of precipitation. More properly, the ratio between evapotranspiration and pan evaporation should have been treated as a constant for the permanently moist parts of the basins, such as flood plain, swamp, or lake areas, and as a function of precipitation, according to Bouchet's theory, elsewhere in the basin. However, the quantity and quality of the available data did not appear to warrant this refinement, particularly as the period of record was about 20 percent wetter than normal (2,200 versus 1,800 mm).

The stream discharge per unit drainage area is listed in column 3. For those streams that drain volcanic terrane there is no reason to assume that the topographically derived drainage areas (column 5) may be in error; therefore, anomalies in the figures for streamflow per unit area cannot be ascribed to errors in drainage area. Not so, however, for the streamflow per unit area from limestone basins; for those streams there is an inherent difficulty in

TABLE 2.—*Water-budget results of the north coast limestone belt for the period November 1969–October 1970*

	Streamflow site	(1) Rainfall P, mm	(2) ET, mm	(3) Discharge Q, mm	(4) $\pm\Delta S$, mm	(5) Drainage area, km²	(6) Pan evaporation, mm
	Basins in volcanic terrane						
1	Upper Camuy	2,210	1,240	960	0	19.7	1,370
2	Criminales	2,210	1,240	1,120	−140	11.7	1,370
3	Arecibo below Lago	2,360	1,200	1,090	+70	438	1,320
4	Upper Tanamá	2,230	1,240	920	+70	47.8	1,370
5	Upper Manatí	2,540	1,140	1,270	+130	330	1,320
6	Upper Cibuco	2,360	1,200	1,040	+120	39.0	1,370
7	Mavilla	2,440	1,170	1,730	−460	24.6	1,370
8	Unibón	2,230	1,240	1,200	−210	13.7	1,370
9	Cialitos	2,310	1,220	960	+130	44.0	1,370
10	Upper Guajataca	2,210	1,240	860	+110	8.3	1,400
	Basins in limestone terrane [1]						
11	Guajataca to Lago	2,230	1,240	760	+230	79.0	1,800
12	Guajataca to mouth	2,030	1,220	560	+250	76.6	1,650
13	Lower Camuy	2,110	1,240	840	+30	170	1,520
14	Lower Tanamá	2,080	1,240	560	+280	103	1,500
15	Lower Arecibo	1,860	1,200	15	+650	76	1,570
16	Lower Manatí	1,860	1,200	860	−200	174	1,320
17	Lower Cibuco	2,030	1,220	890	−80	170	1,500
18	Lajas	2,080	1,220	1,090	−230	21.8	1,370
19	Quebrada de los Cedros	1,730	1,170	25	+530	37.8	1,800
20	South Canals	1,320	1,040	51	+220	53.4	1,800
21	Caño Tiburones	1,320	1,040	2,110	−1,830	46.3	1,800
22	Laguna Tortuguero	1,730	1,170	510	+50	43.5	1,570

[1] For basins that begin in volcanic terrane, discharge is the difference between total downstream flow minus upstream flow. Other data refer to limestone portion of basin only. Location of sites, including those in volcanic terrane, is shown on plate 1.

computing drainage areas for the basins. The drainage areas shown in column 5 for the limestone basins represent a first estimate, to be tested for hydrologic reasonableness as shown later.

The term $\pm\Delta S$ of column 4 is simply the residual from the budget equation:

$$\pm\Delta S = P - ET - Q \qquad (9)$$

where P represents precipitation, ET is evapotranspiration, and Q is stream discharge per unit area. Assuming that ground-water inflow and outflow from the basin are negligible. ΔS represents the change in water storage per unit area in the basin; a plus sign indicates that water was taken into storage, while a minus sign indicates that water was released from storage.

A plot of the streamflow per unit area versus the difference between the rainfall and the estimated evapotranspiration is shown in figure 33. The deviations of the points from the 45-degree line indicate change in storage, ground-water inflow or outflow across the borders of the basin, or data error. Most of the points fall within a band ±20 percent of the 45-degree line. One basin in volcanic terrane plots slightly over +30 percent. There are, however, four basins in the limestone terrane that deviate excessively from the 45-degree line, and their deviation must be explained. The basin numbered 21 is Caño Tiburones. Its discharge per unit area was computed from a drainage area of 47 km²; from plate 1, this represents the immediate surface drainage area as interpreted from the topographic divides. It should be remarked that the actual outflow from Caño Tiburones is a mixture of freshwater and seawater. The discharge shown in table 2 represents only the freshwater portion, calculated on the basis of a chemical rating table. Clearly this freshwater discharge of Caño Tiburones cannot be accounted for by a drainage area of 47 km²; thus the discharge must include a large proportion of ground-water flow from the area to the south (pl. 1), which has no apparent drainage to the sea. This area includes extensive outcrop areas of the Aymamón and Aguada Limestones, and smaller outcrop areas of the Cibao Formation and Lares Limestone. (The flow into Caño Tiburones may also include a small amount of leakage from the artesian zones of the Cibao and Lares; this would represent ground-water inflow even in terms of the extended drainage area.) A new calculation of streamflow per unit area was therefore made for the Caño Tiburones, in which the previously unassigned drainage area to the south was included (refer to pl. 1 for drainage area boundaries). Rainfall and evapotranspiration were taken equal to those of the lower Arecibo basin. It can be seen from figure 33 that, with the new drainage area, Caño Tiburones plots within the main scatter field, thus indicating that the newly assumed drainage boundaries are generally correct.

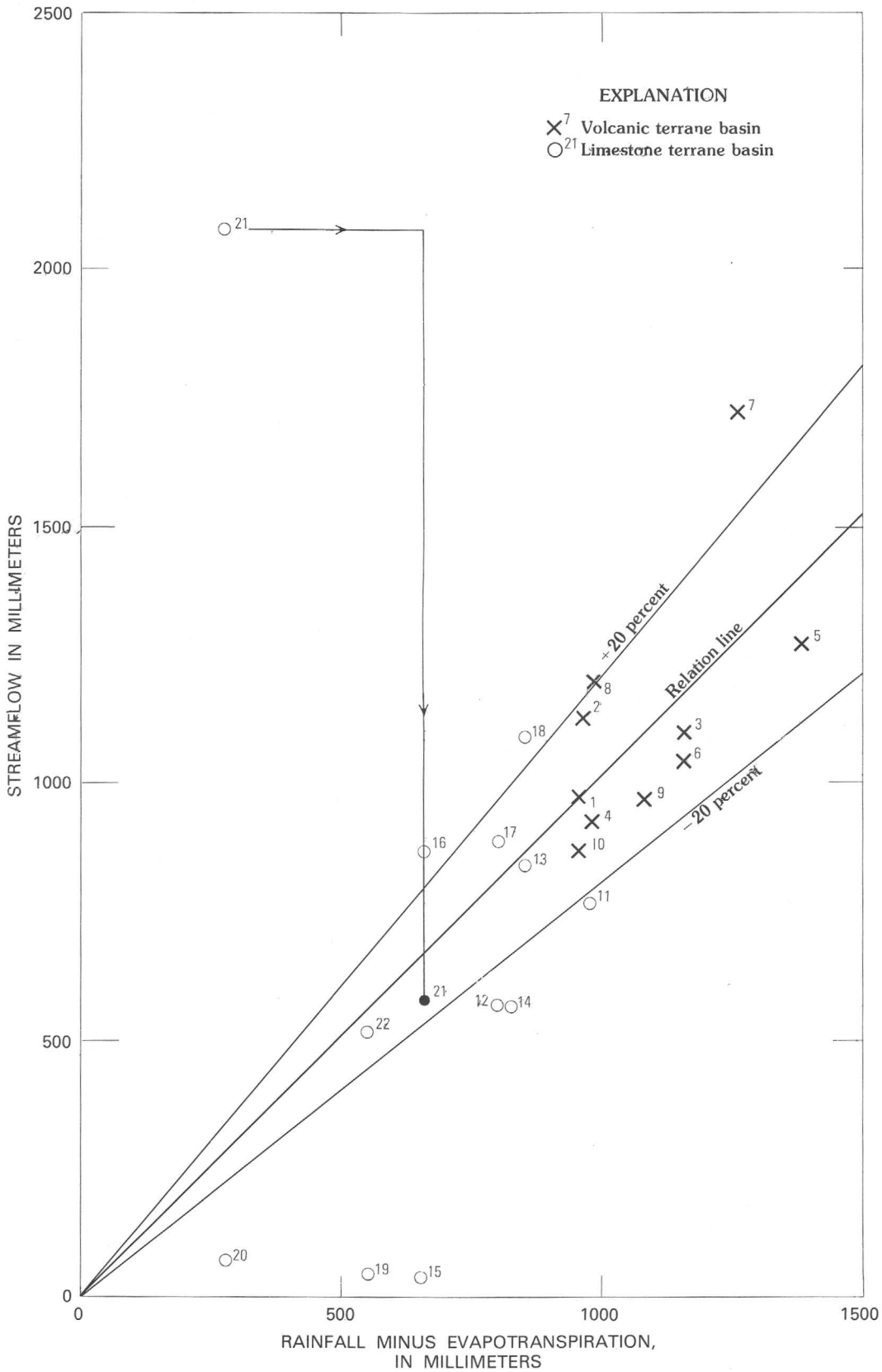

FIGURE 33.—Streamflow versus differences between precipitation and evapotranspiration. Data from table 2.

The basin numbered 15 is the lower Arecibo. It consists largely of valley plain downstream from Lago Dos Bocas. A yearly discharge of 56 mm is obtained by including the discharge of one spring whose flow is diverted from the basin for public supply (a direct subtraction of upstream from downstream flow would have resulted in a negative flow, indicating a loss). To a certain extent, the valley of the Río Grande de Arecibo acts like a sponge, absorbing water from the river during high flow and releasing it to the stream channel during the dry season, with an apparent near-zero net yearly contribution to the streamflow. Actually, from figure 23, for a rainfall of 1,800 mm, the drainage area between the upstream and the downstream site should yield a discharge of 600 mm for the year, about 550 mm greater than calculated. The excess probably flows into Caño Tiburones through the very permeable upper part of the Aymamón Limestone. The cluster of springs at the west end of Caño Tiburones is interpreted to mark the outflow area for this interflow from the Río Grande de Arecibo basin.

The remaining two basins showing excessive deviation from the 45-degree line of figure 33 are numbers 19 and 20. They are, respectively, Quebrada de los Cedros, and an area to the south of Caño Tiburones, which is drained by canals. Quebrada de los Cedros is usually dry, as its bed lies above the water table; it flows only after prolonged rainfall. Its drainage area is, therefore, only that part of the basin which has direct communication with the main channel, or fraction of the 38 km^2 assigned to it on the basis of sinkhole alinement. In addition, during storm runoff, this stream loses water through its bed all along its course. The canal-drained area south of Caño Tiburones (area 20) was assigned a drainage area of 54 km^2. Evidently the canals flow only in response to direct rainfall, and most of the rainfall outside their immediate area emerges as springflow in Caño Tiburones.

BASE FLOW

The separation of streamflow into components of floodflow and base flow involves definitions that are somewhat arbitrary. As used in this report, the term "floodflow" refers to that part of streamflow that produces discrete and clearly defined peaks on the hydrograph. (See fig. 34.) The remainder of the streamflow is considered base flow. It should be noted these definitions are based upon the shape of the surface-water hydrograph, rather than upon the origin of the water making up the various flow components.

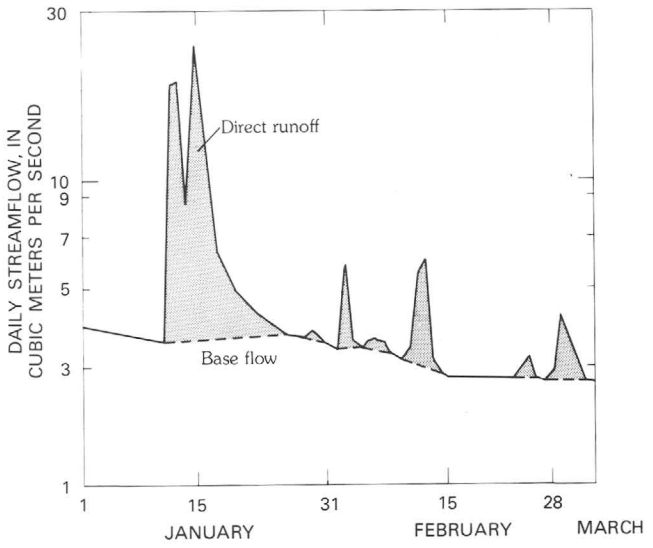

FIGURE 34.—An example of base-flow separation by computer.

A computer program to separate base flow from the total streamflow was adapted for the purposes of this study by T. D. Steele of the U.S. Geological Survey. This program is based on the recognition of points of minima in the hydrograph of daily flows; an empirical function allows for the separate computation of base flow and direct runoff, with the sum of the two being the total discharge. An example of this base-flow separation is shown in figure 34. In general, the program served its purpose well except for a few sites where the base-flow component was somewhat underestimated. The results are shown in table 3.

Two results of the hydrograph separation analysis deserve comment. The first is that the ratio of base flow to total flow, which is plotted against total flow in figure 35, is generally lower, for the major rivers, in the limestone than in the volcanics. The second is that the total base-flow from the limestone region is considerably higher than the total computed ground-water flow in table 1.

Both of these results can be explained by assuming that a certain fraction of the water which infiltrates the land surface in limestone terrane is routed rapidly to the streams through shallow circulation. In some cases this may represent circulation above the normal water table, through conduits which are dry except following a recharge event; in other cases it may represent rapid infiltration to the water table, followed by a correspondingly rapid discharge

TABLE 3.—*Base flow of limestone basins during period November 1969–October 1970*

	Streamflow site	Average base flow (m^3/s)	Lowest flow recorded (m^3/s)	Total flow (m^3/s)	Ratio of base flow to total flow
	Basins in volcanic terrane				
1	Upper Camuy	0.32	0.10	0.60	0.53
2	Criminales	.25	.062	.44	.57
3	Arecibo below Lago	----	----	----	----
4	Upper Tanamá	.89	.25	1.37	.65
5	Upper Manatí	3.50	.84	13.40	.26
6	Upper Cibuco	.48	?	1.30	.37
7	Mavilla	.55	?	1.31	.42
8	Unibón	.23	?	.52	.44
9	Cialitos	.52	.07	1.33	.39
10	Upper Guajataca	.094	.008	.21	.44
	Basins in limestone terrane [1]				
11	Guajataca to Lago	----	----	----	----
12	Guajataca to mouth	0.50	0.13	1.35	0.37
13	Lower Camuy	1.25	.54	4.46	.28
14	Lower Tanamá	1.05	.27	1.81	.58
15	Lower Arecibo	2.15	----	.07	30.00
16	Lower Manatí	2.00	.77	4.65	.43
17	Lower Cibuco	.94	.28	4.48	.21
18	Lajas	.18	.023	.75	.24
19	Quebrada de los Cedros	0	0	----	0
20	South Canals	.002	----	.07	.03
21	Caño Tiburones	2.45	2.0?	3.06	.80
22	Laguna Tortuguero	.55	.30	.74	.75

[1] For basins that begin in volcanic terrane, discharge is the difference between total downstream flow minus upstream flow. Other data refer to limestone portion of basin only. Location of sites is shown on plate 1.

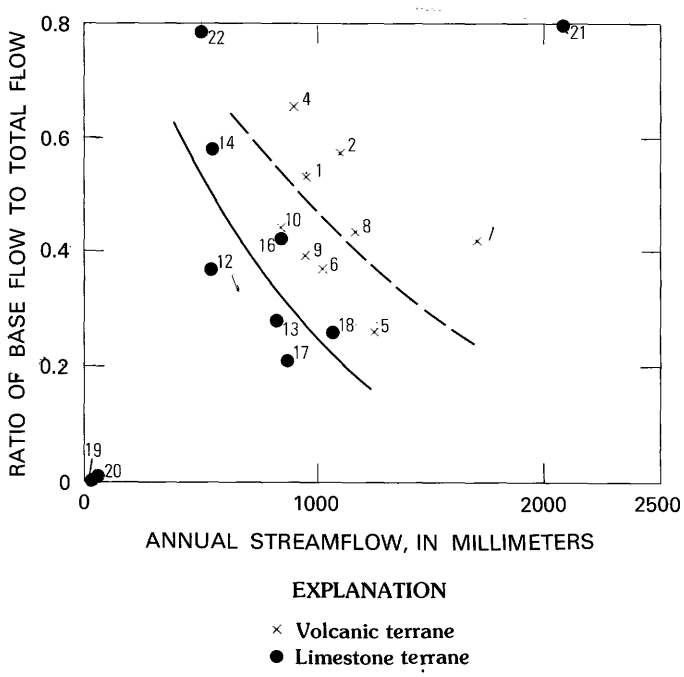

FIGURE 35.—Ratio of base flow to total flow versus discharge per unit area. Data from tables 2 and 3.

to the streams through the shallowest part of the saturated zone. The dye tracing results of Jordan (1970), in which a velocity of about 1.2 cm/s was calculated for water infiltrating to the Río Tanamá through shallow solution channels, confirm that such rapid circulation does occur.

One effect of this type of rapid circulation is that some of the water which infiltrates limestone terrane during a recharge event appears in the stream before "flood peak" has passed. Thus even though this water has infiltrated below land surface, it contributes to the flood peak rather than to base flow and causes the ratio of base flow to total flow to be lower than might be expected. The shallow circulation also persists, however, after passage of the flood peak, and thus also contributes to the base flow of the stream. As a result the total base flow is higher than the total ground-water flow as computed from head gradients in table 1; the computed flow, which is based on average long-term water levels, would not include shallow transient components. The situation forms a marked contrast to that in the volcanic basins, where infiltrating water tends to be held in storage in the weathered zone, and released slowly to the streams, generating a typical base flow recession curve, in which ground-water flow and base flow are presumably equivalent. The results are generally similar to those noted by Olmsted and Hely (1962) for the Brandywine Creek basin in Philadelphia, which flows through a gneiss-schist terrane.

It should be noted that the data for the Caño Tiburones and the Laguna Tortuguero do not fit

the pattern outlined above. Base flow forms a high percentage of the total flow for these features and coincides reasonably well with the computed groundwater flow as given in table 1. The hydrologic role of these coastal discharge features differs from that of the major rivers, and neither direct runoff nor transient shallow circulation can form a major component of their discharges.

In table 3 are listed also the lowest streamflow measurements during the period 1959–70. This period includes the severe droughts of 1964 and 1965, which are rated to have frequencies of occurrence of several decades. Therefore these discharges indicate the order of the minimum flows.

DIRECT RUNOFF

The difference between total flow and base flow is generally termed the direct runoff. This terminology is retained in this report even though, as explained in the preceding paragraphs, this component of the streamflow in the limestone terrane would include a contribution from transient shallow ground-water circulation, in addition to direct overland flow. Figure 36 was obtained by plotting total direct runoff during each month for each major stream entering the limestone from the south, versus the corresponding monthly direct runoff of the same stream at its downstream gaging site, after crossing the limestone. Data points which fall below the 45° line, or equality line, on figure 36, represent instances in which the direct runoff component was smaller at the downstream site than at the upstream site. It is possible that in a few instances this effect could be caused by differences in hydrograph characteristics, through which flow classified as direct runoff at the upstream site is classified as base flow at the downstream sites. In the majority of cases, however, points falling below the equality line on figure 36 must indicate a loss in the flow across the limestone, during periods of high flow. The basins that have well-developed flood plains, the Río Cibuco and the Río Grande de Manatí, show a loss for small inflows. The Río Grande de Arecibo consistently shows a loss. For the Río Grande de Manatí and the Río Cibuco the loss may represent water taken into temporary storage by the flood plain, to be released later as base flow. For the Río Grande Arecibo valley, as already noted in the yearly water budget, a probable transbasin flow to Caño Tiburones is indicated. The large scatter of the data suggests that the network of solution channels in the limestone basins is complex and responds to rainfall in different ways under different conditions, and that the traditional methods used in hydrology of interstation correlation are unreliable for estimating the contribution from the karst. In total flow, however, a fairly reliable correlation exists between the monthly flows of the upstream and downstream sites. It must be noted, however, that the correlation is biased, statistically, because the total flow downstream includes the upstream flow.

GEOCHEMISTRY

The development of the karst arises from an interaction between a slightly acidic rainfall and the soluble limestone. It is, therefore, instructive to analyze some of the chemical and physical properties of the limestones in relation to those of rainfall and to analyze further the properties of the water after this interaction between rainfall and limestones has taken place. The background for the following discussion was obtained by a selective sampling of rocks and of water. The water was field analyzed for pH, bicarbonate, and temperature. The locations of the sample sites are shown on plate 1 and figures 37 and 38 and the data are presented in tables 4, 5, 6, and 7.

THE LIMESTONES

Some physical and chemical properties of the limestones are shown in table 4. The analyses, listed by site, are by the author and by W. H. Monroe (written commun., 1970). Whereas Monroe's data provided detailed information on the geochemistry of the rocks, the samples collected by the author were chemically analyzed only for the more important constituents. Some effort, however, was spent to obtain a measure of rock density and porosity which was unavailable from the literature. The color of the dry rock powder or the "streak" was also obtained and is expressed in units of the Munsell scale as measured from a Rock Color Chart issued by the Geological Society of America. Porosity was measured by leaving oven-dried (at 110°C) rock chips (approx 50 g) in distilled water for 72 hours and recording the amount of water absorbed by the rock. The density was calculated as the ratio of the weight of the oven-dried chips divided by their volume which was in turn measured by the water volume displaced by the water-saturated chips.

The data of table 4 show that the limestones are pure. The Lares Limestone and the Montebello Limestone Member of the Cibao Formation in the central part of the limestone belt range from 94 to 96 per-

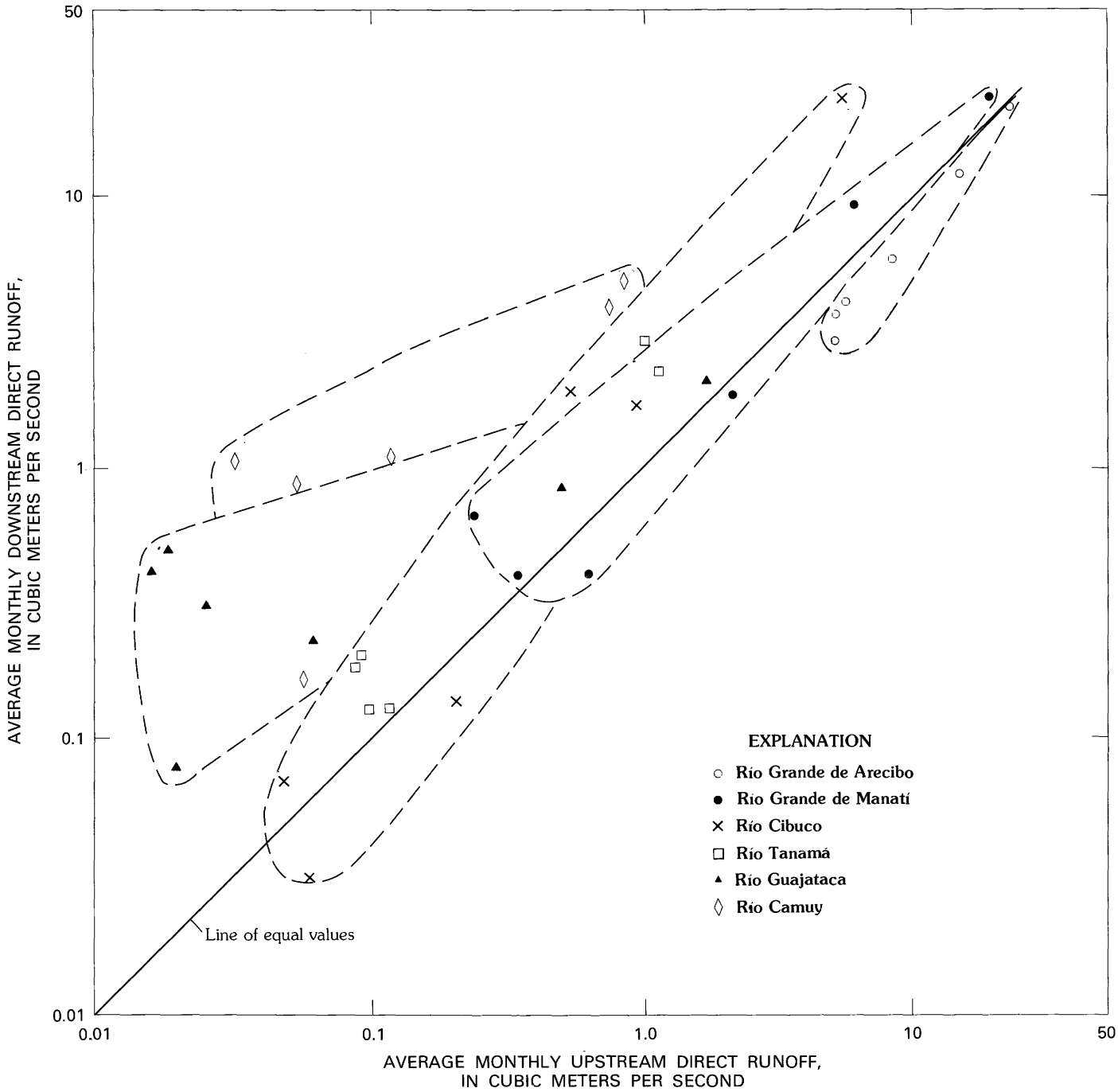

FIGURE 36.—Downstream direct runoff versus upstream direct runoff for those streams that begin in volcanic terrane and cross the limestone belt.

cent $CaCO_3$; the Aymamón Limestone ranges even higher—to 99 percent, but there is an indication from a few samples that these formations are less pure to the east and west. The Cibao Formation ranges from 59 to 91 percent $CaCO_3$, reflecting its variability as previously noted in the description of the geologic formations. The Aguada Limestone is somewhat less pure than the Aymamón and Lares, ranging from 82 to 94 percent; whereas, the Camuy Formation proves to be the most variable of all, ranging from 50 to 95 percent. The magnesium content of the limestones is generally low, less than 2 percent of $MgCO_3$, except for a few samples from the upper part of the Aymamón and the Camuy which show up to 39 percent $MgCO_3$, making these samples calcitic dolomites.

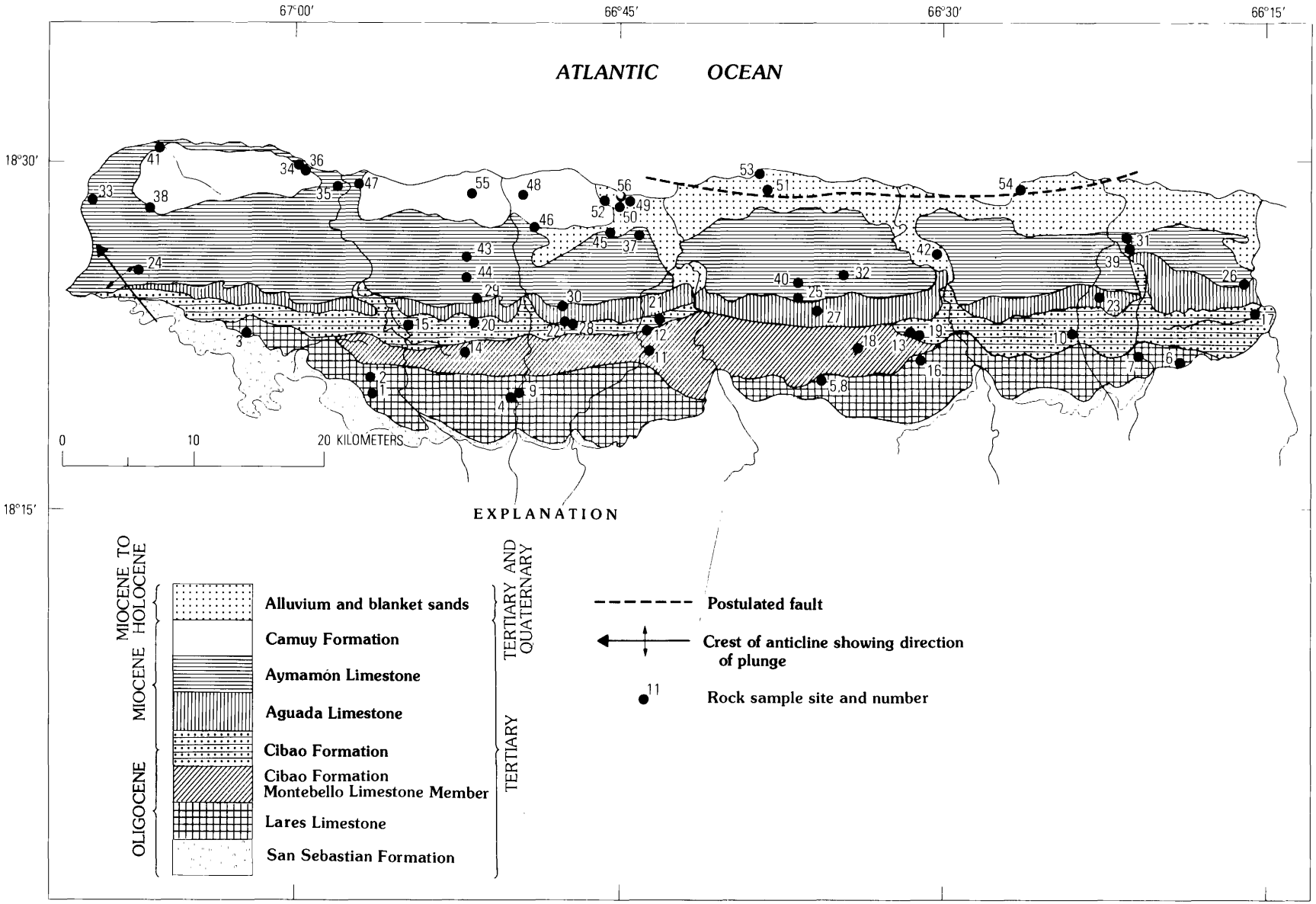

FIGURE 37.—Rock sample sites (data in table 4).

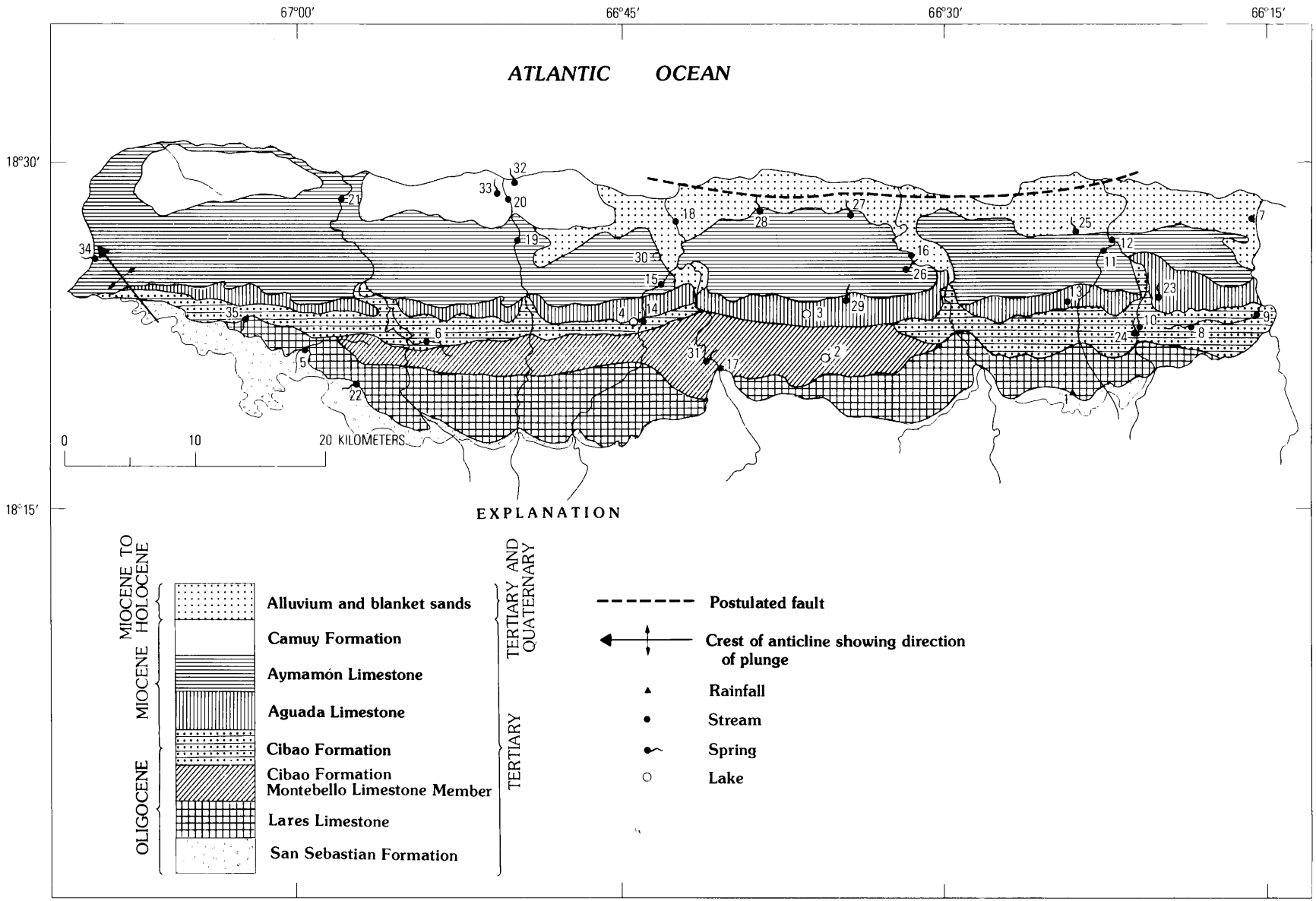

FIGURE 38.—Water sampling sites (data in table 5).

TABLE 4.—*Chemical and physical data of north coast limestone*

[Location is shown in fig. 37. Items in parentheses are from W. H. Monroe (written commun., 1970). Values of silica which are set in italics are from the relation of fig. 39]

No.	Geologic unit	Data, in percent						Porosity	Bulk density (g/cm^3)	Powder color (dry), Munsell scale [1]
		SiO_2	Al_2O_3	Fe_2O_3	$CaCO_3$	$MgCO_3$	Insoluble residue			
(1)	Lares Limestone	6.4	2.7	2.3	83.8	2.5	---	--	---	---
(2)	----do	1.2	.5	0	94.3	1.9	---	--	---	---
(3)	----do	16.9	5.1	2.2	68.7	3.3	---	--	---	---
(4)	----do	.3	.1	0	97.0	.8	---	--	---	---
(5)	----do	.6	.2	.1	95.4	.6	---	--	---	---
6	----do	*24*	--	2.8	60	2.5	34.7	.32	1.39	10 *YR* 6/4
7	----do	*1.5*	--	.1	95	1.1	1.9	.16	1.48	10 *YR* 8/2
8	----do	*.9*	--	0	97	.8	1.1	.19	1.37	5 *Y* 9/1
9	----do	*2.0*	--	.2	94	1.2	2.5	.15	1.98	10 *YR* 8/2
(10)	Cibao Formation	4.0	1.2	1.0	88.7	1.7	---	--	---	---
(11)	Montebello Limestone Member.	.1	.1	0	97.0	.8	.5	--	---	---
(12)	----do	.2	.1	.1	97.8	.8	.7	--	---	---
(13)	Quebrada Arenas Limestone Member.	.4	.3	.2	96.5	.6	.8	--	---	---
(14)	Cibao Formation	3.4	1.0	.4	91.4	1.9	---	--	---	---
(15)	----do	12.3	4.5	1.6	74.8	2.1	---	--	---	---
(16)	----do	8.6	2.8	1.1	83.8	.8	10.0	--	---	---
17	----do	*5.1*	--	.8	90	1.9	6.3	.17	1.73	10 *YR* 8/2
18	Montebello Limestone Member.	*.5*	--	.1	96	.6	.6	.30	1.54	5 *Y* 9/1
19	Cibao Formation	*17*	--	.8	76	.7	20.6	.12	1.98	10 *YR* 7.5/4
20	----do	*29*	--	1.4	59	1.3	35.9	--	1.10	5 *Y* 7/4
21	Aguada Limestone.	6.6	1.2	.6	89.2	.6	7.5	--	---	---
(22)	----do	4.0	2.7	.9	88.8	1.0	---	--	---	---
(23)	----do	1.2	.7	.2	93.6	.4	1.3	--	---	---
(24)	----do	4.4	2.8	1.1	86.5	.8	---	--	---	---
(25)	----do	7.2	2.0	.3	88.4	.6	9.0	--	---	---
26	----do	*9.8*	--	.3	84	.8	11.9	.16	1.81	10 *YR* 7/5
27	----do	*12*	--	.6	82	1.0	14.3	.11	2.13	10 *YR* 8/2
28	----do	*2.6*	--	1.9	93	.7	3.2	.03	2.53	10 *YR* 5.5/3
29	----do	*6.7*	--	1.0	87	.9	8.2	.04	2.16	10 *YR* 8/4
30	----do	*1.7*	--	.6	95	.6	2.1	.09	2.22	10 *YR* 6.5/2
(31)	Aymamón Limestone.	.0	0	0	98.8	.2	---	--	---	---
(32)	----do	.5	.3	.1	97.5	.6	.8	--	---	---
(33)	----do	.5	.2	0	61.6	34.5	---	--	---	---
(34)	----do	.7	.6	0	61.2	35.5	---	--	---	---
(35)	----do	.5	.4	0	57.7	38.9	---	--	---	---
(36)	----do	.7	.3	0	62.7	34.3	---	--	---	---
(37)	----do	.1	.1	0	97.8	1.0	.3	--	---	---
(38)	----do	.8	.4	0	95.5	.6	---	--	---	---
39	----do	*.4*	--	.1	97	.6	.5	.18	1.95	*N* 9
40	----do	*2.5*	--	.4	94	.8	3.1	.06	1.38	5 *YR* 8/4
41	----do	*9.5*	--	1.3	84	1.9	11.7	.17	1.59	10 *YR* 7/6
42	----do	*0*	--	.2	99	.7	0	.13	1.88	5 *Y* 9/1
43	----do	*.9*	--	.2	96	.6	1.1	.28	1.63	10 *YR* 8/4
44	----do	*0*	--	.1	99	.7	0	.18	1.86	10 *R* 8/2
45	----do	*.2*	--	.2	98	.9	.3	.21	1.59	10 *YR* 8/4
(46)	Camuy Formation	8.3	3.0	3.7	79.6	1.5	---	--	---	---
(47)	----do	3.4	.8	.3	55.5	36.0	---	--	---	---
(48)	----do	2.2	.6	.3	93.6	.8	---	--	---	---
(49)	----do	10.6	1.7	1.3	82.2	.8	12.7	--	---	---
(50)	----do	31.7	4.2	1.9	57.0	1.0	39.5	--	---	---
(51)	----do	9.2	2.0	.9	84.8	1.0	11.3	--	---	---
(52)	----do	7.0	1.2	.6	88.8	1.0	7.7	--	---	---
(53)	----do	2.4	.6	.5	94.8	1.5	2.9	--	---	---
(54)	----do	*1.9*	--	.4	---	40.0	2.3	.26	1.23	5 *Y* 8/1
(55)	----do	*21*	--	.2	70	.9	26.4	.24	1.67	5 *YR* 9/1
(56)	----do	*38*	--	.5	50	.8	46.2	.18	1.93	10 *YR* 7/3

[1] See Goddard and others (1948).

TABLE 5.—*Miscellaneous chemical and physical data on water from north coast limestone*

[Data in milligrams per liter except temperature in degrees Celsius, and specific conductance in micromhos per centimeter at 25°C. Location of sites is shown in fig. 38. Number in parentheses are acidified samples]

	Temperature, °C	SiO_2	Ca		Mg		Na	K	HCO_3		SO_4	Cl	NO_3	Dissolved solids	Specific conductance	pH	
									Laboratory	Field						Laboratory	Field
1. Rainfall, average at Morovis.	---	--	1.2	-----	.6	-----	--	--	4.7	---	1.8	4.5	.5	18	----	6.1	--
2. Lago near Montaña.	25	2.1	4.2	(4.9)	1.0	(.9)	2.6	3.5	17	17	0.8	5.5	.7	29	53	6.1	6.3
3. Lago near Alianza.	26	3.8	22	(22.8)	1.1	(.9)	4.3	4.0	66	67	2.6	9.8	.8	81	155	6.7	6.7
4. Lago at Esperanza.	26.7	2.8	58	-----	1.7	-----	6.9	1.9	168	---	12.0	12.0	5.0	183	332	7.3	--
5. Río Guatemala at San Sebastián.	27	8.0	59	(59)	5.8	-----	8.1	1.2	182	181	24	13	2.4	212	364	8.0	7.4
6. Río Chiquito -----	23.5	5.9	88	(90)	5.2	(5.2)	5.1	.9	274	276	17	8.5	2.7	268	469	8.0	7.4
7. Ciénega Higuillar--	24.5	8.7	33	(33)	10	(10.4)	32	3.8	130	181	10	57	1.3	220	419	7.4	7.2
8. Río Lajas at Hwy 823.	24	8.9	85	(93)	6.5	(7.3)	7.9	.7	268	320	14	15	4.7	275	493	7.7	7.8
9. Río Lajas at Toa Alta.	23.4	11.0	78	(81)	4.9	(5.7)	9.8	1.2	240	288	15	19	4.5	262	469	7.7	8.0
10. Río Cibuco at Hwy 647.	23.6	26	38	(41)	7.9	(8.3)	11.0	1.9	142	141	13	16	5.9	190	308	7.6	7.9
11. Río Indio at Hwy 160.	22.8	16	73	(75)	5.8	(6.9)	12	1.8	228	234	13	19	5.6	258	451	7.7	8.0
12. Río Cibuco at Hwy 2.	23.2	21	56	(58)	7.4	(7.8)	12	2.1	190	194	14	17	5.9	230	391	7.6	7.8
13. Quebrada Hicatea-	---	11	119	-----	6.3	-----	14	2.8	356	---	---	----	.3	----	659	7.3	--
14. Río Tanamá near La Esperanza.	24.5	12	47	(52)	3.9	(4.3)	6.3	.7	154	158	8.0	7.0	2.3	163	279	7.6	7.3
15. Río Tanamá at Hwy 10.	22.0	18	47	(46)	3.7	(4.2)	5.9	.6	156	156	4.0	7.3	2.1	166	290	8.0	7.2
16. Río Grande de Manatí at Hwy 2.	26	23	36	(42)	7.7	(4.9)	9.8	1.3	136	146	7.0	11	2.1	166	281	7.2	7.0
17. Río Grande de Arecibo below dam.	24.5	24	21	(21)	6.0	(6.0)	10	1.4	85	78	13	10	3.3	131	197	7.2	7.0
18. Río Grande de Arecibo at Cambalache.	26	17	40	(42)	5.2	(3.9)	8.4	1.2	140	---	4.4	11	4.3	160	290	7.2	7.8
19. Río Camuy at Salto Máquina.	24	7.4	58	(64)	3.8	(3.7)	6.4	.7	184	200	10	9.0	4.1	191	333	8.0	7.6
20. Río Camuy at gaging station.	25	7.4	63	(57)	3.7	(4.1)	6.4	.9	198	191	9.4	9.8	3.4	202	361	7.8	7.6
21. Río Guajataca at gaging station.	25	4.7	56	-----	4.1	-----	7.0	1.1	184	---	11.0	9.8	1.6	186	335	7.9	--
22. Spring, Salto Collazo.	23	4.4	72	(74)	3.2	(3.2)	4.5	.8	220	---	12	8.4	1.6	215	385	7.8	7.5
23. Spring, Hwy 647 near Vega Alta.	25.3	9.4	85	(86)	3.9	(4.7)	9.3	.7	264	266	3.4	21	4.5	267	496	7.8	7.4
24. Spring, El Convento, Hwy 647.	24.5	6.6	86	(89)	6.1	(7.0)	6.4	.4	276	283	4.6	14	10	270	498	7.7	7.3
25. Spring, Comunidad El Ojo del Agua.	25.5	7.3	96	(98)	10	(9.9)	44	1.6	268	267	16	92	11	410	791	7.6	7.2
26. Spring near Manatí.	24.8	6.6	90	(92)	3.2	(3.9)	8.3	.6	278	278	2.8	15	5.1	269	498	7.8	7.3
27. Cáncora Garrochales.	28	8.9	168	(170)	34	(33.6)	241	.8	276	284	53	562	11	1,210	2,300	7.7	7.1
28. Spring north of Garrochales.	25.5	5.6	97	(100)	16	(15.6)	118	.5	266	270	29	218	13	628	1,160	7.3	7.3
29. Spring Riachuelo-	24	15	89	(91)	3.8	(4.2)	6.6	.5	276	274	2.8	10	6.4	270	483	7.7	6.9
30. Spring, Central Los Caños.	25	15	83	(85)	3.9	(3.9)	10	1.1	258	257	4.0	18	12	274	483	7.5	6.7
31. Spring, Los Chorros.	23	7.4	56	(61)	2.5	(2.9)	5.6	.4	174	182	4.2	8.8	3.3	174	305	7.8	7.6
32. Spring near Hatillo.	23.5	11	77	-----	19	-----	108	11	268	---	27	190	3.7	581	1,040	7.7	--
33. Spring, Camuy at Hwy 2.	24.5	8.9	102	(109)	30	(30)	225	8.7	288	---	60	402	7.7	986	1,800	7.6	--
34. Spring in Aguadilla.	25	7.7	83	(88)	4.5	(4.6)	7.6	.9	266	264	3.2	12	12	262	469	7.7	6.8
35. Spring near San Sebastián.	26	25	119	(144)	7.3	(7.3)	11	.5	376	460	19	12	1.6	381	628	7.5	6.9

Most of the insoluble residue from the limestone samples is silica (81 percent) as is shown in figure 39. Minor amounts of aluminum and iron are present in the quantities shown in table 4. Measurable quantities of strontium and titanium and traces of other metals not listed in table 4 were also found.

The primary porosity ranges from a minimum of 0.03 for a sample from the Aguada to a high of 0.32 for a sample from the Lares. In general, the Aguada seems to be the least porous, and the Camuy the most. The densities measured are inversely related to the porosity, with the Aguada clearly denser than all other formations.

The streak of the dry powders of most samples showed very pale colors in the orange section of the color spectrum. The chalky limestones were generally white or very pale gray.

TABLE 6.—*Chemical and physical data from ground water of the north coast limestone*

[Data in milligrams per liter except temperature in degrees Celsius, specific conductance in micromhos per centimeter at 25°C, and pH]

	Well Nos.[1]	Geologic unit	Temperature °C	SiO_2	Ca	Mg	Na	K	HCO_3	SO_4	Cl	F	NO_3	Dissolved solids	Specific conductance	pH
1.	26–24	Aymamón Limestone.	---	9.0	81	3.2	----24----		256	2.0	28	0	19	335	534	7.9
2.	27–20	Aymamón Limestone.	29	6.8	50	4.4	19	0.8	154	8.8	38	0.1	1.4	205	384	8.0
3.	26–33	Lower part of Aymamón Limestone.	---	7.0	110	3.4	12	.0	144	9.0	34	0	26	345	581	7.6
4.	24–25	Aguada Limestone--	---	6.2	88	9.8	----------		302	2.1	18	.1	2.2	283	485	7.4
5.	26–55	Aguada Limestone--	---	21	100	4.1	----35----		385	3.8	19	--	---	523	---	7.2
6.	24–19	Cibao Formation --	---	8.5	112	12	----22----		370	4.4	39	.1	18	404	680	7.7
7.	22–31	Cibao Formation --	29	4.8	103	1.7	6.2	.5	300	5.2	10	0	12	291	514	7.4
8.	22–47	Cibao Formation --	24.4	7.4	88	9.8	-----3.2---		300	28	11	.2	2.3	273	667	7.8
9.	26–33	Montebello Limestone Member, artesian.	---	7.3	37	9.1	8.8	1.5	136	19	14	.1	.4	---	---	--
10.	25–33	Montebello, Limestone Member, artesian.	---	3.6	78	10	6.2	.3	272	7.2	10	--	4.5	254	458	7.9
11.	26–33	Lares, Limestone artesian.	---	16	50	52	69	5.1	310	181	30	4.2	---	560	906	7.8
12.	25–33	Lares Limestone artesian.	---	5.8	69	18	7.8	.6	284	10	12	.2	3.2	266	485	7.5

[1] Well numbers are minutes north of lat 18° for first 2 digits, and minutes west of long 66° for next 2 digits; and can be used to locate the well roughly.

TABLE 7.—*Average values of dissolved constituents and of physical properties of surface water in the north coast limestone belt*

[Data in milligrams per liter except specific conductance in micromhos per centimeter at 25°C, and pH. Note that averages shown are means of samples and are not adjusted for discharge]

	Name and location of stream[1]	Rock type	SiO_2	Ca	Mg	Na	K	HCO_3	SO_4	Cl	NO_3	Dissolved solids	Specific conductance	pH
1.	Guajataca at Lares (10)--	Volcanic ------	29.8	26.5	5.8	11	1.7	114	6.0	9.0	3.6	150	230	7.5
2.	Camuy near Lares (1) ---	----do --------	21.8	13.9	5.3	7.5	1.0	57.5	17.3	6.7	1.6	103	154	7.5
3.	Criminales near Lares (2)-	----do --------	21.9	10.2	4.5	6.5	1.0	47.5	7.8	6.7	2.7	85	121	7.2
4.	Arecibo below Dos Bocas (3)	----do --------	21.6	19.3	5.9	10.1	1.7	78.3	15.0	10.1	1.6	124	189	7.2
5.	Manatí at Ciales (5) -----	----do --------	27.4	21.1	8.7	11.0	1.4	102	8.4	12.2	1.9	147	230	7.5
6.	Cialitos at Ciales (9) -----	----do --------	29.9	23.7	6.5	10.2	1.4	109	3.4	10.5	2.8	142	222	7.5
7.	Cibuco below Corozal (6) -	----do --------	33.4	25.9	10.6	14.0	2.2	124	12.4	17.2	3.8	181	290	7.6
8.	Mavilla near Morovis (7)--	----do --------	28.9	19.5	8.7	12.2	2.6	85.7	10.9	15.3	4.8	150	234	7.7
9.	Unibón near Morovis (8)--	----do --------	23.3	24.8	9.6	11.6	2.1	118	10.6	14.9	2.7	163	261	7.7
10.	Guajataca, below Lago (11).	Limestone and volcanics.	8.6	57.5	4.9	7.5	1.0	185	9.1	12.4	3.1	195	355	7.8
11.	Guajataca at mouth (12)--	----do --------	7.7	58.9	5.4	6.7	1.0	190	8.9	14.0	3.9	203	368	7.9
12.	Camuy near Camuy (13)---	----do --------	9.9	54.5	4.2	6.5	.8	175	7.6	9.4	3.4	184	327	7.9
13.	Tanamá at Charco Hondo (14).	----do --------	13.0	42.7	4.0	6.1	1.2	144	6.4	7.2	1.7	154	266	7.9
14.	Arecibo at Cambalache (15).	----do --------	21.5	30.4	5.3	8.3	1.3	114	12.2	9.6	2.8	148	233	7.5
15.	Manatí at Highway 2 (16)-	----do --------	20.0	28.9	6.5	8.8	1.5	96.4	7.6	10.6	3.2	144	244	7.5
16.	Cibuco at San Vicente (17).	----do --------	21.5	49.6	8.4	12.6	2.1	170	12.4	18.2	3.1	217	373	7.8
17.	Caño Suroeste[2] (20)-------	Limestone -----	10.4	15.5	3.2	6.7	5.7	47	14	9.0	1.2	86.5	136	6.8
18.	Caño Noreste[2] (20) -------	----do --------	9.7	22.0	6.3	27.0	3.8	66	----	50	2.3	177	312	6.7
19.	Caño Tiburones[2] (21)-----	----do --------	10.3	126	69.0	498	20	80	248	910	2.6	1,880	5,320	7.3
20.	Laguna Tortuguero (22) --	----do --------	6.9	88.2	52.1	328	11.4	140	113	721	1.0	1,440	2,680	7.8
21.	Lajas at Toa Alta (18) ---	----do --------	10.9	86.2	6.3	10.4	1.7	242	13.9	20.3	2.8	287	505	8.0

[1] Numbers in parentheses identify stations listed in tables 2 and 3.
[2] High flows.

THE WATER

RAINFALL

Chemical and physical data on the water of the study area are given in tables 5, 6 and 7. However, whereas the data of tables 5 and 6 refer mainly to once only sampling for each given site, those of table 7 on rivers are averages from about 12 samples collected at each site.

The first row of table 5 shows the averaged mineral composition of rainfall at Morovis. These data were provided by Raúl Díaz (written commun., 1970). As expected for an island, chloride salts are the main constituents in the rainfall. The average pH of the rainwater is 6.1 (slightly acidic). A sample of rainfall analyzed in the field immediately after collection showed a pH of 6.2; thus the average of 6.1 of Díaz' samples, which were kept in storage for prolonged periods prior to analysis, can be considered valid.

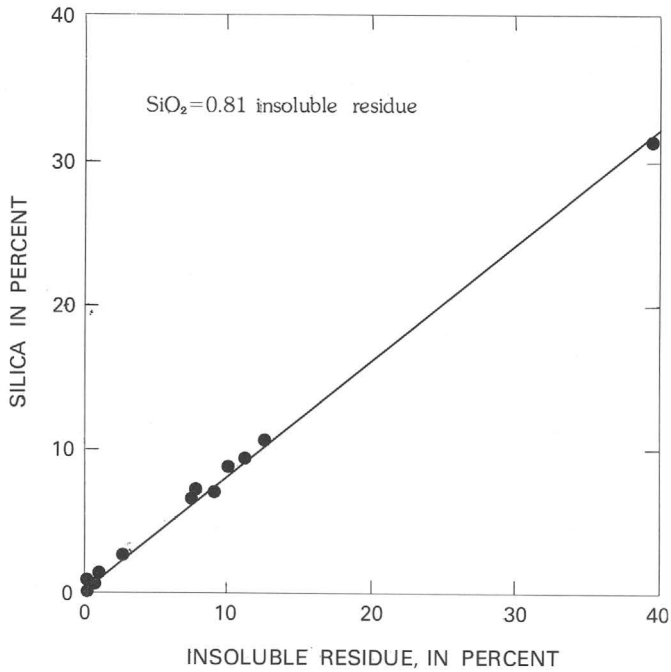

FIGURE 39.—Relation between silica and insoluble residue.

LAKES

The lake water analyses, shown in table 5, were taken from three lakes at progressively lower altitudes, and the results clearly indicate a general increase of mineral concentration. The first analysis—2, a pond resting on terra rossa receiving only direct runoff—shows a concentration similar to that of rainwater, the slight increase of some constituents, particularly calcium, being no more than a leaching of terra rossa or slight concentration from evaporation. The pH is the same; thus the capacity of this water to take limestone into solution remains unaltered. The terra rossa, as mentioned by Birot and others (1967), provides an inert medium for surface water flowing or resting on it. The samples were collected in 1970–71; the fact that these years are considered wet years lessens the possibility of general increase of mineral concentration from evaporation. Analyses 3 and 4, which are lakes that are partly spring-fed, especially 4, show a rapid increase of mineral concentration—especially, calcium.

SPRINGS

Analyses 22 to 35, table 5, are from waters which have been in contact with the limestones. Spring analyses that show sodium and chloride concentrations much larger than the rest, such as 27 and 28, are from springs which lie in the zone of diffusion between ground water and sea water. (See fig. 38.) The generally high chlorides and nitrates of all the springs and, in fact, of all waters of the north coast limestones, are not acquired from dissolution of limestone, but rather arise from the minerals introduced by the rainfall (especially the chlorides) or by residues of biological activities

There are no great differences among the waters from the various formations. The Aguada and the Cibao seem to have a larger SiO_2 content (about 10 mg/L) than the Lares and the Aymamón (about 6.7 mg/L), but the sampling can hardly be considered exhaustive. Spring 35, which flows about 100 L/h (liter per hour) has the highest SiO_2 content of all the springs sampled. This spring issues from the Cibao Formation, which has a large SiO_2 content. The source of the spring, therefore, may explain, in part, the high silica content; however, the increase in concentration could also result from direct evaporation or evapotranspiration.

The calcium content of the springs which are not in the saline zone near the coast ranges from 56 to 119 mg/L. The lowest value is for the spring shown in figure 31 which is associated with travertine deposition, whereas the high value is for spring 35 for which evaporation may be responsible for the higher-than-average calcium concentration. The average concentration of calcium in spring water seems to be about 85 mg/L.

GROUND WATER

Data on the major chemical constituents of ground water are given in table 6. The chemical analyses show that the water from the various formations is similar. The general similarity of the ground water to the spring water is also noted, and most comments about spring water apply to ground water, except that ground water has a high mineral concentration without the effect of evaporation. Of special interest are the data for the deep artesian wells, analyses 9 to 12. The fact that artesian aquifers show smaller concentrations of calcium than water-table aquifers indicates possibly precipitation of $CaCO_3$ through crystallization within the aquifer, for which there is much field evidence (figs. 40 and 41), or simply loss of $CaCO_3$ from the samples after collection (the analyses were not made with acidified samples).

RIVERS

The average composition of water from streams is shown in table 7. The data in table 7 are mainly from low flows, which are normally more concentrated than high flow, and thus the averages are

FIGURE 40.—Evidence of recrystallized limestone.

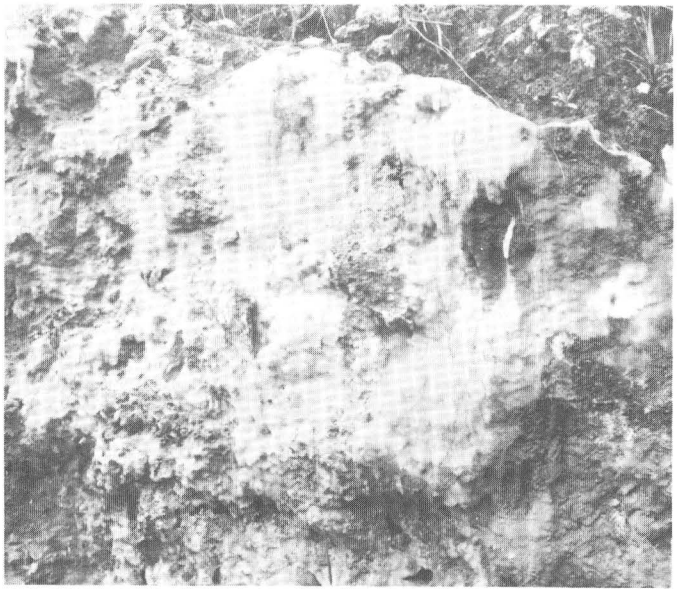

FIGURE 41.—Recrystallization of limestone (close up of fig. 40).

somewhat higher than a true average such as would be obtained from a continuous sampling that would incorporate data from more diluted high flows. Concentration of mineral constituents, as shown by the relation of $CaCO_3$ to discharge in figure 42, in the water is an inverse function of streamflow. This inverse relationship is most applicable to the streams flowing out of volcanic terrane; the limestone streams have a more nearly constant concentration. To the extent that table 7 serves as a comparison between streamflow from the volcanic terrane and that from limestone, the remark about the averages of table 7 is of little importance. It should be taken into account, however, if a comparison is made with data that are averaged relative to the flow. An example of a proper averaging of chemical constituents is shown in the rating table of figure 43 used to compute the equivalent freshwater outflow of Cãno Tiburones.

As expected, the main difference between the streamflow from the volcanic terrane and that from the limestone is the increase in concentration of calcium and, inherently, of bicarbonate, and a slight decrease of all other measured constituents. For those streams that originate in the volcanic terrane and cross the limestone belt, the decrease may be a dilution process, especially in the case of silica. The only sample valid for comparison from purely limestone terrane is from the Río Lajas (station 21 in table 7) that mainly drains the Cibao Formation which, in the Lajas basin, is an impure limestone. Assuming that no precipitation of silica takes place along the stream channel, the contribution of silica from the limestone is of the order of 10 mg/L for the Cibao Formation and perhaps for the Aguada Limestone, and of 6–7 mg/L for the Lares Limestone and Aymamón Limestone.

At the upstream volcanic terrane sites, the streams have a silica content in excess of 20 mg/L and less than half this value at the downstream sites after the streams have crossed the limestone belt. Assuming no streamflow losses through the limestone belt (as borne out by the water-budget results) and ignoring losses by evapotranspiration, one can write:

$$C_u \cdot Q_u + C_L \cdot Q_L = C_D \cdot Q_D \qquad (10)$$

where

C = concentration of silica
Q = streamflow
u,L,D = upstream, limestone, and downstream, respectively, and
$Q_L = Q_D - Q_u$

For the Río Camuy (including the Río Criminales), for example, using the water-budget data from table

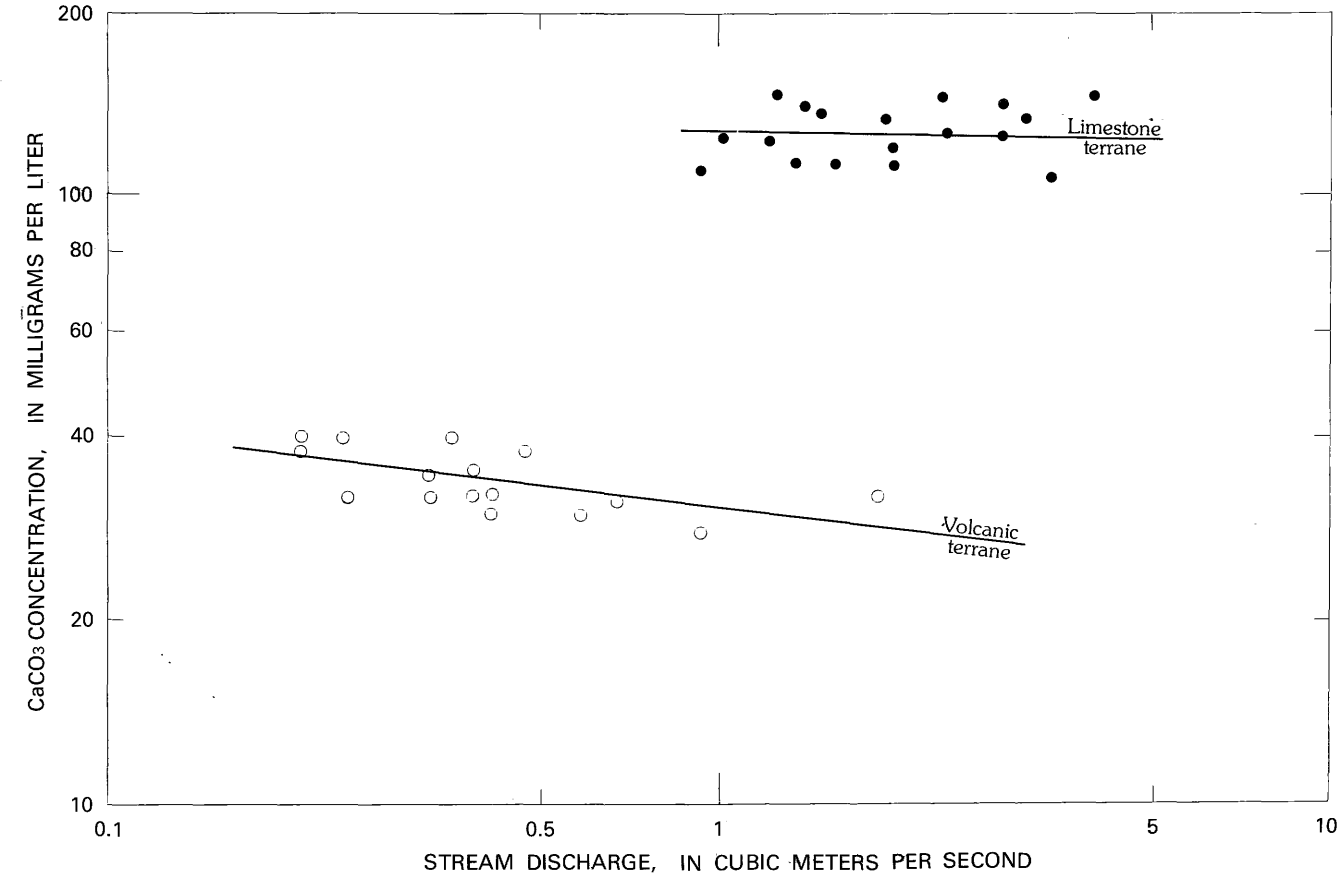

FIGURE 42.—Relation between $CaCO_3$ concentration and discharge (instantaneous values).

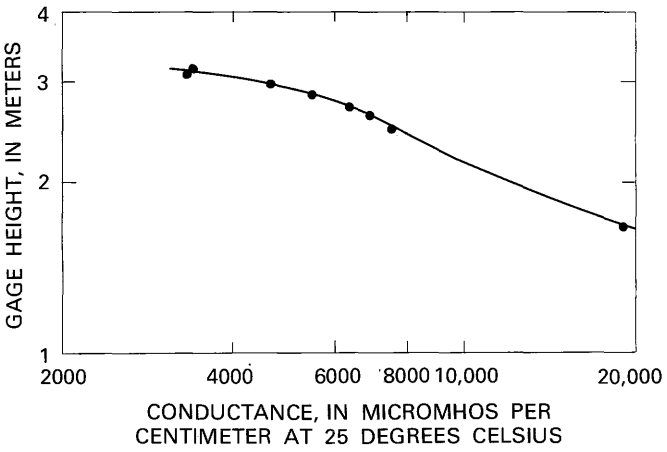

FIGURE 43.—Rating curve used to compute the equivalent freshwater discharge of Caño Tiburones.

2 converted to cubic meters per second, and the concentrations in milligrams per liter of table 7,

$$(21.8)\cdot(0.59)+(21.9)\cdot(0.33)+(X)\cdot(3.4)=(9.9)\cdot(4.3).$$

Solving for X, the silica concentration for the limestone part of the basin, gives a value of 6.6, which is about the concentration of silica found in Lares and Aymamón waters. Although more work is needed, it would seem that silica may provide a good natural tracer to compute the streamflow at the downstream end of those rivers that originate in volcanic terrane.

Samples 14, 15, and 16 are from sites on streams with substantial flood plains. Silica concentrations approach those from upstream sites in volcanic terrane, suggesting that the flood plain itself contributes silica to the water; possibly from contact with clay minerals.

THE SOLUTION PROCESS[1]

The ability of rainfall to interact with carbonate rocks is a function of the pH of the water. The potential for solution of calcium carbonate can be demonstrated by determining the chemical equilibria for rainfall which is given by

$$\frac{[H^+]\,[HCO_3^{-2}]}{[H_2CO_3]}=K_H\,CO_3^{-2}10^{-6.4}. \qquad (11)$$

[1] The following chemical considerations are based on Garrels and Christ (1965), Back (1963), and F. Quiñones (oral commun., 1970).

where K is the equilibrium constant.
It is accepted that in the equilibria of carbonic acid in water, both CO_2 and H_2CO_3 molecules are present, but it has been customary to represent CO_2 as H_2CO_3.

The carbonate system in equilibria is represented by the relation

$$\frac{[Ca^{+2}]\ [CO_3^{-2}]}{[CaCO_3]} = KCaCO_3 = 10^{-8.3}. \qquad (12)$$

In both equations above, activities are expressed in moles per liter. For $CaCO_3$ the activity is unity. Further developing the equilibria for the constant of bicarbonate ions,

$$\frac{[H^+]\ [CO_3^{-2}]}{[HCO_3^-]} = KHCO_3 = 10^{-10.3} \qquad (13)$$

and adding the general equilibria equation for water

$$\frac{[H^+]\ [OH^-]}{[H_2O]} = 10^{-14.0} \qquad (14)$$

while taking the activity of H_2O as unity, the systems of equations can be solved as described by Garrels and Christ (1965).

To examine the influence of rainfall on the solution of the carbonate rocks, one must consider the chemical equilibria of the ions. From equation 11 we know that CO_2 and water ionize into H^+ and HCO_3^- forming H_2CO_3. From equations 11 and 12.

$$CaCO_3 + CO_2 + H_2O \leftrightharpoons Ca^{+2} + 2HCO_3^- \qquad (15)$$

which is the basic equation for the solution of $CaCO_3$. In the system, the equilibria are regulated by the CO_2 concentration; and changes in CO_2 will cause a shift of the equilibria. Taking the rainfall pH as 6.1 from table 5, or $[H^+] = 10^{-6.1}$ and substituting in equation 11

$$\frac{[HCO_3^-]}{[H_2CO_3]} = \frac{10^{-6.4}}{10^{-6.1}} = 10^{-0.3}. \qquad (16)$$

The equilibria of CO_2 is (from Garrels and Christ, 1965)

$$\frac{[H_2CO_3]}{PCO_2} = 10^{-1.47}, \qquad (17)$$

where P = partial pressure.
For a partial pressure of CO_2 in the atmosphere of the order of $10^{-3.5}$

$$[H_2CO_3] = 10^{-1.47} \times 10^{-3.5} = 10^{-5.0} \qquad (18)$$

and, substituting in equation 16

$$[HCO_3^-] = 10^{-0.3} \times 10^{-5.0} = 10^{-5.3}. \qquad (19)$$

Therefore the total amount of dissolved carbonates in rainwater would be

$$(CO_3^{-2})_{Sol} = [H_2CO_3] + [HCO_3^-] = 10^{-5.0} + 10^{-5.3} = 10^{-4.75} \qquad (20)$$

and the concentration of Ca^{+2} in equilibrium would be

$$[Ca^{+2}] = \frac{10^{-8.3}}{[CO_3]} = \frac{10^{-8.3}}{10^{-4.75}} = 10^{-3.55} \qquad (21)$$

which is equivalent to a maximum concentration of 11.2 mg/L of Ca^{+2} that can be dissolved by rainfall. Because the average concentration of calcium in rainfall from table 5 is 1.2 mg/L, we may conclude that the effective reactive ability of rainwater for calcite is almost totally available prior to the solutioning process on the limestone rocks. Once the reaction with the limestone is completed, a new equilibrium is reached. The nature of this mechanism is discussed in detail by Garrels and Christ (1965) who conclude that at a pH of 9.9 a concentration of $CaCO_3$ of 14 mg/L in the solute from the rainfall-calcite reaction will be in equilibrium —thus pointing out the low reactive capacity of rainwater. This reasoning is also followed by Birot and others (1967) who concluded that, to explain the high calcium content of some of the waters of the north coast limestone belt, additional CO_2 must be picked up from the soil by the percolating rainfall. In turn the CO_2 in the soil is obtained from the decomposition of organic acids into CO_2 and water. These are also the views first presented by Monroe (1966).

The relative importance of this enrichment in CO_2 from the breaking down of organic acids is examined by analyzing as an example the $CaCO_3$ dissolved from the Río Lajas basin which drains limestone terrane only. A mean annual base flow of about 0.1 m^3/s is computed from figure 35 adjusted for the mean annual rainfall. From a concentration-discharge correlation similar to the one shown in figure 42, an average concentration of 200 mg/L of $CaCO_3$, coinciding with the low-flow field-measured sample of table 5, is obtained—an annual load from base flow of 630 tonnes per year. From the previous data for rainfall at a maximum reactive value of 28 mg/L of $CaCO_3$ (11.2 mg/L of Ca^{+2}), and 0.1 m^3/s of base flow as the rainfall percolated, a total discharge load of 88 t/yr may be attributed to the effect of rainfall. If 88 t/yr $CaCO_3$ potential solution is by rainfall and 630 t/yr $CaCO_3$ is actual solution, then 542 t/yr $CaCO_3$ is derived from solution through CO_2 contributed from

the soil. According to these data the enrichment in rainwater of CO_2 in the soil from the decomposition of organic acids is responsible for about 86 percent of the solution process, and the acidity of rainwater itself is responsible for 14 percent of the solution of the limestones. Birot and others (1967), from a series of samples collected during overland flow following a storm, estimated that at least three-fourths of the acidity was derived from CO_2 from the soil.

CARBONATE EQUILIBRIA

In calculating the degree to which the water of the north coast limestones is saturated with calcium carbonate, it must be realized at the outset that the computations are carried out with reference to pure calcite for which reasonable equilibrium constants are available. It is not known to what extent the computed results reflect field conditions, that is, whether the limestones depart substantially from pure components.

Back (1961) gives the two reactions

$$CaCO_3 = Ca^{+2} + CO_3^{-2} \quad (22)$$

and

$$HCO_3^- \rightleftharpoons CO_3^{-2} + H^+ \quad (23)$$

whose equilibrium constants are

$$K\ (CaCO_3) = \frac{[Ca^{+2}]\ [CO_3^{-2}]}{[CaCO_3]} \quad (24)$$

and

$$K\ (HCO_3) = \frac{[CO_3^{-2}]\ [H^+]}{[HCO_3^-]} \quad (25)$$

with $[CaCO_3] = 1$, and the basic definition of activity

$$[\ ] = m \cdot \gamma \quad (26)$$

where m is the molality and γ is the activity coefficient. Solving for $[Ca^{+2}]$ from equation 24, inserting $[CO_3^{-2}]$ from equation 25, and making use of equation 26, one obtains

$$m\ Ca = \frac{K(CaCO_3)}{K\ (HCO_3)} \cdot \frac{1}{\gamma Ca \cdot \gamma HCO_3} \cdot \frac{[H^+]}{mHCO_3^-} \quad (27)$$

Because interest is in the ratio of Ca (observed) to Ca (computed), equation 27 can be expressed as

$$\frac{m\text{Ca (obs.)}}{m\text{Ca (comp.)}} = \frac{K(HCO_3)}{K\ (CaCO_3)} \cdot \gamma Ca \cdot \gamma HCO_3 \cdot \frac{m\text{Ca (obs.)}\ mHCO_3}{[H]} \quad (28)$$

and using the symbol S (saturation) for the left hand side of the equation, and expressing molality in units of milligrams per liter and [H] as pH

$$S = \frac{1}{2.44 \cdot 10^9} \frac{K(HCO_3)}{K(CaCO_3)} \cdot \gamma Ca \cdot \gamma HCO_3 \frac{Ca \cdot HCO_3}{10^{-pH}} \quad (29)$$

The ratio of the equilibrium constants and the product of the activity coefficients are a function of temperature and ionic strength, so that a function ϕ can be defined such that

$$\phi = 0.41 \frac{K(HCO_3)}{K(CaCO_3)} \cdot \gamma Ca \cdot \gamma HCO_3 = f(T,I) \quad (30)$$

where

$$I = \text{ionic strength} = 1/2 \Sigma m_i z_i^2, \quad (31)$$

where

m_i is the molality,

z_i is the charge of the ith ion in the solution, and

T is water temperature in degrees Celsius.

By keeping values of the ratio of the equilibrium constants near 1 (that is, taking out 10^{-2}) equation 29 becomes

$$S = \phi\ (T,I)\, Ca \cdot HCO_3 \cdot 10^{\{[pH]-11\}} \quad (32)$$

The function $\phi(T,I)$, with the equilibrium constants and the activity coefficients taken from Back (1961), is graphed in figure 44 versus the ionic strength and temperature. With this and equation 32 one can compute the degree of saturation with respect to calcite of the water from the limestone belt.

In a discussion of the errors involved in these computations, Back (1961) states that pH, bicarbonates, and temperature must be determined in the field. The data of table 5 on pH and bicarbonates are given as determined in the laboratory and in the field, augmented by pH data from Back (1961), and the correlation between the two sets of data are shown in figure 45. The concentration of bicarbonates determined in the field is higher than the concentration of those analyzed in the laboratory by at most 20 percent (excluding one point that is 40 percent higher than the laboratory). Most are well within 10 percent of those determined in the laboratory. The pH tends to be lower in the field, especially, as expected, in tests of water from springs. Those samples that show a lower laboratory pH are not readily explainable and as it occurred to Birot and others (1967) in their sampling of karstic water, cannot be ascribed to random instrumental or operator's errors.

As is apparent from equation 32, the pH is overwhelmingly significant in the computation of satura-

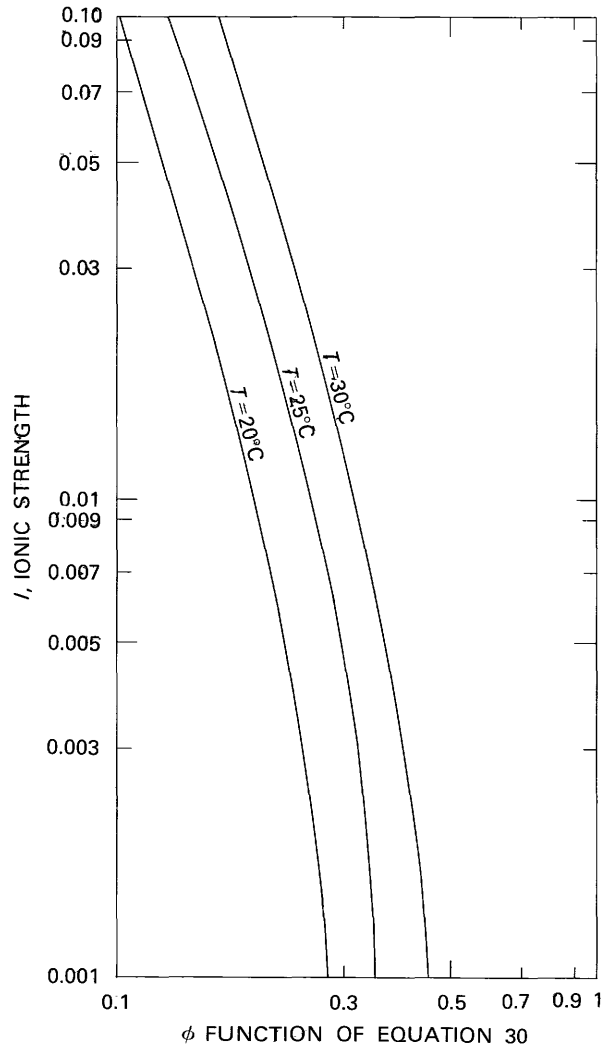

FIGURE 44.—Relation between ϕ of equation 30 and ionic strength and temperature.

tion. Further simplifications of equation 32 are possible from empirical expressions that relate the bicarbonate concentration and the ϕ function to the calcium concentration of the solution at an average temperature of 25°C. These relations are shown in figure 46, and the correlation between Ca and HCO_3 is well defined, with 95 percent of the points falling within an error band of ±30 percent. The relationship Ca versus ionic strength shows larger scatter and it breaks down, as expected, for more concentrated water with ionic strength greater than 0.01. Still, the ϕ function of figure 44 shows that its range of values is quite restricted so that, for diluted solutions, even the approximate value of the ionic strength that can be obtained from the calcium versus ionic strength relation is sufficient to give workable values. So, by using the results of figure 46 saturation can be expressed as a function of calcium concentration and pH only as given by the equation

$$S=\phi'(\mathrm{Ca})^2\,10^{\{\mathrm{pH}-11\}} \qquad (33)$$

where ϕ' is a function of calcium concentration for a temperature of 25°C.

The expression above is graphed in figure 47 with the data of tables 5 and 6 plotted therein. Also shown as vertical lines is the deviation between the more precise saturation values computed from equation 32 and those from the empirical approximation using calcium and pH data only. The results are nearly the same except for a few of the empirical saturation values which depart somewhat from the theoretical ones. In no case is the saturation boundary crossed (that is, all the theoretically unsaturated or oversaturated samples are also from the empirical approximation). The lake samples, as previously noted, are undersaturated and only one, spring-fed, approaches saturation. At the other extreme, all the ground water (from routine well-water analyses) is either supersaturated or near saturation. For a clearer discussion the saturation ratios (exclusive of well data) are plotted in figure 48 next to the sampling points. The streams are all undersaturated before entering the limestone belt and become saturated or supersaturated before reaching their mouth. The sampling was not extensive enough to determine whether the saturation is progressively increased or decreased in a downstream direction. During a trip down the Río Guajataca, travertine was seen along the stream channel, so it is evident that some precipitation of calcium carbonate takes place. The combination of degree of saturation in relation to the stream velocity that leads to the precipitation of travertine is unknown. There is an indication that water from the Cibao Formation is more supersaturated than that of other limestone formations, but the reasons for this are not known.

RECONSTRUCTION OF THE GEOLOGIC AND HYDROLOGIC HISTORY

Paleontological evidence from the sequence of about 1,400 meters of limestone and minor sedimentary clastics that are now exposed on the north coast of Puerto Rico indicates deposition started about middle Miocene according to Gordon (1959), or middle Oligocene to middle Miocene according to most investigators, and continued possibly until middle Pliocene according to G. A. Seiglie (oral commun., 1969). Assuming that middle Miocene, middle Oligocene, and middle Pliocene correspond to

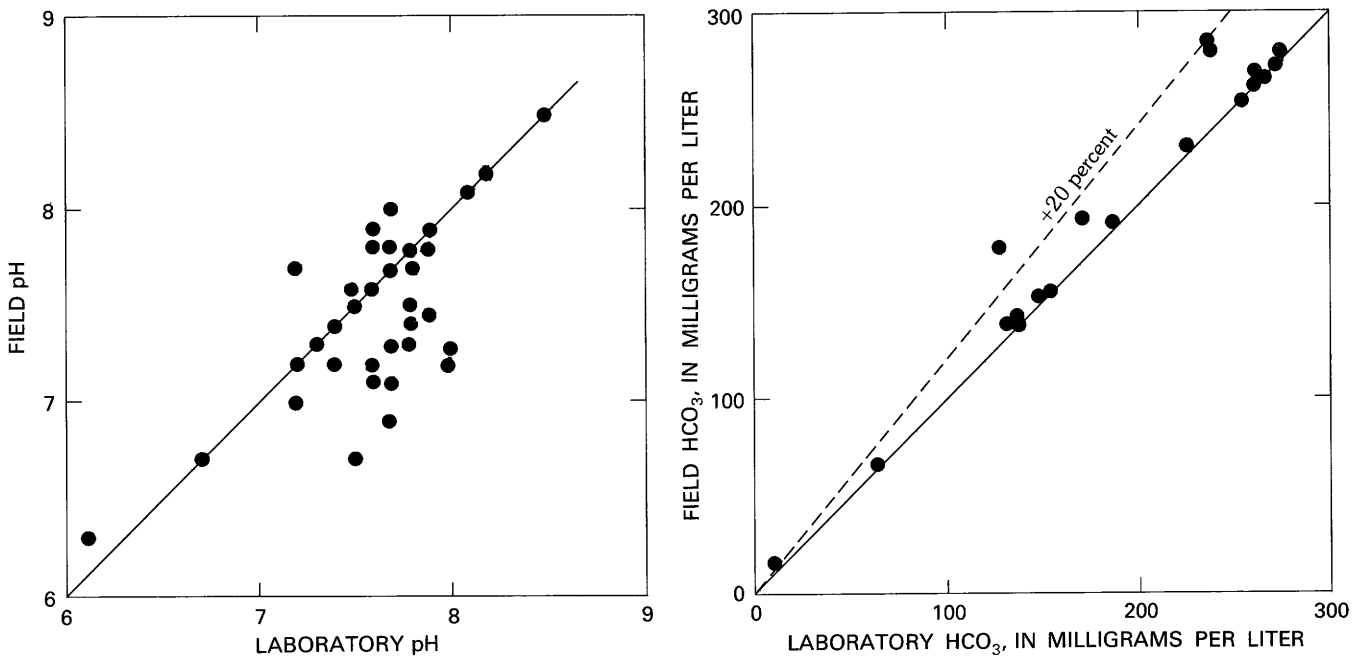

FIGURE 45.—Correlation between field and laboratory determinations of pH and bicarbonate concentration.

about 17, 32, and 5 million years ago, respectively, the rate of sedimentation would calculate to be about 0.12 mm per year (1,400 meters per 12 million years) or 0.05 mm per year (1,400 meters per 27 million years) making no adjustment for change of thickness resulting from compaction.

The rate of sedimentation based on a middle Miocene age for the oldest sediments appears to be too high if compared with maximum rates of sedimentation of 0.01 to 0.02 mm per year reported by Keunen (1950) for *Globigerina* ooze and the chalky deposits of the Paris basin. For this reason, the beginning of sedimentary deposition on the north coast of Puerto Rico is considered to be middle Oligocene in age—a view held in most of the literature. Sedimentation closed near the end of the Tertiary Period with the deposition of the Camuy Formation; the deposition of the Camuy was followed by or was contemporaneous with the arching up of the Puerto Rican platform.

On the basis of the hydrologic and geochemical data presented it is possible to determine, albeit roughly, the time when the limestones emerged from the sea and their dissolution began. Several assumptions and approximations are needed in making such an assessment:

1. The present bioclimatological conditions (vegetation cover and rainfall-evaporation) do not depart greatly from those of the past, either in quality or quantity.
2. It is possible to reconstruct the general configuration and height of the original limestone surface.
3. The physical and chemical properties of the dissolved material were not different from those measured on the material of the present surface.
4. No large vertical tectonic movement occurred, after the emergence of the limestones.
5. The lowering of the original limestone surface took place largely through the solution process.

Assumption 1 is justified by the fact that the limestone belt is presently as densely covered with vegetation as it can be and enrichment of CO_2 in the soil through the decomposition of organic matter should be at a maximum. Man's activities, with the accompanying increase of erosion and solution, are at a minimum within the general area and nearly absent in the more rugged part of the limestone belt. Therefore, the rock and water samples collected are free of or negligibly influenced by man. The rainfall-evaporation function has varied, no doubt, through geologic time. The consolidated sand dunes of the north coast bear testimony to both the lowered sea level of glacial times—hence to an increase of sand supply—and to lower rainfall (because under present rainfall conditions, vegetation grows readily nearly up to the strandline and would have trapped the sand available during periods of lower sea levels. However, glacial times would have increased the

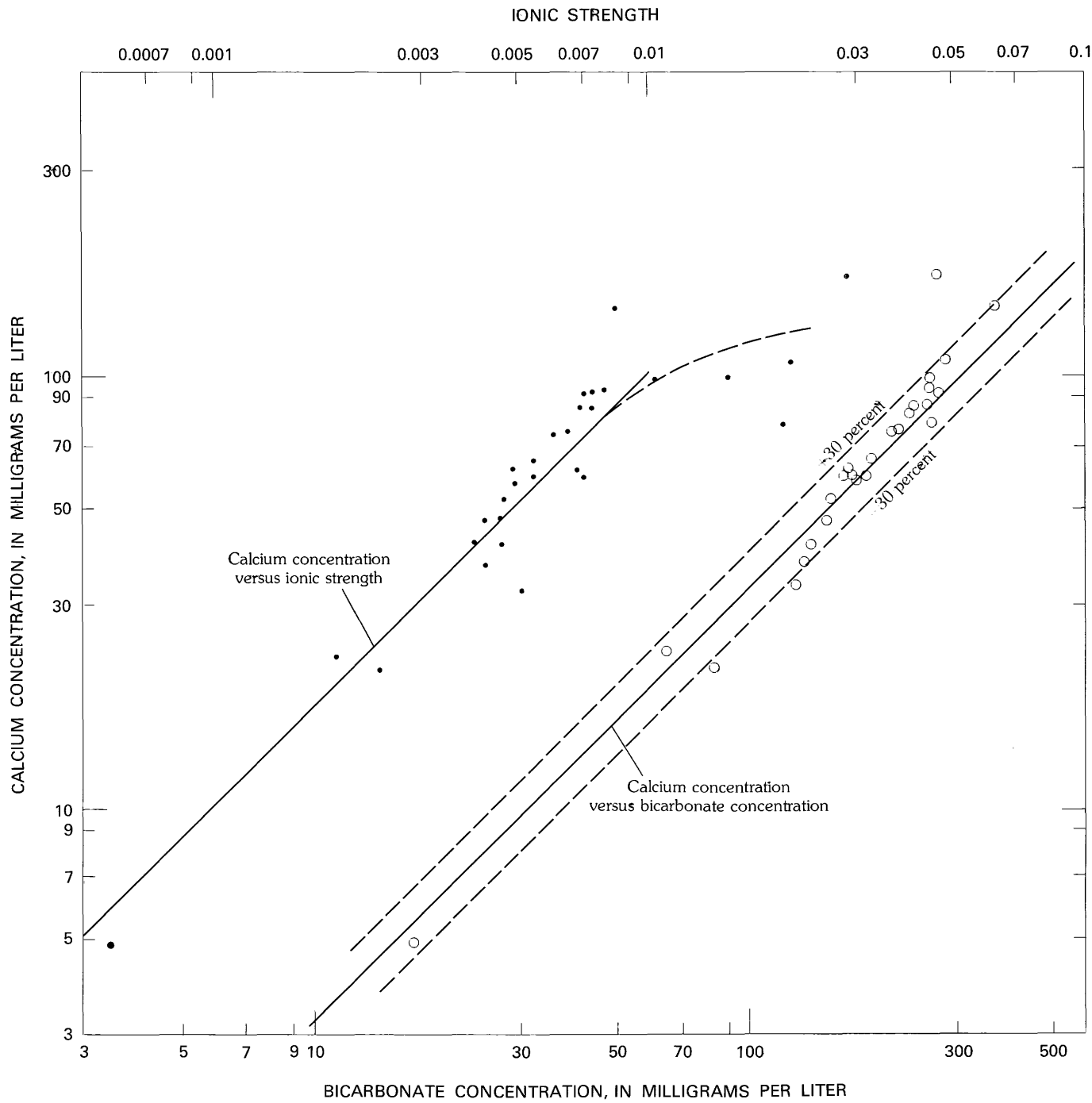

FIGURE 46.—Relation between calcium concentration and ionic strength and between calcium concentration and bicarbonate concentration.

limestone solubility through a lowering of temperature, so that some justification exists for using present rainfall-evaporation functions, and present calcium concentration values.

Assumption 2 is justified because the simple wedge structure and the uniformity of dip of the limestones permit a usable reconstruction of the height of the original surface. Of the other assumptions, 3 seems reasonable if some allowance is made for the more clastic nature of the original surface material especially toward the contact with the volcanic core; and 5 can accommodate with no great error the possible presence of an ancestral fluvial system formed on more clastic material, with lesser

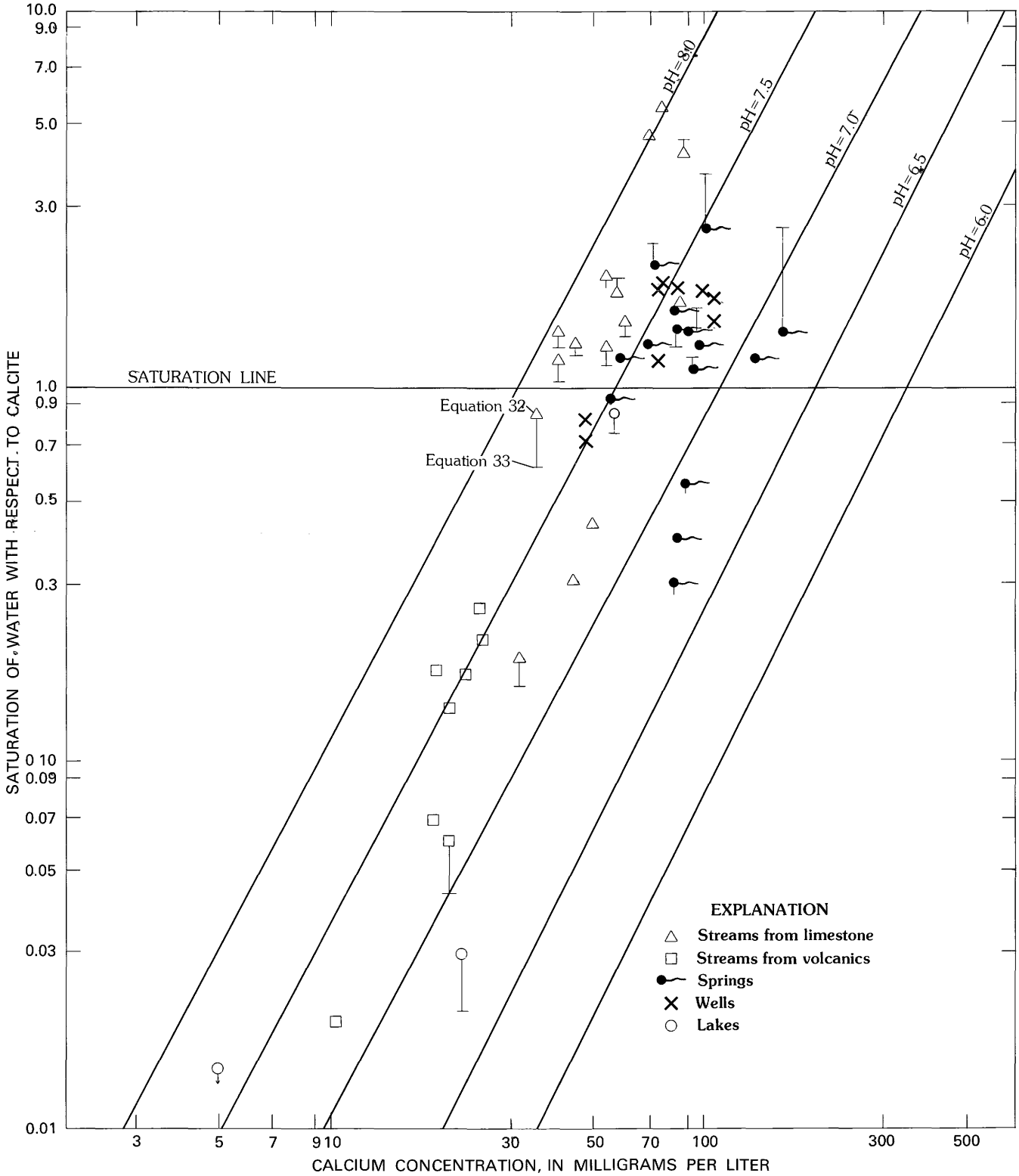

FIGURE 47.—Saturation of water with respect to calcite as a function of calcium concentration and pH. Vertical lines represent saturation values from equations 32 and 33 in text.

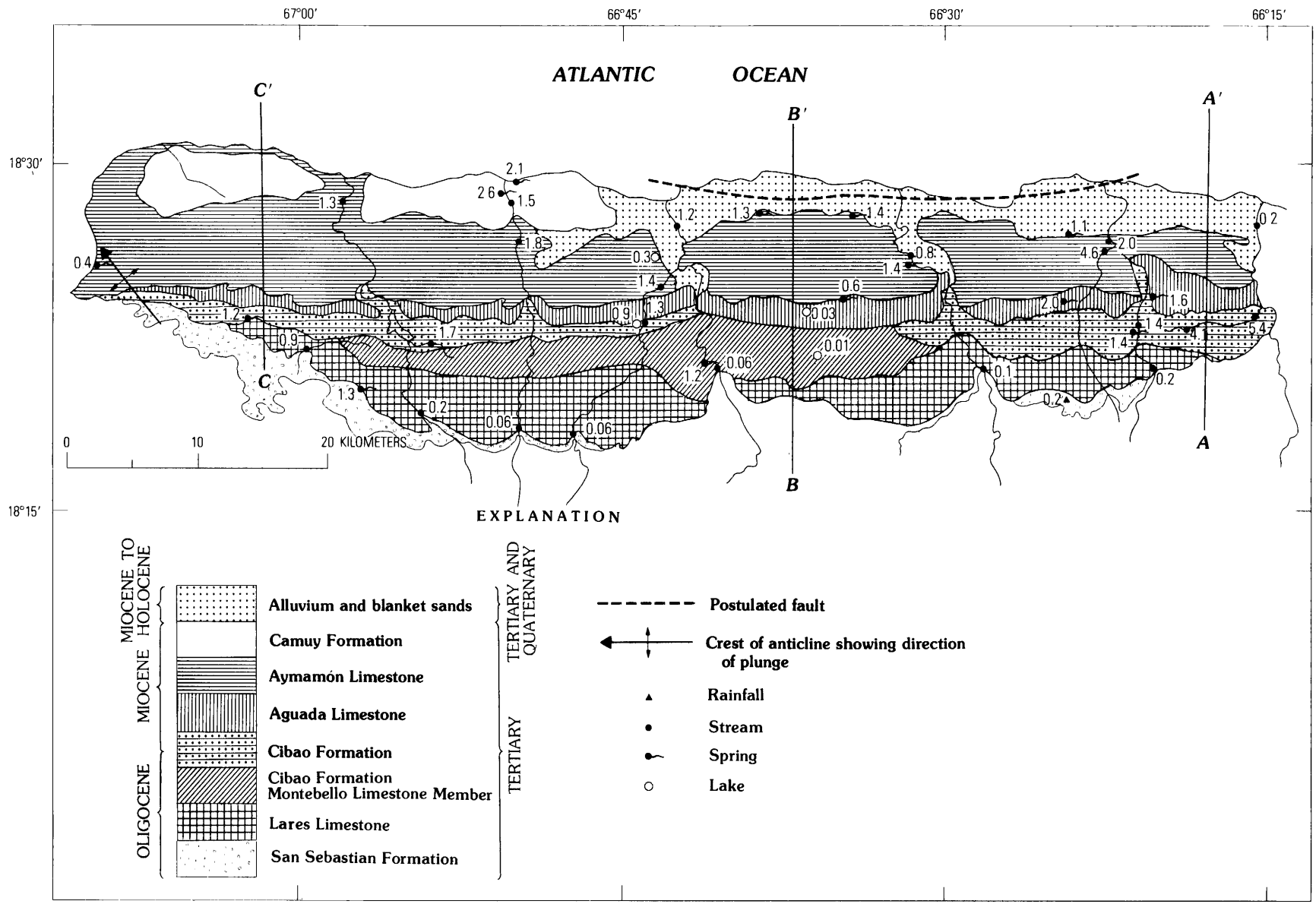

FIGURE 48.—Saturation ratio of waters from north coast limestone and volcanics.

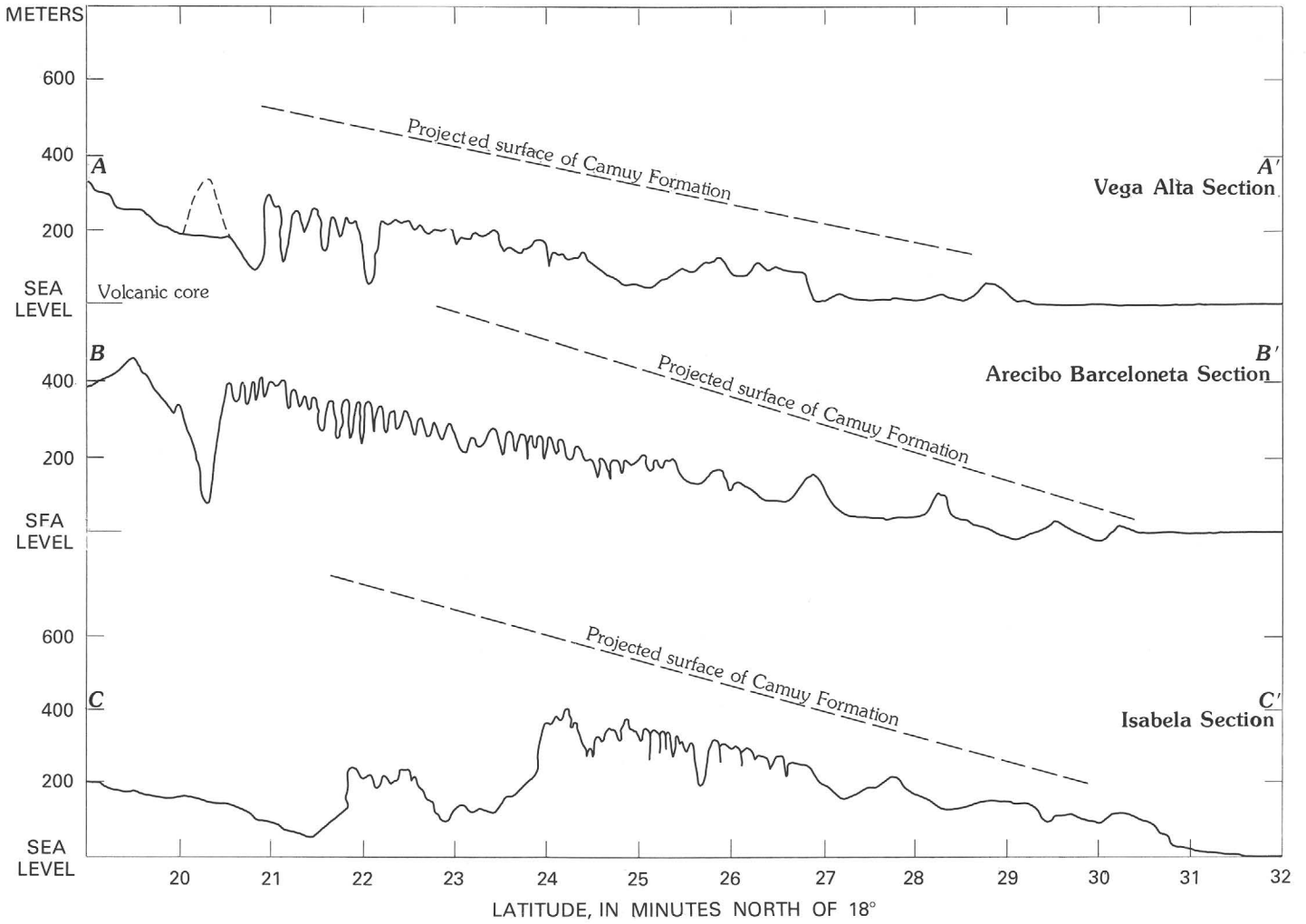

FIGURE 49.—Sections south-north through the limestone belt, with projected original surface of the Camuy Formation. (See figure 48 for location of sections.)

solution and more abrasion. No evidence is reported in the literature for or against assumption 4 other than possible tilting in Pleistocene time. The computations of the time when the limestones began to be dissolved shall be used to test this assumption.

An interpretation of profiles of the original surface is shown in figure 49 for three sections thought to be representative. The surface has been projected according to the dip of the formations and to their thinning southward as best as can be calculated from the detailed geologic maps of Monroe (1962, 1969a) and Briggs (1961), and from the few deep wells drilled in the area. The Camuy Formation is assumed to have been about 150 m thick near the coast, an estimated average based on the maximum thickness of 180 m for the Camuy given by Briggs and Akers (1965). The difference between the projected surface of the Camuy and the mean altitude of the present land surface (fig. 12) represents the amount of limestone removed since the time of emergence of the Puerto Rican platform. To compare the total volume of the calcium carbonate of the limestone removed by solution with the calcium carbonate concentrations measured in the water, the following factors are involved:

1. the calcium carbonate content.
2. the primary intergranular porosity.
3. the secondary porosity of the formation, accounting for the space between larger pieces of limestone; fractures, bedding planes or reef structures (figs. 50 and 51).

Data for 1 and 2 were obtained from table 4, and 0.1 was taken as the value of porosity for 3. Having obtained a slab thickness of pure calcium carbonate by the method just outlined, the next step was to obtain the thickness of calcium carbonate removed annually. For this, figure 23 was used together with

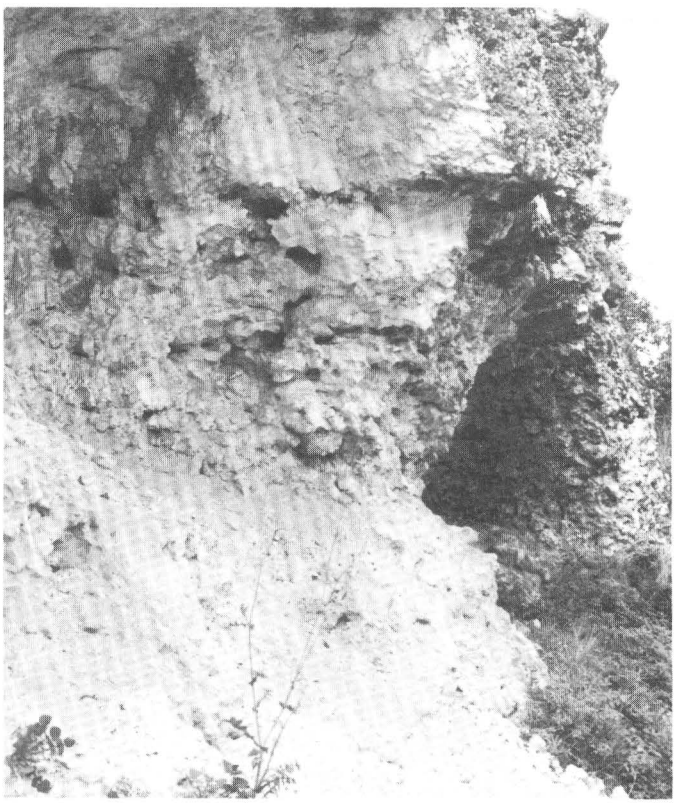

FIGURE 50.—Secondary permeability developed on chalky Aymamón Limestone. In this solution riddled limestone, water moves through much as through a sponge.

the average annual rainfall to compute the evapotranspiration and the subsequent discharge. The discharge is further assumed to carry an average concentration of 200 mg/L of $CaCO_3$ as obtained from the data of table 5. No adjustment was made for the $CaCO_3$ carried by rainfall—a negligible amount. An example is shown of the computations carried out for a piece of the cross section *B–B′* of figure 49 between latitude 18°22′ N. and 18°23′ N.

Altitude of original surface = 550 m
Mean altitude of present surface = 230 m
Thickness of removed slab = 320 m
Average $CaCO_3$ content = 0.85, average primary porosity = 0.15, average secondary porosity = 0.10
Thickness of equivalent $CaCO_3$ slab = $320 \times 0.85 \times 0.85 \times 0.90 = 210$ m
Average annual rainfall = 1,750 mm
Average annual evapotranspiration = 1,000 mm
Average annual outflow = 750 mm
Average concentration of $CaCO_3$ in outflow = 200 mg/L = 0.2×10^{-3} g/cm^3 = 0.074×10^{-3} (using a $CaCO_3$ density of 2.72 g/cm^3)

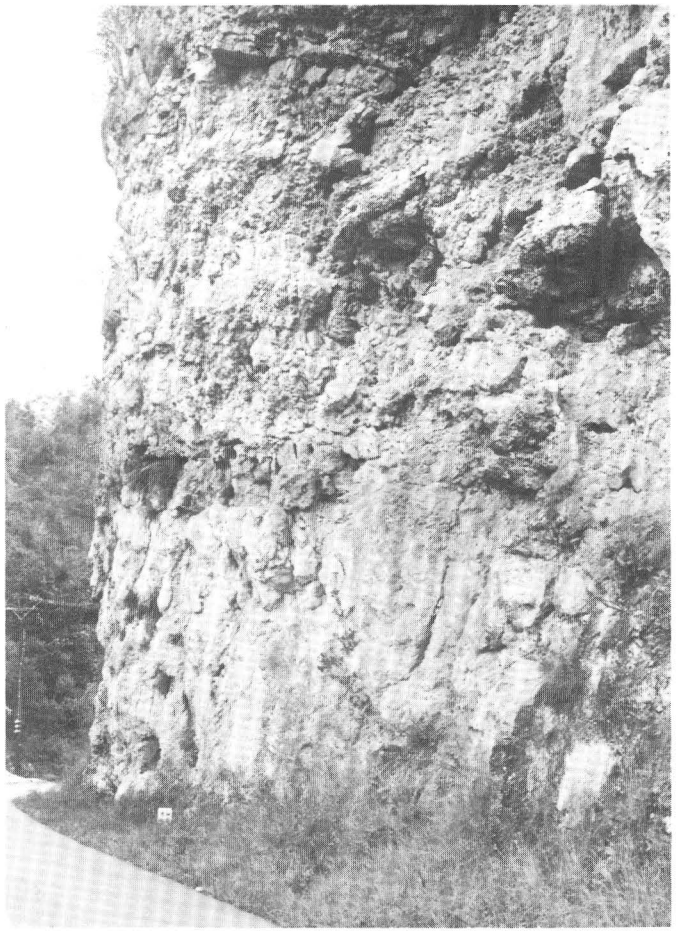

FIGURE 51.—Secondary permeability developed on Aguada Limestone. Water moves through openings between larger limestone clasts.

Average solution rate = 750 mm/yr $\times$ 0.074 $\times 10^{-3}$ = 0.055 mm/yr
Time needed to dissolve 210 m of $CaCO_3$ = 3.8 million years

This value of 3.8 million years is computed assuming only solution. Where fluvial drainage is present it is possible to compute the contribution to erosion of the abrasion process. In section *A–A′* of figure 49 between latitude 18°22′ N. and 18°23′ N. the karst surface is cut by a river. If we assume that the next 1-minute of latitude of the section immediately to the south underwent only solutioning from the same beginning time, we can write for the Vega Alta section:

Between latitude 18°21′ N. and 18°22′ N.

Solution rate $\times$ time = thickness of equivalent $CaCO_3$ slab, or 0.055 mm/yr $\times t_1 = 280$ m

Between latitude 18°22′N. and 18°23′ N.

(Solution rate + abrasion rate) × time = thickness of equivalent $CaCO_3$ slab, or

(0.055 mm/yr + abrasion rate) $t_2 = 290$ m

and, assuming that $t_1 = t_2$

$$\text{Abrasion rate} = 0.007 \text{ mm/yr}$$

and the relation between abrasion and solution rates is

$$\frac{\text{Abrasion rate}}{\text{Solution rate}} = \frac{0.007}{0.055}$$

or

$$\text{Abrasion rate} = 0.13 \text{ Solution rate.}$$

The calculations shown refer to an area where one small river has cut a canyon through the karst surface, perhaps through collapse of a former underground channel. The abrasion rate computed is probably a minimum.

The previous computations carried through in the area between latitude 18°21′ N. and 18°23′ N. of the Isabela section *C–C′* where a true fluvial system is present, give much larger results for abrasion: there

$$\frac{\text{Abrasion rate}}{\text{Solution rate}} = \frac{0.024}{0.063} = 0.38$$

or

$$\text{Abrasion rate} = 0.38 \text{ Solution rate}$$

and this can probably be considered a more significant ratio.

The solution rates and the time since solution began, computed for the three sections of figure 49, adjusted for abrasion rates where applicable, are shown in table 8. The variability in time since the onset of solution among the sections is probably due to sampling error except for the uniformly lower values of section *C–C′*. These lower values are thought to be indicative of the Pleistocene tilting and, taking an age of 3.6 to 4 million years as an average for the beginning of the erosion process or the time of emergence of the limestones, and 2.6 to 3.0 million years as the apparent age of the most seaward part of the Isabela section, the tilting can be dated as the difference in the two times, or about 1 million years ago.

Birot and others (1967) compute 2 million years as the time needed to erode a circular doline 100 m deep, and this is the same order of time computed here for an equivalent thickness of limestone.

The author's view is that tectonic movements have been responsible for the high Pleistocene terraces and eolianities described by Monroe (1968a) and Kaye (1959), but these investigators prefer eustatic movements (changes in sea level) as the explanation.

HISTORICAL DEVELOPMENT OF THE PUERTO RICAN KARST

According to the computations of the previous section, about 4 million years ago the north coast of Puerto Rico completed its emergence from the sea and the dissolution of the limestones began (it had probably started earlier near the contact of the limestones with the volcanic mountain core). A view of the area as it might have looked about 3.8 million years ago is shown in figure 53.

The drainage in the limestone belt in the west near the contact with the volcanics is assumed to have been southward to the ancestral Río Culebrinas, which was cutting a deep canyon at the volcanics-limestones contact. Subterranean drainage in a slight northwesterly direction is assumed to have been taken by all the rivers west of the city of Arecibo. All the rivers from the city of Arecibo east are presumed to have cut through the limestone belt by this time (fig. 52). It is further assumed that a mature karst existed in the east and that an incipient karst was forming in the west.

TABLE 8.—*Solution rates (in millimeters per year) and times (in million years) since solution began*

Latitude	Sections in figure 49					
	A–A′		*B–B′*		*C–C′*	
	Solution rate (mm per yr)	Time since solution began	Solution rate (mm per yr)	Time since solution began	Solution rate (mm per yr)	Time since solution began
18°29′	----	--	----	--	0.028	2.6
28′	----	--	----	--	.032	3.0
27′	----	--	0.035	4.0	.035	3.0
26′	0.035	3.7	.040	3.7	.042	3.3
25′	.040	3.2	.040	4.1	.049	3.4
24′	.040	3.8	.045	4.2	.052	3.6
23′	.045	3.5	.050	3.8	.056	[1] 3.6
22′	.050	[1] 3.5	.055	3.8	.063	[1] 3.6
21′	.055	3.1	.060	4.0	.063	[1] 3.6
20′	----	--	.060	4.0	----	--

[1] Adjusted for abrasion.

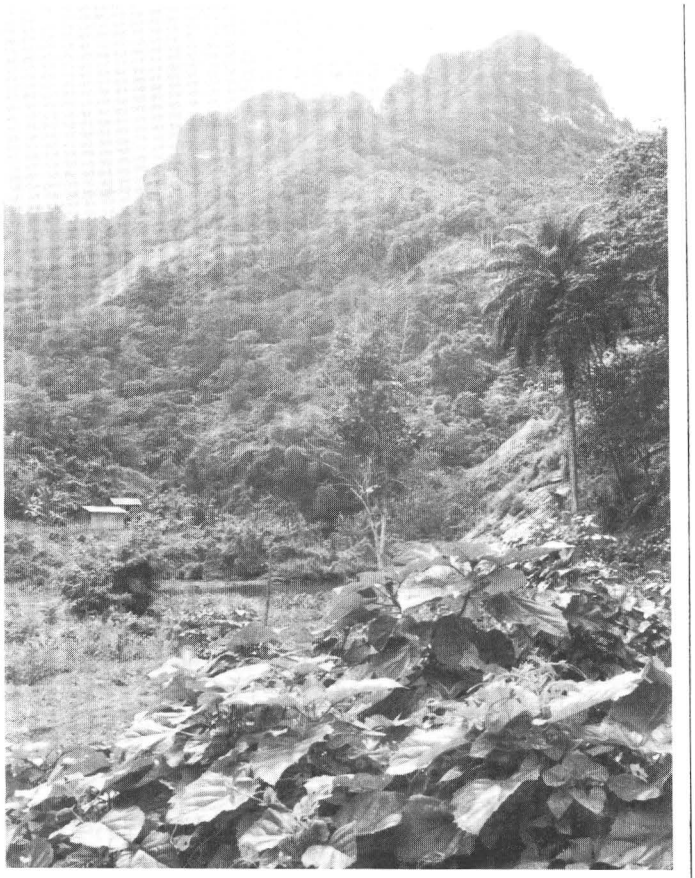

FIGURE 52.—Limestone knobs left as residuals on top of volcanic rocks by downcutting of the Río Grande de Arecibo.

Solution presumably continued to about 1 million years ago; during the process geomorphic development led to capture of part of the south-draining karst by the Río Guajataca, development of part of the Ríos Camuy and Tanamá, and the development of flood plains in the eastern rivers. At that time the karst between the Río de la Plata and the Río Grande de Arecibo is thought to have entered its final phase, characterized by the formation of mogotes covered by blanket sands weathered in situ or carried northward from higher altitudes. In the west, cockpit karst developed in the permeable formations, and a fluvial system formed on the more impermeable rocks.

About a million years ago tectonic activity raised the north coast limestones in the northwest and tilted eastward the entire Puerto Rican platform. The rise and tilt brought about a shift in the direction of drainage, as is interpreted from figure 54, a series of histograms of stream channel orientation for the various limestone formations. Qualitatively, attention is called to the multipeaked distribution of all the flow directions and to the flow directions

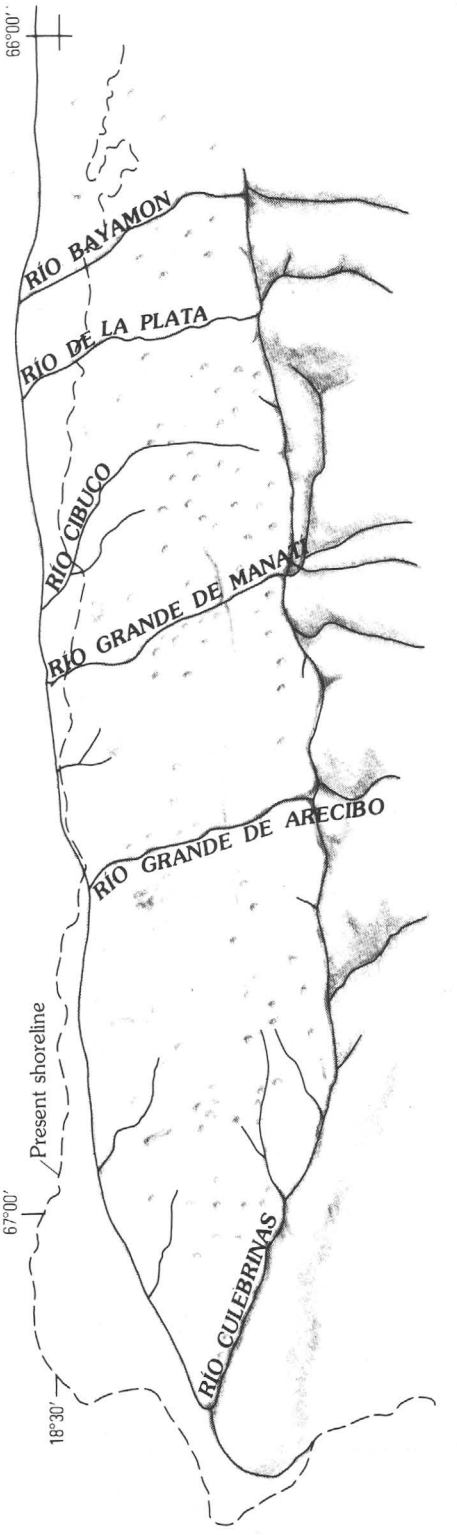

FIGURE 53.—A view of the north coast belt 3.8 million years ago.

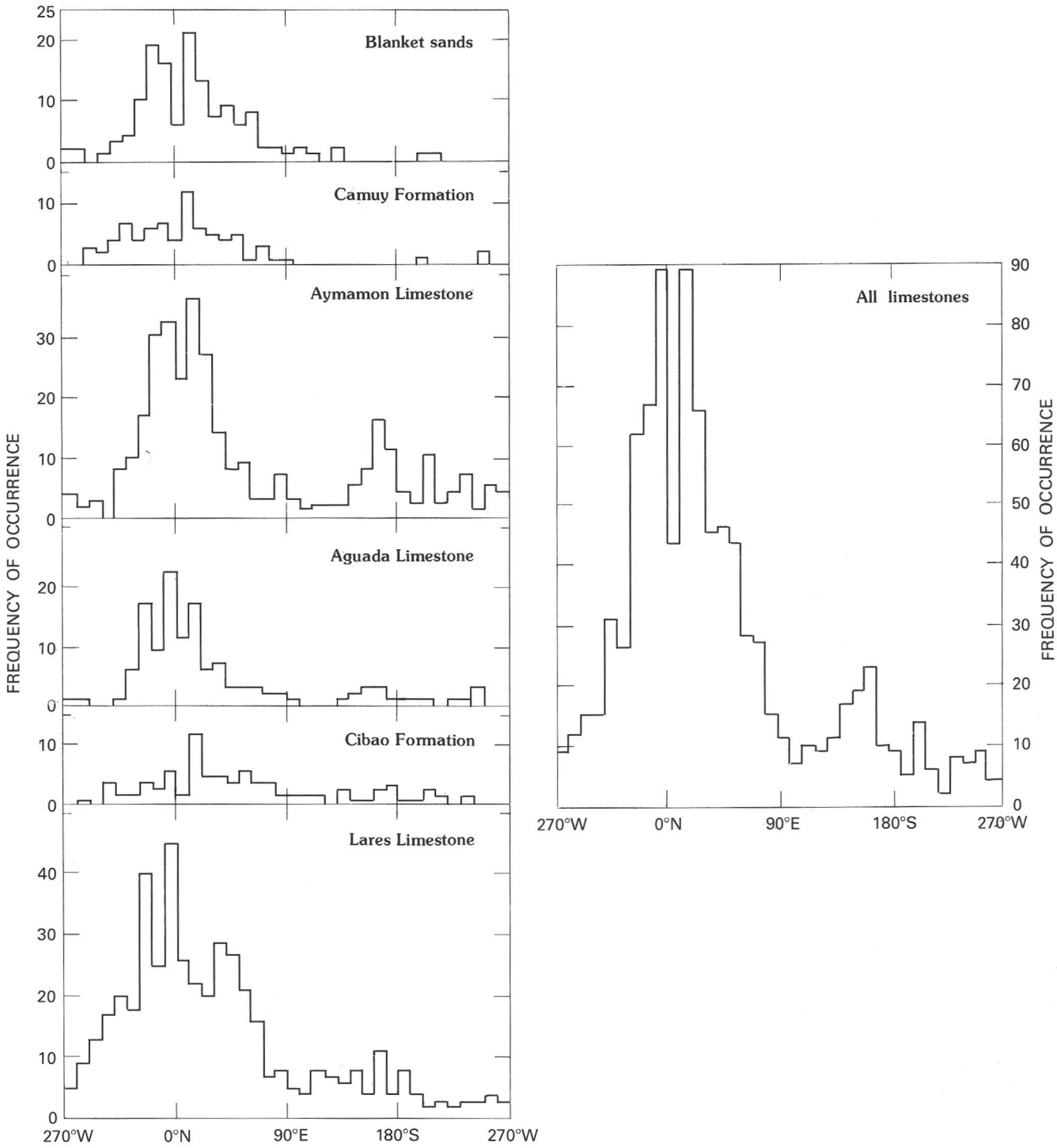

FIGURE 54.—Distribution of stream channel orientations in the north coast limestones.

of those formations exhibiting clearly multipeaked distribution .The main western peak in these cases (modal values of about −10° or 350°, is interpreted as a fossil drainage direction from pre-tilt times. Two formations are either single peaked (assuming that the ups and downs of the histograms are due to sampling errors) or weakly multipeaked: (1) the Camuy, which is the youngest, most lithologically variable, and most seaward formation, and (2) the Cibao, which is a formation that has a clearly developed fluvial system. The lack of a predominant peak in the histogram to show a preferential direc-

tion west of north is inferred to indicate that the abrasion process has erased the evidence of the vestigial drainage direction still present in the other formations. In the purer limestones the solution process has etched in depth the former paths of flow. It should also be noted in figure 54, that all mean values of the distributions would only indicate an orientation of stream channels in an eastward direction and thus fail to disclose the admittedly subjective assignment of some drainage to a westward direction as just discussed. The tilt of the Puerto Rican platform is also taken to have affected the directional pattern of subterranean drainage, leading to development of springs mainly on the west side of rivers, especially in the western part of the belt. The coastal swampy area east of Arecibo is also ascribed to the tilt, as is the raised shoreline west of Arecibo.

FACTORS OF KARSTIFICATION

The north coast Puerto Rican karst, with its peculiar landscape called "lunar" by Monroe (1968b) and, with Gallic sagacity, "á mamelons" by Birot and others (1967), is notably different from the classic karst of Yugoslavia: there are no uvalas (depressions 1 to 10 kilometers in diameter), no poljes, and karren or lapiez are scarce. Perhaps some forms of mogote karst are a local equivalent of the uvalas and poljes; certainly they do not look the same. Birot and others (1967) find it difficult to explain the differences of this karst from that of other areas, particularly that of the temperate zone. In a search for explanations temperate zone karst investigators suggest climatic differences, though they admit to having no final answer. Monroe, (1966) as already discussed, favors, lithologic and stratigraphic differences to explain the various landforms of the Puerto Rican karst; he has not yet compared this karst to that of other places. Traditionally, of course, climate, percentage of $CaCO_3$ in the rocks, and the regional structure have been set forth as the cause and, in particular, since most investigators of karst have been European, fracturing has invariably been suggested as the primary condition for the beginning of the karst. The Puerto Rican limestones of the north coast, however, are not obviously fractured as the European limestones are. Jointing is inconspicuous as can be seen from the photographs shown so far, including one (fig. 55) taken on a cut in the Lares Formation. There are, to be sure, open spaces between the larger pieces of limestone, through which water can percolate and even create vertical caves (fig. 56), but there are no vertical shafts or obvious fractures. The absence of joints, however, does not keep water from infiltrating; on the contrary it does so quite readily, much as it does in fine alluvial material or through soil, and even if the limestones had no void space between the larger clasts, water could infiltrate through the primary openings of the rocks. (See table 4.) The development of the karst only requires that water infiltrate—no significance is attached to the manner in which infiltration takes place.

Presently the limestones are being preferentially dissolved under the blanket sands because of the existence of the hardened limestone shell covering the mogotes, as explained by Monroe (1966). However, on a larger scale it may be argued, and Birot and others (1967) tacitly assume it, that there are regional fractures and joints such that dolines are formed at the intersection of the fracture planes and mogotes are formed in the area between the fractures. This view deserves testing, as clearly then there should be a preferential arrangement of

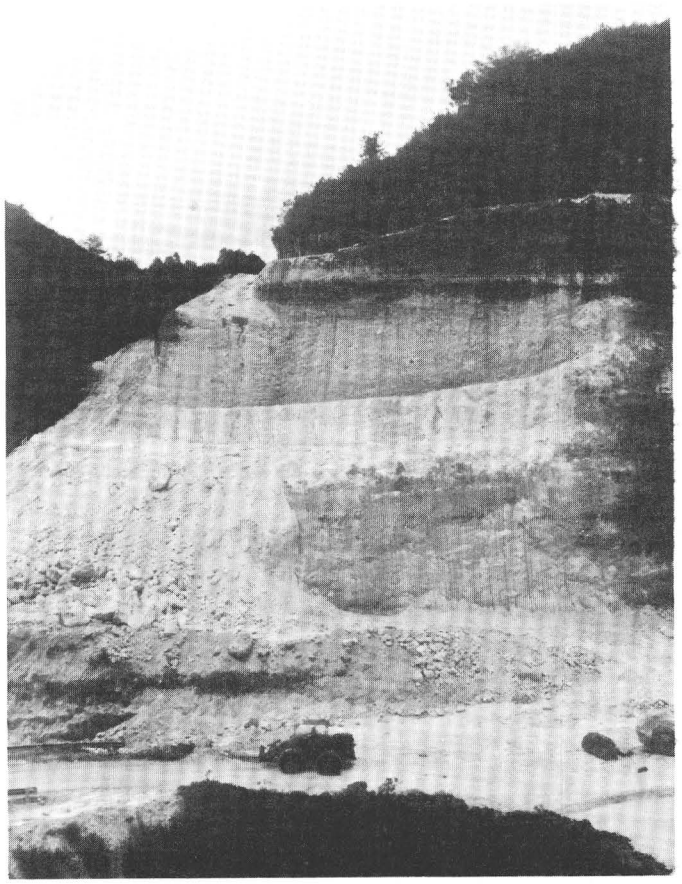

FIGURE 55.—A cut through a mogote of Lares Limestone. Note the absence of fracturing. (Photograph by Rafael Dacosta).

FIGURE 56.—Small cave in Aguada Limestone. Water percolates much as through soil layers—no fracturing.

dolines in some direction. A qualitative test of this interpretation is demonstrated in figure 57, which shows a random arrangement of dolines (drawn from a table of random numbers), two actual examples from the north coast karst, and an assumed geometrical arrangement of dolines. A distribution of orientations can be obtained by counting the number of dots recorded within a plastic strip (about 2.5 cm wide) superimposed and rotated on the various arrangements of dots of figure 57. Using six strips orientations and assuming equal count per orientation, valid intuitively for a random arrangement, a chi-square test can be used.

The results of this test, shown in table 9, indicate that dolines are located randomly within the space of the two sampled areas. As expected, the geometrical arrangement of dolines tested to be nonrandom. Therefore, it is concluded that water infiltrates through no preferential path and that dolines are randomly distributed. The flow directions that show preferential orientation at the scale of the entire belt resulted from the topographic gradient and were not the result of jointing or fracturing. (See Williams (1965), p. 67–80.)

Leopold and Langbein (1962) have investigated the development of river drainage networks and have derived by random walks river networks quite similar, at least on a gross scale, to the real ones. It appears that an equivalent condition is present in the karst of Puerto Rico through random arrangement of solutional features. If this is so then, it is not the "classical" European karst that we should look to for a more clear understanding of the beginning of karst development, and certainly it should not be taken as the standard to which other karsts are to be compared. The karst of the north coast of Puerto Rico, showing as it does, all degrees and shades of karstification, from the incipient stage forming on the raised platform of the northwest to the completed denudation of the northwestern coastal flats, offers a vast field of profitable investigation on its own. And because this karst appears to be the product of random solution on a structurally simple wedge and on relatively young unfractured limestones which, at places, seem to have the consistency of freshly deposited material (fig. 58), it may be regarded as the sequence of erosional stages which the limestone terrane goes through when newly emerged from the sea.

The question of rock hardness or density and fracturing is thought to be of crucial importance for determining the type of karst features that will develop on a carbonate-rock terrane. There are, for example, among the Cretaceous and older Tertiary limestones of Puerto Rico (fig. 1), areas where the rocks are fractured and indurated; in these areas the similarity (on a small scale) to the European karst becomes more apparent, for both karsts contain lapie fields and funnel-shaped dolines. Clearly the different morphologies cannot be explained by climatic differences because the climate where the Cretaceous and older Tertiary limestones are located is nearly the same as that of the north coast limestones. Even the dismissal of a lack of an extensive karst development on the limestone belt of the south coast because of an arid climate, may be erroneous as Moussa (1969) points out. Nonetheless one would expect climate to exert some influence on karst development and on its morphology in that the rate at which rock solution takes place, other things being equal, depends in part on the amount of net precipitation coming in contact with the limestones. Furthermore soils and vegetation are thicker and more abundant in humid than in arid areas and thus there is a better opportunity for the

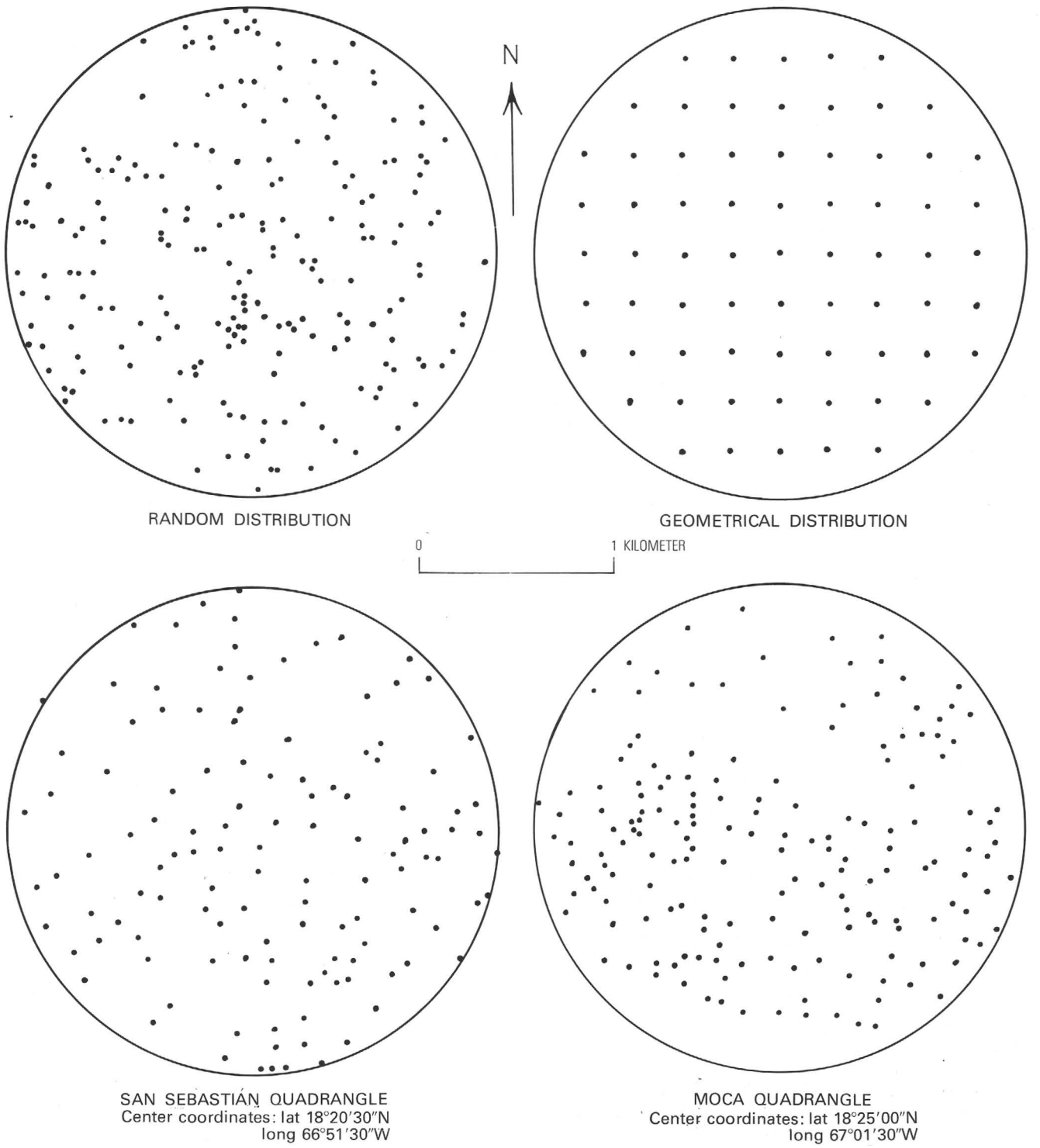

FIGURE 57.—Spatial distribution of dolines.

development of organic acids which contribute significantly to the solution process.

Clearly the $CaCO_3$ content of the rocks determines the threshold between the formation of a karst or a fluvial drainage (for example, the lithology of the Cibao Formation). Given that the limestones are sufficiently pure as to be readily dissolved by acidic water, it is thought that the two primary factors which determine the karst morphology at a given stage in time are vertical and lateral rock

TABLE 9.—*Chi-square test of doline orientation*
[Areal distribution shown in figure 57]

Orientation, degrees	Observed frequency, in percent				Theoretical frequency, in percent
	Random dolines	Grid-alined dolines	Actual dolines		
0–180	12	25	11	22	16.7
30–210	20	12	14	14	16.7
60–240	10	12	18	19	16.7
90–270	22	25	23	19	16.7
120–300	19	12	20	11	16.7
150–330	17	12	14	16	16.7
χ^2(5df)	6.67	13.54	5.95	4.73	---

permeability (either primary or from fracturing) and the primary porosity or rock density. Climate, lacking proof to the contrary, is tentatively placed at a lower level of importance.

SUMMARY AND CONCLUSIONS

The north coast limestone area of Puerto Rico is underlain by a sequence of six formations which range in age from middle Oligocene to middle Miocene (or as young as middle Pliocene(?)). These formations from oldest to youngest are known as San Sebastián Formation, Lares Limestone, Cibao Formation, Aguada and Aymamón Limestones, and Camuy Formation. All the formations, except for the first, which is mainly a claystone and the third which is a mixture of marl, chalk, sand, and clay, are nearly pure limestones. Little structural deformation is shown by the formations, and this broad mass of rocks can be described as forming a homocline gently inclined to the north.

All degrees of karst development can be found on the limestone surfaces except for the San Sebastián Formation and parts of the Cibao Formation; these two formations have developed a dendritic fluvial drainage. The surface and subsurface paths taken by precipitation falling on the karst are different from those found in fluvial drainage basins and even in alluvial ground-water provinces. In terms of the water balance, however, most of the

FIGURE 58.—The limestone is so soft, in places, that a knife is sufficient for this modern sculptor. Montebello Limestone Member of Cibao Formation at entrance of Arecibo Astronomical Observatory. (Photograph by Rafael Dacosta).

rainfall on the karst can be accounted for by streamflow or lagoonal discharge, when consideration is given to losses by evapotranspiration.

The climatic factors which condition this discharge are:

1. Average rainfall ranging from 1,550 mm on the coast to 2,300 mm at the higher elevations, or 1,800 mm as an overall average.
2. Incoming total solar radiation (direct plus diffuse sky), expressed as about 4,000 mm of evaporated water for cloudless sky or about 2,900 mm under the average cloud cover; resulting in an average potential evapotranspiration of about 1,500 mm.

For the average climatic conditions, the actual evapotranspiration is about 1,100 mm and the discharge is about 650 mm. The discharge may follow surface or subsurface paths whose pattern is controlled by the karst development. In the impure Cibao Formation and in the northwestern part of the Lares Limestone area, discharge is predominantly by surface drainage with subsequent infiltration in the karst of the Aguada Limestone, where the Cibao dips under it. Elsewhere in the karst the discharge is subsurface partly as transient tributary flow to those rivers alined in the general direction of the ground-water flow (south to north) and partly as saturated flow in the areas between the rivers.

The ground-water flow is under water-table conditions in the Aymamón and Aguada Limestones; discharge occurs in a strip near the coastline along a freshwater–seawater interface created by the difference in density between freshwater and seawater. East of Arecibo, much of the ground water discharges landward of the shoreline, in springs, lakes, and swamps, and is dissipated by evapotranspiration or by surface outflow to the sea. The direct discharge to the sea in this area probably emerges uniformly (rather than through springs) through the seabed and diffuses into the sea. West of Arecibo, and in increasing amounts toward Aguadilla, however, the ground-water discharge appears to be predominantly on the seaward side of the shoreline and may emerge in places as spring flow through the sea bottom.

In the downdip parts of the Montebello Limestone between Arecibo and Mantatí, the groundwater flow is under artesian conditions, confined by low-permeability layers of massive limestone and by certain nearly impermeable sections of the Cibao. The artesian flow emerges through submarine outflow areas at an unkown distance from the coast and possibly, in part, through the fault proposed by Briggs (1961) into the swampy areas of Caño Tiburones and Laguna Tortuguero.

There is an indication that the lateral permeability of the aquifer decreases exponentially with stratigraphic depth, ranging in value from about 1 cm/sec for the upper part of the Aymamón Limestone to 10^{-4} cm/sec for the basal Lares. No data are available for the vertical permeability although it can be inferred that it must be high because the water table is but a few meters above sea level in certain parts of the upper part of the Aymamón where the altitude of the land surface is more than 100 meters.

The water table is extremely flat in the most seaward Aymamón thus reflecting its high permeability. The increase in water-table gradient through the Aguada is ascribed to its relatively low lateral permeability and to the effect of the underlying impermeable Cibao. In the Cibao and the Lares the water table is again quite flat, possibly indicating that lateral flow through the water-table zone is less significant than downdip flow into the artesian system.

Streamflow from the volcanic terrane south of the limestones is increased during rainy periods by contribution from the karst, mainly by shallow transient subsurface flow through solution channels. The base-flow component of streamflow is less in basins in limestone than in volcanic terrane. On an annual basis, water-budget results indicate, however, that the flow of the rivers, after they have traversed the limestone belt, is about the same as it would have been had they continued flowing on volcanic terrane.

The flood plain provides a dampening effect on the storm runoff, absorbing part of the floodflow through bank storage, and releasing it later as base flow. However, one flood plain, the Río Grande de Arecibo, seems to be responsible for an overall apparent loss of flow. This loss is probably flow that bypasses this basin to emerge as spring flow in Caño Tiburones.

It is not possible to define a unique drainage area for that portion of the limestone belt that is drained by Caño Tiburones and the Río Grande de Arecibo because the base flow of Caño Tiburones is almost all ground-water flow from much of the belt to the south, whereas its direct runoff is from the area of the Caño itself. The best interpretation that can be made of the flow pattern and associated drainage areas of the north coast limestones is shown in figure 59.

The overwhelming effect of the limestones on the chemical quality of the water is to increase its bicarbonate and, therefore, its calcium concentration. Silica content in the limestone water is less than half (6–10 versus 15–30 mg/L) that found in the waters from the volcanic terrane.

The acidity of rainfall is insufficient to explain the measured quantity of $CaCO_3$ in the limestone water, and it is calculated that as much as 86 percent of the limestone solution takes place mainly through the enrichment of rainwater with CO_2 by the decomposition of organic material in the soil. Except for the water of lakes resting on terra rossa, most limestone waters are saturated or supersaturated with respect to calcite. Some of this calcite is probably reprecipitated as is evidenced by the crystalline limestone and the stalactitic deposits seen in most roadcuts. On the average, about 0.047 mm per year of $CaCO_3$ is discharged with the water flowing out of the limestones. Accordingly, the average land-denudation rate from solution is about 0.070 mm per year. Scant evidence indicates that abrasion in fluvial systems contributes about another 40 percent to the calculated denudation rate based on solution only.

A span of about 4 million years is computed as the time it would take present denudation rates to reduce a reconstructed original limestone surface to the present land surface. It is inferred, therefore, that the limestones of the north coast of Puerto Rico emerged from the sea about 4 million years ago. Some lower computed ages for the northwestern part of the limestone belt are thought to be indicative of later emergence related to the eastern tilting of the Puerto Rican platform as reported in the literature. By difference between the computed lower ages (about 3 million years ago) and the average, this eastern tilting of the Puerto Rican platform is considered to have occurred about 1 million years ago.

Geomorphic data on orientation of river courses indicate that the present drainage pattern, oriented slightly to the east and in accord with the topographic slope, is superimposed on a vestigial pattern slightly oriented to the west. These drainage patterns are thought to be supporting evidence for the tilting, as is the fact that karstic springs are most prevalent on the west side of river valleys.

An analysis of orientation and distribution of sinkholes reveals no preferred orientation. Thus surface solution is inferred to take place as an areally random process. The absence of preferred

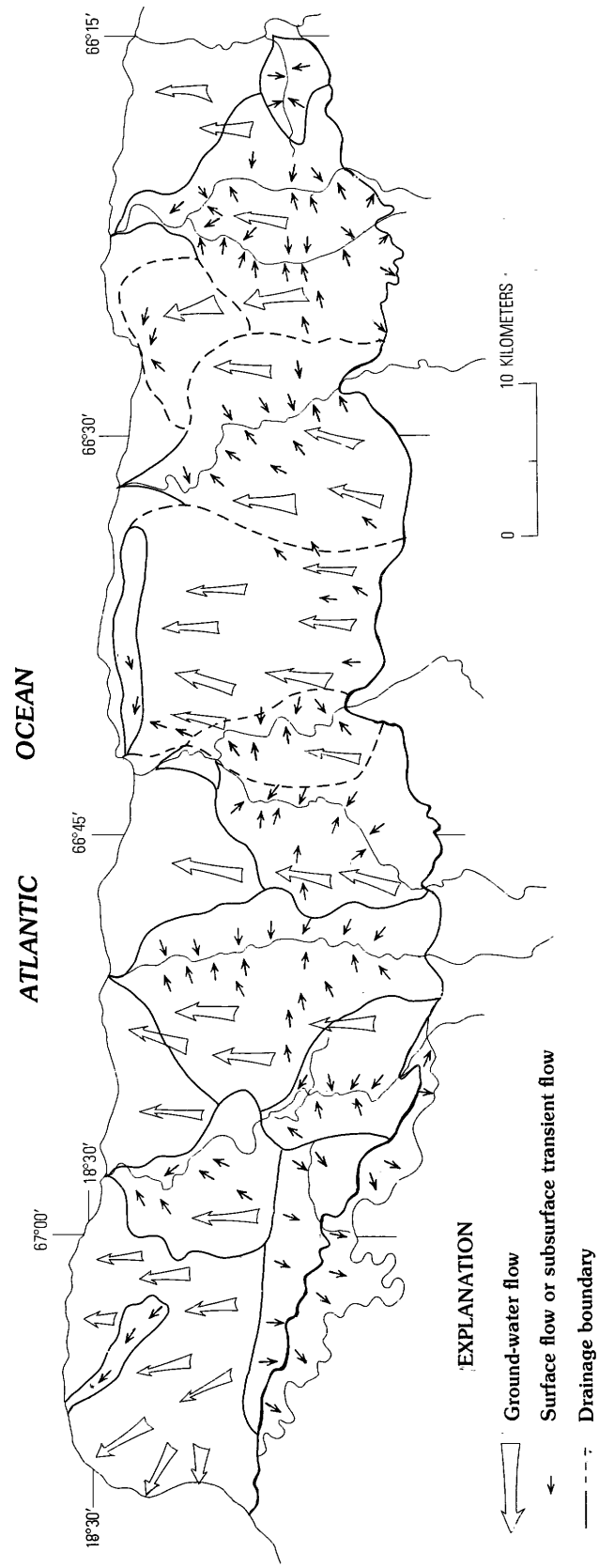

FIGURE 59.—Flow patterns and drainage areas of the north coast limestones.

orientation is taken to imply that large scale limestone joints are rare or absent.

Consideration of the processes that form the surface features of karst on soluble, unjointed, and unfractured limestones in Puerto Rico indicates that the primary controls are the distribution of lateral and vertical permeability and the primary porosity of the rocks. Climate is considered to be of lesser importance.

REFERENCES

Back, William, 1961, Calcium carbonate saturation in ground water, from routine analyses: U.S. Geol. Survey Water-Supply Paper 1535–D, 14 p., 1 pl.

——— 1963, Preliminary results of a study of calcium carbonate saturation of ground water in central Florida: Bull. Internat. Assoc. Sci. Hydr. VIII Année, no. 3.

Bennett, G. D., and Giusti, E. V., 1972, Ground water in the Tortuguero Area, Puerto Rico, as related to proposed harbor construction: Commonwealth of Puerto Rico Water-Resources Bull. 10, 25 p.

Birot, P., Corbel, J., and Muxart, R., 1967, Morphologie des régions calcaires à la Jamaique et à Puerto Rico: compte rendu de deux missions subventionnées par le Comité Nat. Recherche Sci.

Bouchet, R. J., 1963, Evapotranspiration réelle et potentielle, signification climatique: Gen. Assembly Berkely Pub. 62, Bull. Internat. Assoc. Sci. Hydrology, Gentbrugge, p. 134–142.

Briggs, R. P., 1961, Oil and gas possibilities of northern Puerto Rico: Puerto Rico Mining Commission, San Juan, P.R., p. 1–23, illus. including map.

——— 1966, The blanket sands of northern Puerto Rico: Third Caribbean Geol. Conference, Kingston, Jamaica Geol. Survey Pub. 95, Tr., p. 60–69.

Briggs, R. P., and Akers, J. P., 1965, Hydrogeologic map of Puerto Rico and adjacent islands: U.S. Geol. Survey Hydrol. Inv. Atlas HA–197.

Briscoe, C. B., 1966, Weather in the Luquillo mountains of Puerto Rico: Inst. Tropical Forestry, U.S. Forest Serv. Research Paper ITF–3.

Diaz, José Raul, 1973, Chemical quality of water in Caño Tiburones, Puerto Rico: U.S. Geol. Survey open-file report, map series 2.

Garrels, R. M., and Christ, C. L., 1965, Solutions, minerals, and equilibria, New York, Harper and Row.

Giusti, E. V., and López, M. A., 1967, Climate and streamflow of Puerto Rico, Caribbean Jour. Sci., v. 7, no. 3–4, p. 87–93, illus.

Goddard, E. N., chm., and others, 1948, Rock-color chart: Washington, Natl. Research Council (repub. by Geol. Soc. America, 1951), 6 p.

Gordon, W. A., 1959, The age of the Middle Tertiary rocks of northwestern Puerto Rico: Second Caribbean Geol. Conf. (Puerto Rico) Trans., p. 87–90.

Gurnee, R. H., Thrailkill, J. V., and Nicholas, G., 1966, Discovery at the Río Camuy; limestone erosion by ground water can produce caves of impressive size: Explorers Jour., v. 44, no. 1, p. 51–65, illus.

Jordan, D. G., 1970, Water and copper-mine tailings in karst terrane of Río Tanamá basin, Puerto Rico. U.S. Geol. Survey open-file report, 24 p.

Kaye, C. A., 1959, Shoreline features and Quaternary shoreline changes, Puerto Rico: U.S. Geol. Survey Prof. Paper 317–B, p. 49–140, illus.

Kuenen, P. H., 1950, Marine geology: New York, John Wiley and Sons, Inc. p. 376–385.

Leopold, L. B., and Langbein, W. B., 1962, The concept of entropy in landscape evolution: U.S. Geol. Survey Prof. Paper 500–A.

Lobeck, A. K., 1922, The physiography of Puerto Rico: New York Acad. Sci., v. 1, pt. 1 (Survey of Porto Rico).

McGuinness, C. L., 1948, Ground water resources of Puerto Rico: Puerto Rico Aqueduct and Sewer Authority, duplicate report.

Mackin, J. H., 1948, Concept of the graded river: Geol. Soc. America Bull., v. 59, p. 463–512.

Meyerhoff, H. A., 1933, Geology of Puerto Rico: Univ. Puerto Rico Mon., ser. B, no. 1, 306 p.

Monroe, W. H., 1962, Geology of the Manatí quadrangle, Puerto Rico (with text), U.S. Geol. Survey Misc. Geol. Inv. Map I–334.

——— 1964, The zanjón, a solution feature of karst topography in Puerto Rico: U:S: Geol. Survey Prof. Paper 501–B, p. B126–B129.

——— 1966, Formation of tropical karst topography by limestone solution and reprecipitation: Caribbean Jour. Sci., v. 6, no. 1–2, p. 1–7, illus.

——— 1968a, High level Quaternary beach deposits in northwestern Puerto Rico, *in* Geological Survey research, 1968: U.S. Geol. Survey Prof. Paper 600–C, C140–C143.

——— 1968b, The karst features of northern Puerto Rico: Natl. Speleol. Soc. Bull., v. 30, no. 3, p. 75–86.

——— 1969a, Geologic map of the Aguadilla quadrangle, Puerto Rico: U.S. Geol. Survey Misc. Geol. Inv. Map I–569.

——— 1969b, Evidence of subterranean sheet solution under weathered detrital cover in Puerto Rico: Problems of the karst denudation, Brno, Studia Geographica 5, Geografický Ústav, Brno.

Morton, F. I., 1965, Potential evaporation and river basin evaporation: Proc. Am. Soc. Civil Engrs., J. Hydraulic Div., v. 91, HY 6.

Moussa, M. T., 1969, Quebrada de los Cedros, southwestern Puerto Rico, and its bearing on some aspects of karst development: Jour. Geology, v. 77, p. 714–720.

Myers, W. H., 1955, Preliminary results of geophysical exploration for gas and oil on the north coast of Puerto Rico: Puerto Rico Econ. Dev. Admin., Div. Mineralogy and Geology, Bull. 1, 10 p.

Olmsted, F. H., and Hely, A. G., 1962, Relation between ground water and surface water in Brandywine Creek basin, Pennsylvania: U.S. Geol. Survey Prof. Paper 417–A, 21 p.

Picó, Rafael, 1950, The geographic regions of Puerto Rico: University of Puerto Rico Press, Río Piedras, P.R., 256 p., illus.

Roche, M., 1963, Hydrologie de surface: Gauthier-Villars Editeur, Paris, 123 p.

Shurbet, G. L., and Ewing, Maurice, 1956, Gravity reconnaissance survey of Puerto Rico: Geol. Soc. Am. Bull., v. 67, no. 4, p. 511–534, illus.

Smithsonian Meteorological Tables, 1966, Sixth revised edition: Smithsonian Institution.

Solomon, S., 1967, Relationship between precipitation, evaporation, and runoff in tropical-equatorial regions: Water Resources Research, v. 3, no. 1.

Thornthwaite, C. W., 1931, The climates of North America according to a new classification: Geographic Review, v. 21, p. 633–655.

Williams, R. S., 1965, Geomorphology of a portion of the Northern Coastal plain of Puerto Rico: Unpub. thesis, Pennsylvania State University.

Zapp, A. D., Bergquist, H. R., and Thomas, C. R., 1948 (reprinted 1950), Tertiary geology of the coastal plains of Puerto Rico: U.S. Geol. Survey Oil and Gas Inv. Prelim. Map 95.

INDEX

[Italic page numbers indicate major references]

☆ U.S. Government Printing Office: 1977—261-221/157